ARTICLE

New Horizons for Catalysis Disclosed by Supramolecular Chemistry

Received 00th January 20xx,
Accepted 00th January 20xx

DOI: 10.1039/x0xx00000x

Giorgio Olivo*[a], Giorgio Capocasa[a], Daniele Del Giudice[a], Osvaldo Lanzalunga[a] and Stefano Di Stefano*[a]

The adoption of a supramolecular approach in catalysis promises to address a number of unmet challenges, ranging from activity (unlocking of novel reaction pathways) to selectivity (alteration of the innate selectivity of a reaction, e.g. selective functionalization of C-H bonds) and regulation (switch ON/OFF, sequential catalysis, etc.). Supramolecular tools such as reversible association and recognition, pre-organization of reactants, stabilization of transition states upon binding and catalysis regulation offer a unique chance to achieve the above goals disclosing new horizons whose potential is being increasingly recognized and used, sometimes reaching the degree of ripeness for practical use. This review summarizes the main developments that have opened such new frontiers, with the aim of providing a guide to researchers approaching the field. We focus on artificial supramolecular catalysts of defined stoichiometry which, under homogeneous conditions, unlock outcomes that are highly difficult if not impossible to attain otherwise, namely unnatural reactivity or selectivity and catalysis regulation. The different strategies recently explored in supramolecular catalysis are concisely presented, and, for each one, a single or very few examples is/are described (mainly last 10 years, with only milestone older works discussed). The subject is divided into four sections in light of the key design principle: i) nanoconfinement of reactants, ii) recognition-driven catalysis, iii) catalysis regulation by molecular machines and iv) processive catalysis.

1 Introduction

Catalysis – the acceleration of chemical reactions by adding a substance (the catalyst) that is not consumed in the process – is a key enabling technology for chemical industries. Its importance fuels the need to continuously improve current catalysts and design novel ones to address challenges that are still unmet. This is especially true in the application of catalysis to organic synthesis. For instance, most catalytic systems struggle to achieve site-selectivity – mainly in C-H and C=C functionalization[1] - or substrate-selective transformations in mixtures of compounds, crucial for the use of biomasses and wastes as feedstock materials.[2] Other reactions are prohibitively slow or fail to provide the products in any synthetically meaningful yield. Combination of multiple catalytic reactions as an assembly line for the synthesis of complex molecules from simple starting materials remains difficult for organic chemists.[3] Or again, temporal regulation of catalytic activity to promote different reactions at different times is not trivial using conventional catalysis approaches.

The merger of catalysis and supramolecular chemistry (the study of weak, reversible interactions among different molecules) offers a way to face these challenges. Incorporation of supramolecular tools (reversible recognition and preorganization of reactants, stabilization of transition states upon binding, regulation of catalysis) in catalyst design mimics some key features of enzymes and has the prospect to unlock unprecedented reactivity and selectivity. In fact, catalysis has been one of the main research themes in the field of supramolecular chemistry since its very beginning. However, when compared to the other topics of supramolecular science, it certainly poses greater difficulties and hurdles associated to the impossibility to know the precise structure of the transition states to be stabilized by interaction with supramolecular catalysts. Moreover, the structural sophistication of early supramolecular catalysts could discourage their use. Nevertheless, notable examples of supramolecular catalysts have appeared in the literature in the last 50 years that approach the efficiency of natural enzymes. In particular, the last decade has witnessed a significant progress in this field, with a growing number of supramolecular catalysts featuring high activity and selectivity.

Herein, we summarize the main developments that, in our view, have opened new opportunities for catalysis, aiming to provide a guide and an inspiration to the researchers approaching the field. An overview of key works in supramolecular catalysis is given, without pretension to be exhaustive. One or few examples for each approach is (are) explicitly described, followed by a list of references based on an analogous design or reviews and book chapters with a more specific focus to which we direct the interested reader. In particular, we have restricted our analysis to homogeneous, artificial supramolecular catalysts of defined stoichiometry which unlock outcomes that are highly

[a] Dipartimento di Chimica, Università degli Studi di Roma "La Sapienza", Dipartimento di Chimica and ISB-CNR Sede Secondaria di Roma - Meccanismi di Reazione P.le A. Moro 5, I-00185 Rome, Italy. E-mail: stefano.distefano@uniroma1.it and giorgio-olivo@uniroma1.it

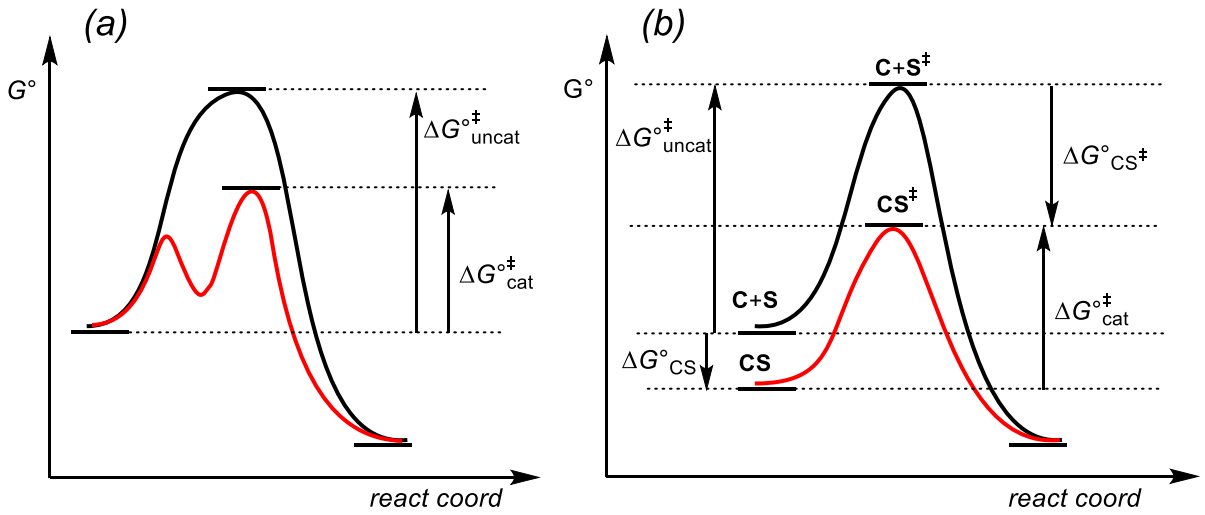

Fig. 1. Two possible catalytic modalities: (a) the catalyst allows a new mechanistic path with a lower activation barrier, (b) the reaction mechanism remains the same but the catalyst binds the transition state more strongly than the initial state, lowering the activation barrier. Free energy variations are referred to 1 M standard states.

difficult if not impossible to attain otherwise - namely unnatural reactivity or selectivity and catalysis regulation. The timeframe of our analysis is mainly focused on the last ten years, with only milestone results before 2010 included, since most of them have been already reviewed.[4] These systems are presented in light of their design: i) nanoconfinement of reactants, ii) recognition-driven catalysis, iii) catalysis regulation by molecular machines and iv) processive catalysis.

1.1 Efficiency and selectivity of a supramolecular catalyst

Generally speaking, a catalyst can accelerate a reaction in two different ways, i) opening a new mechanistic path, unfeasible in the absence of the catalyst, whose activation barrier is lower than that associated to the uncatalyzed reaction (Fig. 1a); ii) lowering the activation barrier of the same mechanistic path of the uncatalyzed reaction by binding the transition state more strongly than the substrate (Fig. 1b).

Most of the supramolecular catalysts as well as several enzymes adopt the second strategy. As a matter of fact, an efficient supramolecular catalyst should possess all the typical features of a natural enzyme, first of all the capability of binding the substrate via weak interactions, which is not contemplated in conventional catalysis. Thus, the thermodynamic and kinetic treatments that have disclosed the origin of the catalytic power of enzymes[5] can also be applied to supramolecular catalysts. As far as strategy ii is concerned (Fig 1b), in both cases (enzymes or supramolecular catalysts) the binding event with the substrate is of paramount importance in the definition of the efficiency and selectivity properties of the catalyst. In the limits of the Eyring theory,[6] the kinetic scheme for a reliable comparison between a one-substrate uncatalyzed and catalyzed reaction is reported in Fig. 2.

Following a simple but operatively effective model due to Linus Pauling,[7] from the thermodynamic cycle depicted in Fig. 2 in which $\Delta G°_{CS}$ and $\Delta G°_{CS\neq}$ represent the standard free energy for the association of the catalyst with the substrate and the transition state, respectively, and $\Delta G°^{\neq}_{cat}$ and $\Delta G°^{\neq}_{uncat}$ the standard free energy activation barriers for the catalyzed and

Giorgio Olivo

Giorgio Olivo *obtained his PhD in 2015 at "La Sapienza" university of Rome (Italy) with S. Di Stefano. Then, he moved to Girona (Spain) as a postdoctoral fellow in the QBIS group of M. Costas (2016-2020), working on a recognition-driven oxidation of remote aliphatic C-H bonds catalyzed by Fe and Mn catalysts. Recently (2021) he moved back to Rome, where his research interests lie in the design and implementation of a supramolecular approach to control selectivity in late-stage functionalization and in bioinspired metal catalysis.*

Giorgio Capocasa

Giorgio Capocasa *was born in Rome in 1993. In 2017, he earned a master's degree in Chemistry at "La Sapienza" University of Rome (Italy) and enrolled in a PhD programme at the same university. In 2021, he gained his PhD with a thesis on supramolecular catalysis applied to hydrocarbon functionalization under the supervision of S. Di Stefano. He is currently working as a post-doc in the M. Costas group at "Universitat de Girona" (Catalunya, Spain) with a project on bioinspired C-H functionalization*

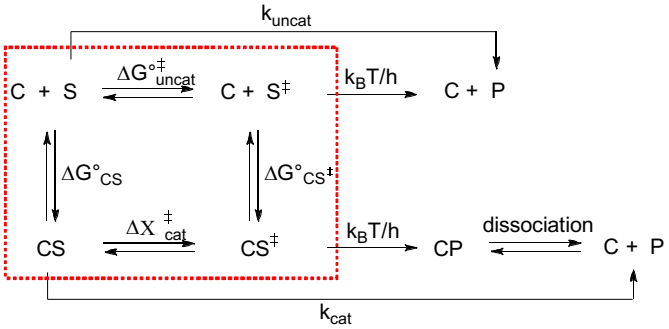

Fig. 2. Comparison between a one-substrate uncatalyzed and catalyzed reaction. The thermodynamic cycle discussed in the text is inside the red square. Dissociation step in considered fast.

uncatalyzed processes, respectively, eqn (1) can be easily derived and rearranged to obtain eqn (2).

$$\Delta G^{\circ}_{CS} + \Delta G^{\circ\neq}_{cat} = \Delta G^{\circ\neq}_{uncat} + \Delta G^{\circ}_{CS\neq} \quad (1)$$

$$\Delta G^{\circ\neq}_{uncat} - \Delta G^{\circ\neq}_{cat} = \Delta G^{\circ}_{CS} - \Delta G^{\circ}_{CS\neq} \quad (2)$$

It has to be noted that eqn (1) can also be rewritten as eqn (3), which is immediately visualized in Fig. 1b.

$$\Delta G^{\circ\neq}_{uncat} - \Delta G^{\circ}_{CS} = \Delta G^{\circ\neq}_{cat} - \Delta G^{\circ}_{CS\neq} \quad (3)$$

Since the rate constants for the catalyzed and uncatalyzed reactions can be written as $k_{cat} = (k_BT/h)\exp(-\Delta G^{\circ\neq}_{cat}/RT)$ and $k_{uncat} = (k_BT/h)\exp(-\Delta G^{\circ\neq}_{uncat}/RT)$, respectively, where k_B and h are Boltzmann and Plank constants, T the absolute temperature and $R = N \times k_B$ (N is the Avogadro number), and since the association constants of the transition state and the substrate with the catalyst are $K_{CS\neq} = \exp(-\Delta G^{\circ}_{CS\neq}/RT)$ and $K_{CS} = \exp(-\Delta G^{\circ}_{CS}/RT)$, respectively, eqn (4) can be directly obtained from eqn (2).

$$k_{cat} / k_{uncat} = K_{CS\neq} / K_{CS} \quad (4)$$

Eqn (4) tells us that the efficiency of a catalyst (k_{cat} / k_{uncat}) that operates with a complexation (binding) mode (Fig.1 b), depends on its capability to selectively stabilize the transition state ($K_{CS\neq}$) with respect to the substrate (K_{CS}).

On the other hand, catalyst selectivity also calls for a strong binding of the target substrate. The selectivity ability of a supramolecular catalyst for a target substrate, exactly like in the case of an enzyme, is indeed properly described by the specificity constant,[8] which is commonly defined as in eqn (5), where K_M is the Michaelis constant. The latter corresponds to the inverse of K_{CS} in the very frequent case of an association between the catalyst and the substrate much faster than the transformation of the bound substrate to products.[8]

$$\text{Specificity constant} = k_{cat}/K_M \ (\text{or } k_{cat} \times K_{CS}) \quad (5)$$

For example, the selectivity of a supramolecular catalyst for one of two substrates can be obtained by the ratio of the two specificity constants for the two substrates, while the selectivity for one of two reaction sites present in the same substrate can

Osvaldo Lanzalunga

Osvaldo Lanzalunga. *received his PhD degree from the University of Rome "La Sapienza" in 1994. After postdoctoral experience in S. Steenken group at the Max Plank Institute fur Strahlenchemie, Mülheim (Germany) he became Researcher and is currently Full Professor in Organic Chemistry at the Dipartimento di Chimica of the University "La Sapienza". His scientific research is mainly focused on the chemistry of radicals and radical ions, on the role of structural and medium effects on hydrogen atom transfer (HAT) and electron-transfer (ET) reactions involving oxygen-centered radicals and on the role of ET processes in organic and bioorganic reactions.*

Daniele Del Giudice

Daniele Del Giudice *was born in Latina in 1995. In 2019 he earned the master's degree in chemistry at the University of Rome La Sapienza, receiving the "Excellent Graduate" award from the same university. Master's degree internship was performed in the laboratory of S. Di Stefano, regarding the development of chemical fuels triggering the motion of acid-base operating molecular machines. Then he enrolled in a PhD programme under the supervision of the same professor, working on the employment of chemical fuels to obtain dissipative control on several kinds of supramolecular systems.*

Stefano Di Stefano

Stefano Di Stefano *received his PhD in Chemical Sciences in 2000 at the University of Rome La Sapienza. After a period in the pharmaceutical industry, he came back to the same University where he is now an Associate Professor. His research interests lie in the field of supramolecular catalysis, dynamic covalent chemistry, and chemically driven molecular machines. For his research work, he received an award from Italian Chemical Society in 2020. He also received the prize for "Excellent University Teaching" in 2014, 2017 and 2018 from the Faculty Dean. He has been involved in many national and international scientific collaborations.*

be obtained by the ratio of the two different k_{cat} values corresponding to each site (K_M is the same).

To sum up, a good supramolecular catalyst must strongly bind the substrate in order to display a high selectivity and at the same time must bind even more strongly the transition state to feature a high catalytic efficiency.

The dissociation from reaction product (Fig. 2) is needed to guarantee turnover. It always represents an issue, which can be circumvented by a rational design of the supramolecular catalyst.

In the following sections, the supramolecular tools at disposal of catalysis practitioners will be reviewed in light of strategies recently used.

2. Nanoconfinement of reactants

Confinement of reactants in a nanometric cavity of comparable size and shape offers a unique chance to modulate reaction outcomes.[9] Encapsulation can remove the solvation shell from reactants and enforce unusual conformations and orientations, altering the energy profile of a reaction. In particular, nanoconfinement can i) accelerate chemical reactions via selective stabilization of transition states; ii) unlock novel or forbidden reactivity by disclosing new reaction pathways; iii) modulate the selectivity by altering the relative orientation of reactants; iv) protect the catalyst shielding the reaction site from the bulk solution (Fig. 3). Herein, we describe selected recent examples that provide an overview of these different approaches, and we refer the interested reader to more specialized and exhaustive reviews.[10]

Nanometric vessels are the cavities of concave or hollow molecular structures - the hosts –which are delimited by organic walls. There is a huge number of possible host structures, ranging from vase-like, covalent macrocycles (cyclodextrins,[11] cucurbiturils,[12] cavitands,[13] hemicryptophanes[14] and so on) to self-assembled super-structures held together by weak interactions (coordination cages[15] or hydrogen bonded capsules[16]). In particular, the ease of synthesis and the modularity of self-assembled cages and capsules makes them especially attractive from a practical point of view. Indeed, most examples in this review rely on such hosts. However, confinement, like other strategies in supramolecular catalysis, faces the great challenge of product inhibition. In fact, true catalysis (turnover) requires expulsion of the reaction products, typically strongly bound to the host, to make room for other substrate molecules. This elusive condition is met when the reactants bind to the host with a higher affinity compared

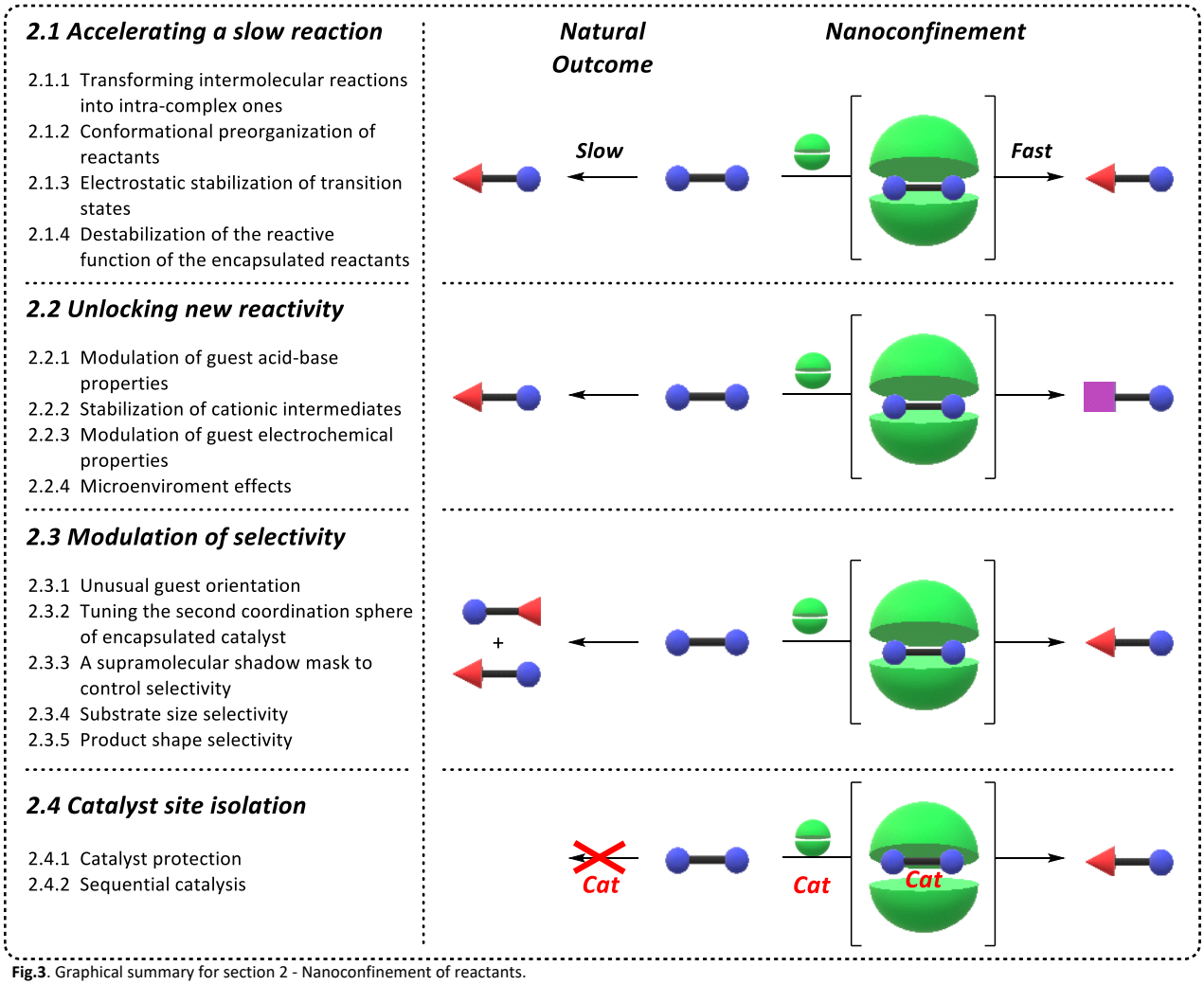

Fig.3. Graphical summary for section 2 - Nanoconfinement of reactants.

to the products, displacing them and starting the catalytic cycle over again. Practically, this implies designing a system where the change in the product shape, charge or properties compared to reactants disrupts its affinity for the cavity and induces its egress. This challenging requirement has been met in several examples, paving the way for practical applications of supramolecular catalysis.

2.1 Accelerating a slow reaction

Encapsulation can enhance reaction rates by bringing in proximity the reactive functions. This is a consequence of reactants pre-organization, which results in the selective stabilization of the transition state of the rate determining step with respect to the initial state (the reactants themselves).[5e] The magnitude of such acceleration can be dramatic, and the timescale of the reactions can be consequently reduced from weeks to minutes, effectively unlocking reactions that are otherwise prohibitively slow. Although selective stabilization of the transition state(s) is always the source of catalysis,[5e] a rough classification based on the main components of the catalytic effect can be of help to visualize the different approaches to the problem and present the tools at disposal of supramolecular catalysis.

2.1.1 Transforming intermolecular reactions into intra-complex ones. When two (or more) reactants are co-encapsulated inside a restricted space, an otherwise intermolecular reaction is transformed into an intra-complex (intramolecular) one with the reactants and their host belonging to the same adduct. As a consequence, the reaction is accelerated essentially for entropic reasons (in an intermolecular bimolecular process, the roto-translational entropy associated to one molecule is lost when the two reactants interact to form the transition state, while an intramolecular reaction does not require any loss of the same kind (this is often called "intramolecularity" effect). Substrate encapsulation pays upfront the entropic cost of bringing the reactants together, reducing the kinetic barrier of the reaction. The acceleration effect can be properly evaluated in terms of effective molarity (EM),[17] which is a measure of the reactivity enhancement

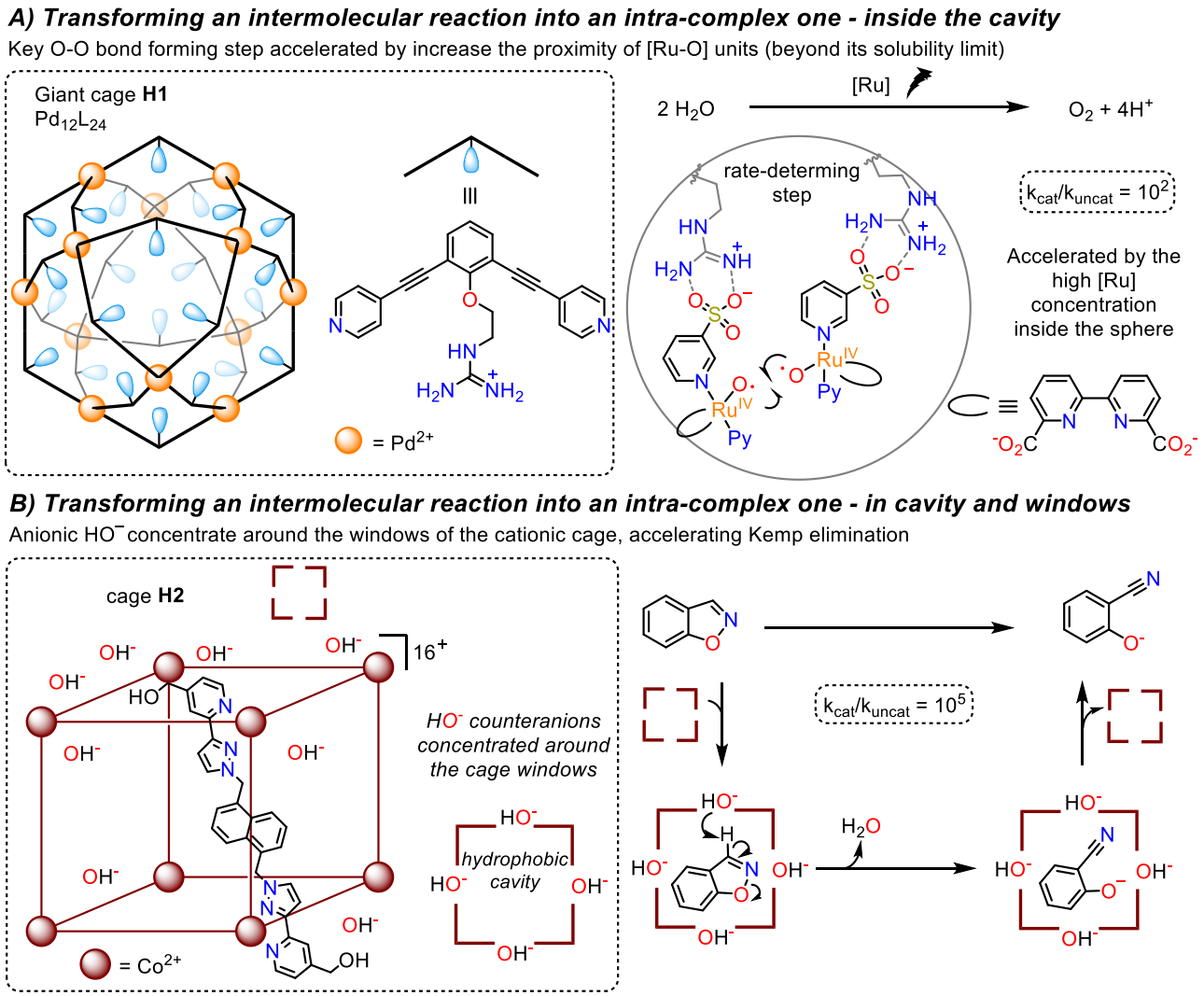

Fig.4. Acceleration of chemical reactions by converting intermolecular reactions into intra-complex ones upon encapsulation. A) Rate enhancement of Ru-catalyzed water oxidation inside a giant cage (ref 18). B) Catalysis of Kemp elimination by preorganization of the hydrophobic substrate inside the cavity and HO^- counteranions around the cage windows. (ref 22a)

caused by the proximity of the reactive functions in a restricted space. In principle, if the corresponding intermolecular model reaction is available to carry out a reliable comparison of reactivity, values of EM up to about 10^7 M can be expected (corresponding to a ~9 kcal mol^{-1} energy gain at 25 °C).[17b,c,d] However, deviations from ideality (presence of strain or imperfect preorganization) typically lead to lower, yet significant EM values. The enhancement of reactivity due to the "intramolecularity" effect is often described as an increase of the "local (or effective) concentration" of one reactive function with respect to the other. A quantitative treatment based on thermodynamic parameters such as that based on EM is however more desirable.[17b,c,d]

Practically, co-encapsulation of two guests in the same cavity usually accelerates bimolecular reactions, as long as the reactants are properly oriented. For instance, the giant coordination cage (host **H1**) contains multiple guanidinium units in its large cavity, which can in turn bind several Ru water oxidation catalysts (WOCs) bearing sulfonate moieties via hydrogen bonds (Fig. 4A). As a consequence, the reactive Ru-O units are pre-organized for radical O-O coupling that forms O_2, and the rate (and yield) of water oxidation experiences a 10^2-fold enhancement.[18] Analogously, several bimolecular reactions were accelerated (and their yields were enhanced) by co-encapsulation of the two reactants.[17c,d,19] Remarkably, sometimes the acceleration can be large enough to unlock forbidden reactions such as Diels-Alder cycloaddition with typically inert partners (i.e. naphthalene).[20]

Another strategy to increase the proximity of reactive functions by means of a cavity exploits the orthogonal affinities for the hydrophobic cavity and for its charged exterior to bring together reactants of opposite polarity.[21,22] As a consequence, their reaction occurs inside the ionic pair and becomes "intra-complex". For instance, encapsulation of isobenzoxazole inside polycationic (16^+) cage **H2** induces a 10^5-fold acceleration of Kemp elimination, mainly because the HO^- counter-anions of the cage are pre-organized at the cage windows close to the encapsulated substrate (Fig. 4B).[22] Catalysis is then allowed by expulsion of the anionic product from the hydrophobic cavity and further accelerated by an autocatalytic process.

2.1.2 Conformational preorganization of reactants.

Encapsulated guests tend to assume peculiar, folded conformations to optimize the occupancy of the cavity (following the 55% occupancy rule)[23] and the interactions with its walls. Such conformations, which can be particularly effective from a reactivity standpoint, can be unlikely in solution for entropic reasons (ordered transition state that requires freezing of a large number of rotable bonds)[17c,d] but become spontaneous upon encapsulation, when this entropic price is paid in advance. A quantitative treatment and rationalization of these effects can be again based on the effective molarity.[17c,d] Preorganization of reactants in these conformations accelerates intramolecular reactions even by orders of magnitude, and often constitutes a key ingredient of cage catalysis.

A prominent example in this regard is the cavitand-promoted macrocyclization described by Rebek's group (Fig. 5). Macrocyclization of flexible compounds is challenging and typically not efficient, as they must assume an unlikely and sometimes strained[17g] U-shaped conformation to bring the reactive functions in proximity. Encapsulation of linear alkyl chains with polar heads in the hydrophobic cavity of a cavitand (**H3**), driven by solvophobic effects, pre-organizes the guest in a folded, U-shaped conformation with nearby polar heads at the vase opening.[13] At this point, addition of suitable reactants readily links these heads together into a macrocycle with almost quantitative yields,[24] while the analogous macrocyclization essentially does not occur in bulk solution. Unfortunately, the product is stuck inside the cavitand, preventing catalytic turnover. Analogous guest preorganization in other capsules or coordination cages also leads to large acceleration of intramolecular reactions.[16,25,26]

Rate enhancement via guest preorganization

Preorganization of alkyl chains in a U-shaped conformation facilitates macrocylization

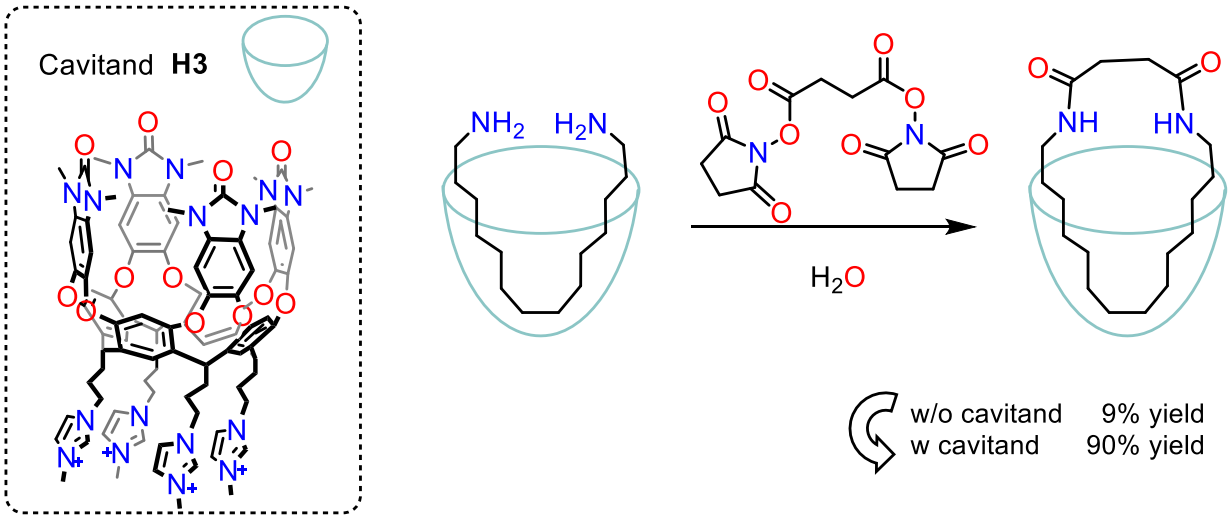

Fig.5. Acceleration of a macrocylization reaction (increase of the yield) via constrictive binding that fixes the substrate in a U-shaped conformation upon encapsulation, with the reactive heads preorganized for macrocylization (ref 24b).

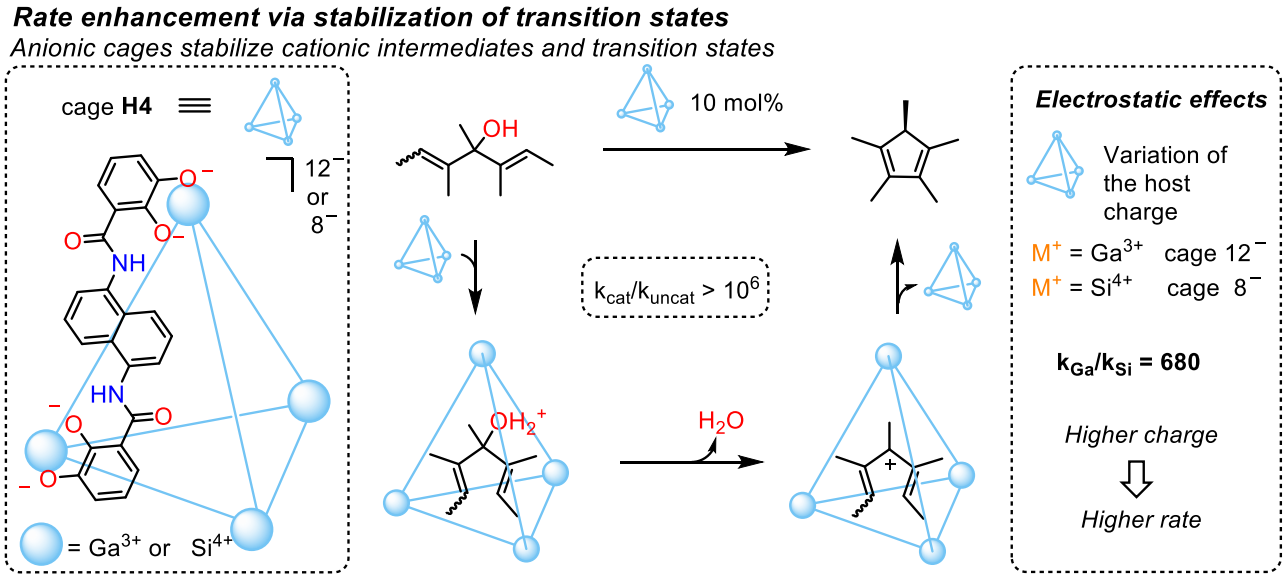

Fig.6. Acceleration of Nazarov cyclization upon substrate encapsulation in an anionic cage. Several factors concur to such a large rate enhancement including an electrostatic stabilization of the cationic transition state (ref 27). The latter effect is quantified by variation of the host charge (ref 29).

2.1.3 Electrostatic stabilization of transition states. High-energy, charged intermediates – and hence the related transition states (TSs) – can be stabilized via electrostatic or cation-π interactions with hosts of opposite charge. If they are selectively stabilized over the reactants, the kinetic barrier is lowered and the reaction rate increased. The extent of such electrostatic stabilization is often difficult to quantify, since it is typically combined with other factors (mainly guest preorganization). However, as found in enzymes, its magnitude can be quite high when charged intermediates or transition states are formed in the slow step.

For instance, Raymond, Bergman and coworkers reported an anionic coordination cage **H4**[26] that encapsulates and stabilizes small cationic guests in folded conformations, accelerating their intramolecular rearrangement. The Nazarov cyclization of a bis-allylic alcohol, where carbocation formation is the slow step, undergoes an impressive 10^6 rate enhancement inside cage **H4** (Fig. 6).[27] The majority of this acceleration is due to preorganization of the guest,[28] but electrostatic stabilization of the transition state plays also a key role: 33% increase of negative charges on the same anionic cage from 8^- to 12^- translates into a 680-fold acceleration, without significant geometric variations observed in the host structure.[29] Along a similar line, an intramolecular S_N2 reaction (with an anionic transition state) undergoes a 10^5-fold acceleration moving from an anionic host to its cationic analogue.[30]

2.1.4 Destabilization of the reactive function of the encapsulated reactants. Another way to lower the kinetic barrier and accelerate a chemical reaction is the relative destabilization of reactive functions of the reactants with respect to the transition state,[31] which is again a selective stabilization of the transition state with respect to the reactants.[5e]

Such concept has recently been used by Fujita's team. Confinement of two amide guests inside coordination cage **H5** induced a twist in the C-N bond from 0 to 34°, as determined by X-Ray crystallography (Fig. 7). Such twist disrupts the resonance along the C-N bond, increasing the amidic carbonyl

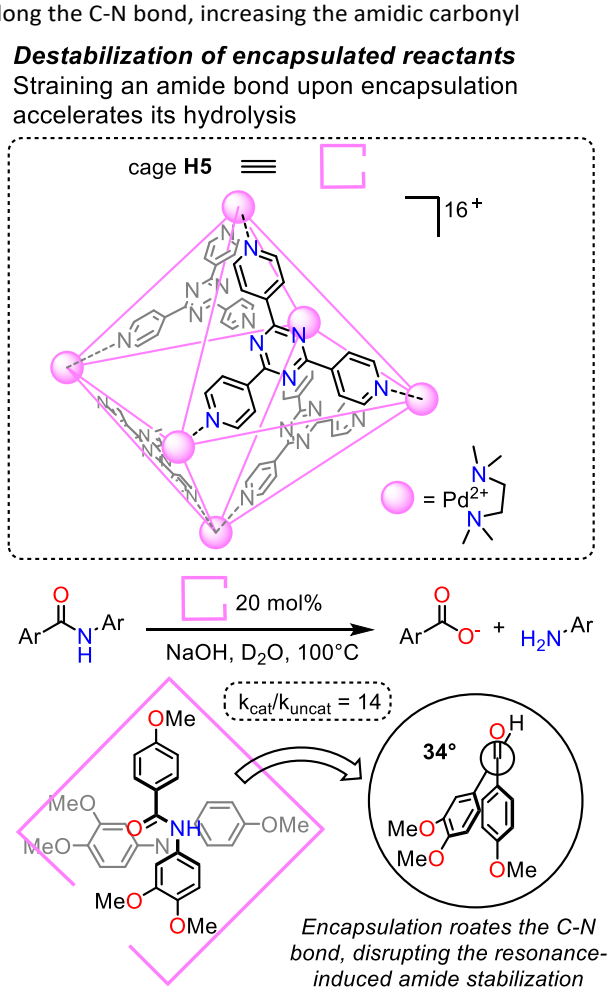

Fig.7. Rate enhancement of amide hydrolysis under basic conditions induced by introduction of strain in the C-N bond upon encapsulation in **H5** (ref 32).

electrophilicity and destabilizing the reactant. This way, the hydrolysis of the amide experiences a 14-fold acceleration.[32]

2.2 Unlocking new reactivity

Perhaps the most fascinating feature of confinement is the chance to fully alter the energy profile of a reaction with the tools described above, unlocking new pathways that lead to unusual products. This is usually achieved by exploiting the different microenvironment in the cavity to selectively stabilize high-energy species difficult to form in solution, leading to divergent reactivity.

2.2.1 Modulation of guest acid-base properties. Encapsulation inside a charged host alters the environment surrounding the guest, effectively stabilizing the development of an opposite charge on the guest via electrostatic (and cation-π) interactions. One way to build up these charges is protonation or deprotonation of the guest; in this case, encapsulation can modify the acid/base properties of a molecule (its pK_a).

For instance, anionic cage **H4** induces an increase up to 4.5 pK_a units of the basicity of neutral guests, preferentially stabilizing their protonated form.[26] As a consequence, reactions that require acid conditions become viable even at neutral or basic pH (Fig. 8). For instance, orthoformates are hydrolyzed only at acid pH, and are stable at neutral and basic pH. Addition of anionic cage **H4** increases their basicity and enables acid catalyzed hydrolysis even in basic solution (pH = 11), a process that does not occur in bulk solution.[33,34] Catalytic turnover is then achieved since the flat, smaller shape of the product has a lower affinity for the cavity. On the other hand, a cationic cage facilitates deprotonation of its guest to form anions, unlocking base-catalyzed reactions at a neutral pH.[19b,35]

2.2.2 Stabilization of cationic intermediates. As discussed above, stabilization of high-energy, charged intermediates via encapsulation can substantially accelerate chemical reactions. In some cases, such stabilization (usually in combination with pre-organization and protection from the outside solution) opens up novel reaction pathways that are precluded in bulk solution.

In organic reactions, such stabilization facilitates the formation of high-energy carbocationic intermediates. Tiefenbacher and coworkers designed a catalytic, selective terpene cyclization[36] inside a self-assembled capsule made up of 6 resorcinarene units[16] (Fig. 9A, **H6**). This capsule binds cationic guests via cation-π interactions and solvophobic effects. Moreover, the water molecules involved in the hydrogen bond network at its rim behave as a strong Brønsted acid.[16a,b,37]

As a result, encapsulated terpenes are easily protonated. Loss of water generates a carbocation, stabilized by the capsule, which triggers multiple tail-to-head cyclizations whose selectivity is controlled by the folded conformation (Fig. 9A). Such cyclization mimics that catalyzed by cyclase enzymes and is a powerful synthetic method. This is currently the shortest total synthesis of several natural products with bi- or polycyclic structures (eucalyptol, δ-selinene, isolongifolene, etc.).[36,38] Building on similar principles, the same cage was shown to catalyze a range of elusive transformations,[16] from carbonyl-olefin metathesis[39] and alcohol dehydration[40] to β-Friedel-Craft alkylation of pyrroles.[41]

The electrostatic stabilization by encapsulation can be applied also to organometallic reactions that involve high-energy cationic intermediates.[42,43] Reductive C(sp^3)-C(sp^3) elimination is prohibitively slow from $L_2Au^{III}(Me)_2$ or $L_2Pt^{IV}(Me)_2$ complexes.[42] However, dissociation of one ligand (L) from these complexes generates a cationic, unsaturated metal center that

New reactivity via modulation of guest acid-base properties

Encapsulation in an anionic cage increases the guest proton affintity by stabilizing cationic species

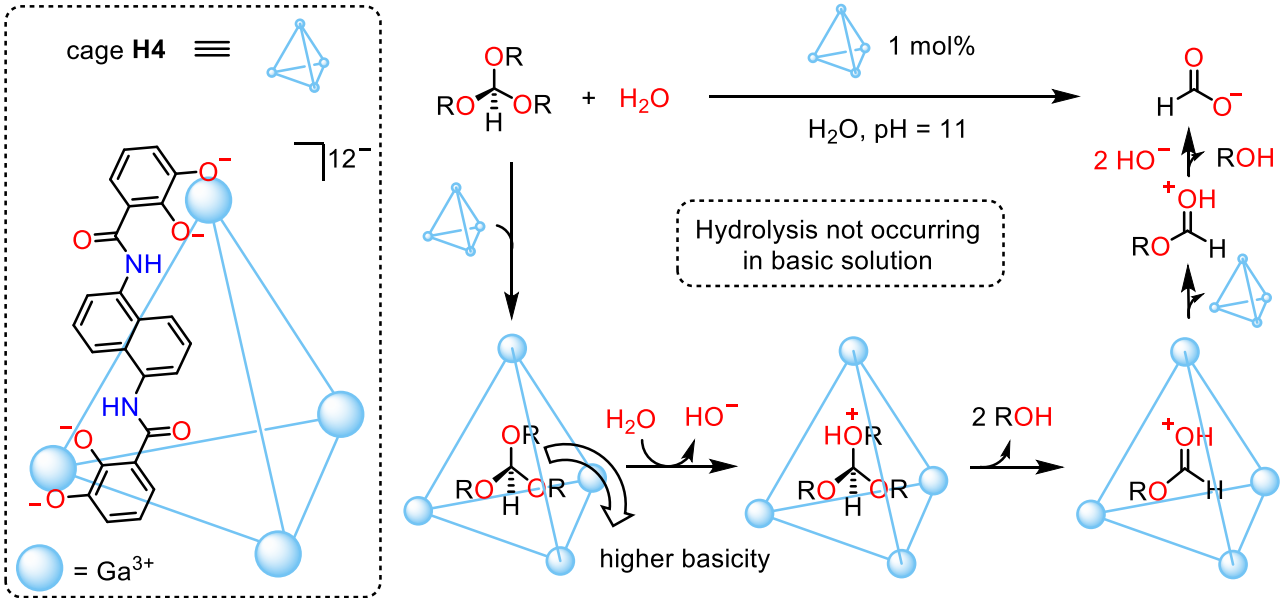

Fig.8. New reactivity (orthoformates hydrolysis in basic solution) unlocked by increasing the basicity upon encapsulation in an anionic cage (ref 33).

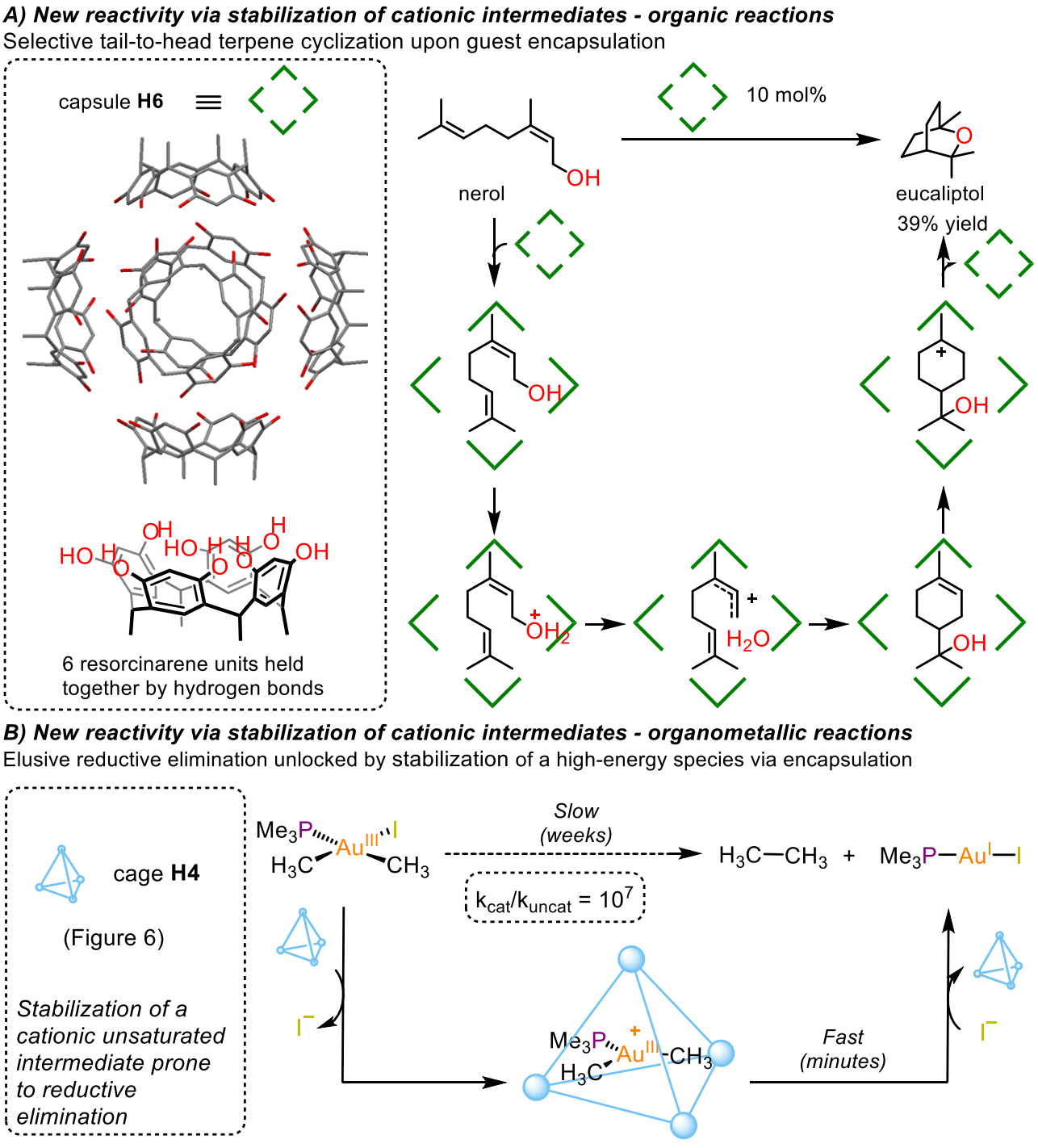

Fig.9. New reactivity unlocked by stabilization of high-energy, cationic intermediates. A) Selective nerol cyclization disclosed by stabilization of folded cationic intermediates inside deprotonated, anionic resorcinarene capsule **H6** (ref 36). B) Challenging reductive elimination unlocked by stabilization of unsaturated, cationic intermediates upon encapsulation into anionic cage **H4** (ref 42).

undergoes facile and rapid reductive elimination to restore a stable Au^{I} or Pt^{II} compound (Fig. 9B). Typically, this unsaturated intermediate is energetically uphill and not spontaneously formed. In stark contrast, addition of anionic cage **H4** stabilizes this cationic species and unlocks this pathway, resulting into a striking 10^4-10^7-fold acceleration, reducing the process timescale from weeks to minutes.[42]

2.2.3 Modulation of guest electrochemical properties.

Stabilization of high-energy, charged intermediates via encapsulation also affects the electrochemical properties of a guest, modulating its ability to lose or accept electrons. In fact, electron transfer from the guest to the host or *vice versa* produces unstable radical cations and anions, which are highly reactive and difficult to form in bulk solution. Moreover, electron transfer can be further favored by the proximity of the reactants as well as by the limited structural reorganization required within the host-guest adduct. Practically, these

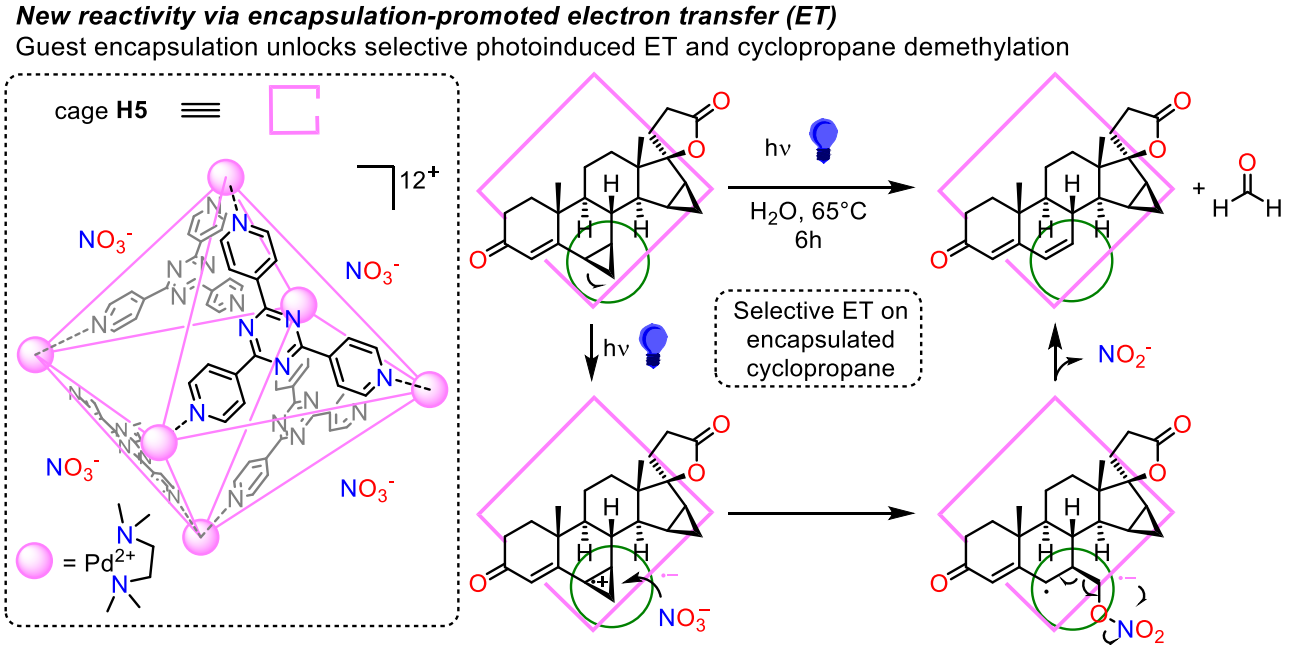

Fig.10. New reactivity (guest-to-host photoinduced electron transfer followed by cyclopropane demethylation) unlocked by encapsulation-induced proximity and stabilization of high-energy, cation-radical intermediates (ref 44).

reactions are usually photo-induced. Irradiation of the host-guest adduct excites one partner (typically the host) and promotes the electron transfer, which then triggers subsequent reactions that thermodynamically drive the whole process.

Host **H5** is photoactive, and can accept electrons from encapsulated guests upon irradiation. For example, it can remove an electron from a cyclopropane moiety, triggering a process that eventually forms a C=C double bond and releases formaldehyde – overall, a formal demethylation of cyclopropanes (Fig. 10).[44] Stabilization of the high-energy radical cation is key to unlock this process that does not usually occur in solution. Remarkably, the reaction is site-selective as it exclusively involves the cyclopropane inside the cage, while another cyclopropane placed outside the cavity is left untouched. Similarly, several photoinduced reactions triggered by electron transfer between guest and host have been developed over the years.[45]

2.2.4 Microenvironment effects. A different strategy to induce divergent reactivity via encapsulation relies on the difference between the microenvironment experienced by confined molecules compared to their typical solvation shell. Given the proximity of a guest to the walls of the nanometric cavity, this microenvironment strongly influences the reactivity of encapsulated molecules.

The hydrophobic cavity of anionic cage **H4** binds small cationic guests in water, such as the iminium terpene derivative depicted in Fig. 11A.[26,46] The folded conformation of the latter favors an Aza-Prins cyclization, that generates a carbocationic intermediate. In bulk solution, this species is rapidly quenched by water to give the product depicted on the left. However, the hydrophobic cavity of **H4** strictly excludes water. Consequently, the reaction follows an unusual path (an elusive [1,5]-hydride shift from an *N*-methyl group) that does not occur in solution. Eventually, the product is released when its positive charge is lost (hydrolysis of the resulting iminium ion), ensuring turnover. Analogous divergent reactivity was observed also in Au-catalyzed cyclizations inside other hydrophobic capsules.[47,48]

The walls of the cavity can take an even more active part in the reaction, triggering unique mechanistic pathways. Raymond and coworkers observed a surprising retention of stereochemistry in the solvolysis of benzylic substrates inside a chiral anionic cage (**H7**, Fig. 11B), independent of the initial substrate chirality.[49] The reaction occurs via a typical S_N2 mechanism, which entails inversion of stereochemistry. In bulk solution, the expected product with inversion of stereochemistry is obtained. However, upon encapsulation in **H7**, the electron-rich aromatic walls of its cavity promote an initial, faster nucleophilic substitution with a first stereo-inversion. The solvent (water or methanol) attacks this intermediate with a second stereo-inversion and yields the product with an overall stereo-retention.

Along a different approach, the walls can also contain reactive groups that are well pre-organized to react with encapsulated substrates.[50] For instance, coordination cage **H8** is decorated with endohedral carboxylic acid groups that create an acidic microenvironment into the cavity. Such acidic cavity catalyzes reactions that do not occur in bulk solution at similar neutral pH, such as the Oxa-Pictet-Spengler one depicted in Fig. 12.[51] The protected aldehyde is exclusively unmasked inside the cavity, triggering the attack by the co-encapsulated alcohol that eventually evolves into the cyclized product.

2.3 Modulation of selectivity

The chance to alter the energy profile of a reaction upon encapsulation can be also used to modulate or even reverse selectivity, favoring the pathway that preferentially leads to one isomer over the other(s). In particular, the shape and size of the

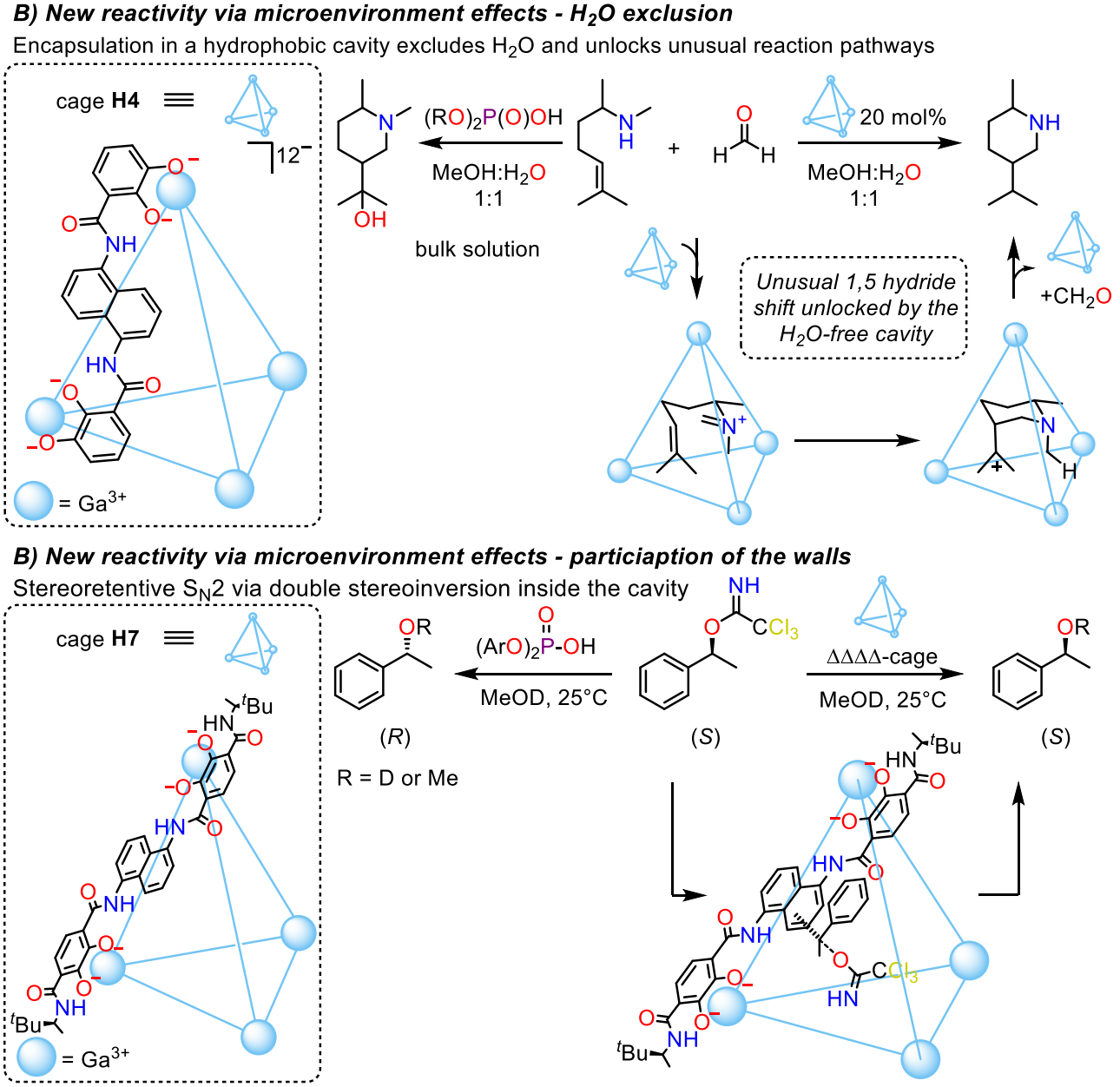

Fig.11. New reactivity unlocked by microenvironment effects: A) Divergent Aza-Prins cyclization enabled by unusual [1,5]-hydride transfer and lack of H_2O inside the hydrophobic cavity (ref 38). B) stereoretentive nucleophilic substitution unlocked by participation of cavity walls in the reaction (ref 49)

cavity modify the relative orientation of encapsulated reactants, enforcing them to follow unusual trajectories of approach. As a consequence, the selectivity of a reaction can be finely tuned by confinement.

2.3.1 Unusual guest orientations. Co-encapsulation of two guests inside a cavity usually fixes their relative orientation to approach the 55% space occupancy[23] and maximize the interactions with the host. This specific orientation can bring together parts of the molecule that are usually less reactive and separate other parts that are typically more reactive. Consequently, the typical selectivity can be altered.

For instance, Diels-Alder reactions with anthracene derivatives usually occur at the most reactive central ring (9,10 adduct; Fig. 13, top). However, Fujita's team reported that hetero co-encapsulation of a substituted anthracene and maleimide in coordination cage **H5** draws the dienophile (maleimide) close to the terminal rather than the central aromatic ring (diene) of a substituted anthracene. Heating up this host-guest adduct leads to an unprecedented cycloaddition on the terminal arene (1,4 adduct), reversing the typical selectivity (Fig. 13).[52] Following this approach, unusual or forbidden selectivities were unlocked in several cycloaddition reactions,[10,20,53] including enantio-selectivity.[54] Remarkably, change of the host structure can lead to orthogonal selectivity – i.e., different cavities furnish opposite isomers of the same product.[55]

2.3.2 Tuning the second coordination sphere of encapsulated catalysts. When a catalyst is confined inside a host, its

New reactivity via microenvironment effects - acidic cavity

The acidic cavity unlocks acetal hydrolysis and cyclization even in usually unreactive conditions

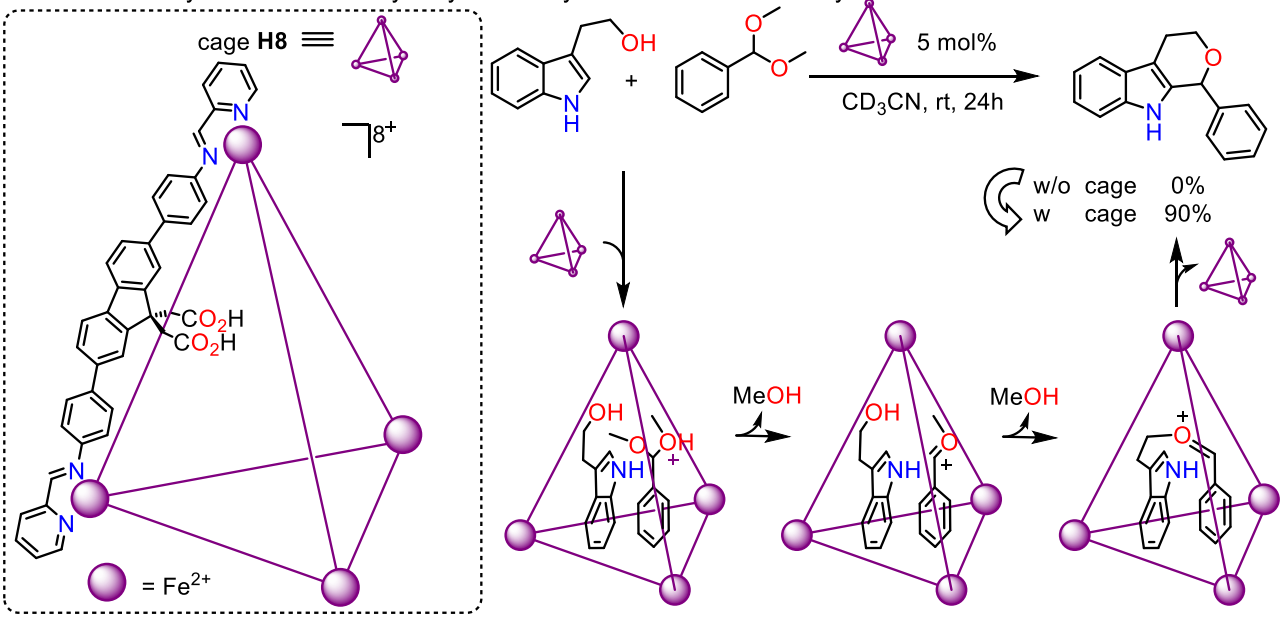

Fig.12. Oxa-Pictet-Spengler reaction enabled by the acidic microenvironment inside **H8** cavity (ref 51).

surrounding environment (second coordination sphere) is substantially altered compared to bulk solution. The limited space available in the cavity and the orientation of its windows forces the substrate to follow specific approach trajectories, which brings near to the catalytic site only specific positions of the substrate or enforce peculiar orientations. The consequence is a substantial alteration of regio-, stereo- and site -selectivity.

Confinement of a Cu^{I} catalyst into the cavity of a cyclodextrin controls the direction of substrate approach, modulating the regioselectivity of alkyne hydroboration (measured as branched/linear ratio, b/l, Fig. 14A). In bulk solution, the linear isomer is strongly favoured (b/l = 5:95). However, the more compact, branched isomer fits better into the cavity and the groove of an *β*-cyclodextrin (**H9**) that contains the catalyst, leading to an opposite, high b/l ratio (91:9).[56] Similar considerations can be applied to regioselectivity tuning via confinement in other reactions, such as olefin hydroformylation[57] or alkyne cyclization.[49,58]

Such a fine control of the approach trajectory can expose only a specific face of the molecule to an encapsulated chiral catalyst, increasing the enantioselectivity. For instance, inclusion of a

Modulation of selectivity via encapsulation

Preorganization of reactants upon co-encapsulation can invert expected selectivity

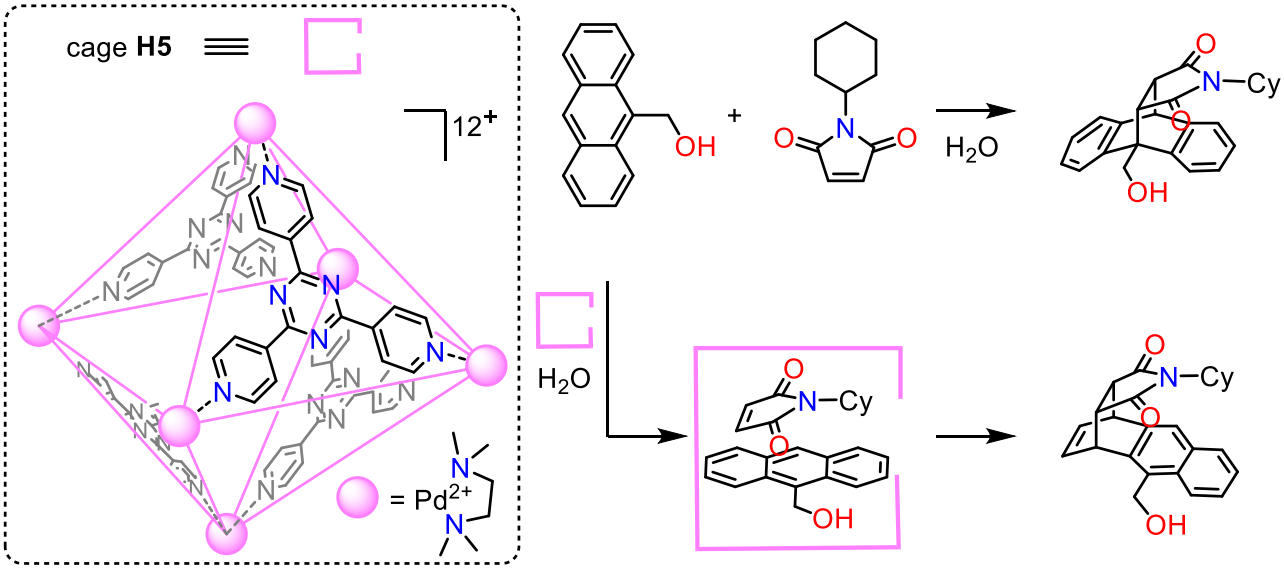

Fig.13. Diverting selectivity upon encapsulation: The selectivity of a Diels-Alder reaction is fully inverted inside cage **H5** (ref 52).

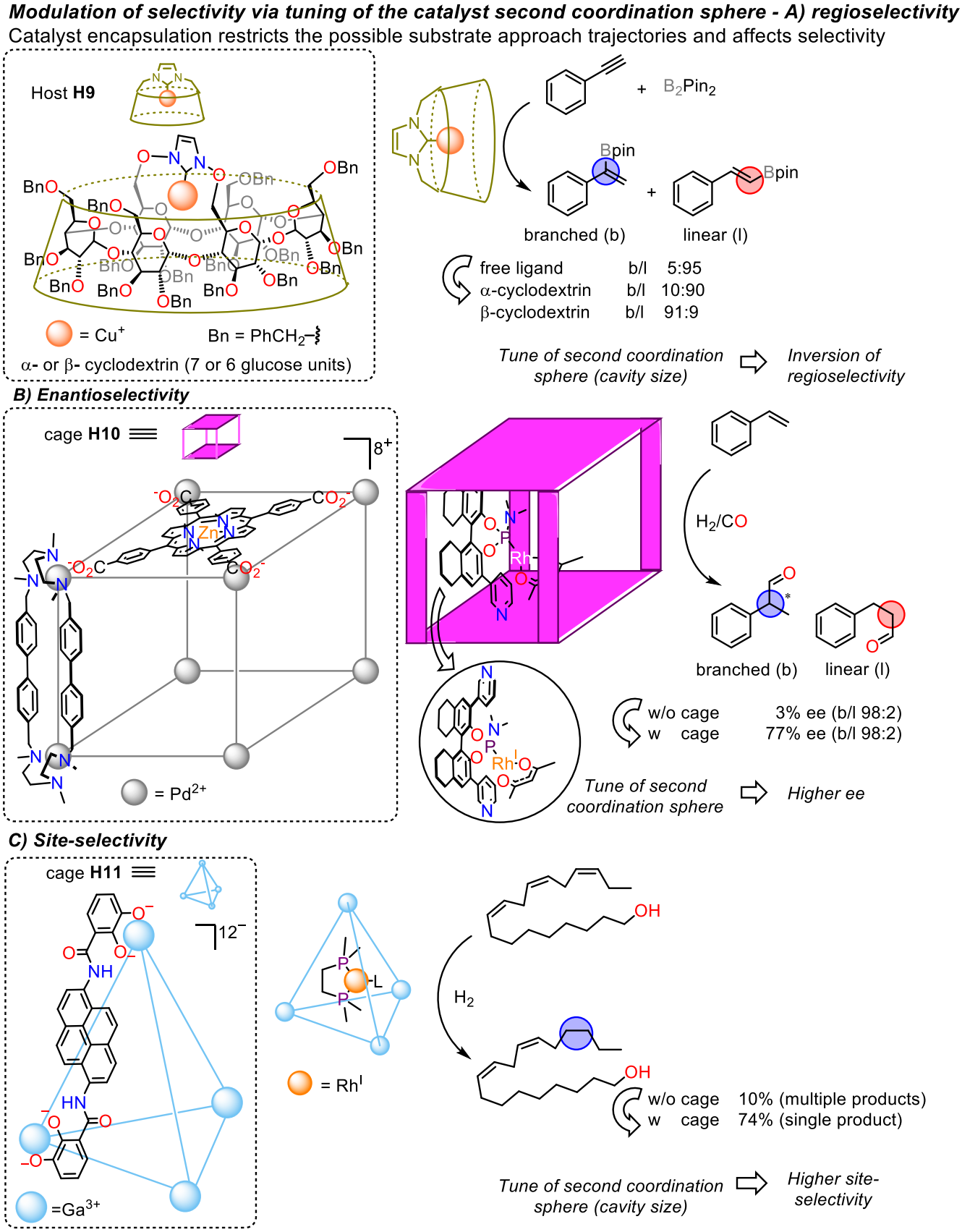

Fig.14. Modulation of selectivity via tune of the second coordintion sphere upon catalyst encapsulation: A) Inversion of regioselectivity controlled by the size and shape of cyclodextrin cavity (ref 56). B) Substantial increase of enantioselectivity upon catalyst encapsulation (ref 59). C) High site-selectivity for the most accessible positions upon encapsulation (ref 61).

chiral Rh hydroformylation catalyst inside coordination cage **H10** forces the substrate to assume specific orientations and leads to a dramatic increase in enantioselectivity from 3 to 77% ee (ee = enantiomeric excess; Fig. 14B).[59] Similar effects were observed also for other reactions.[60]

Finally, the size of the available cavity dictates which position can fit inside together with the catalyst (typically the most accessible sites). For instance, confinement of a Rh hydrogenation catalyst inside anionic host **H11** restricts substrate access only to the less hindered double bond close to the chain tail (Fig. 14C).[61] A related high site-selectivity for the most accessible moieties has been observed also in other reactions.[44]

2.3.3 A supramolecular shadow mask to control selectivity.

When one large guest almost completely fills a cavity, external reactants can approach only the regions of the guest located close to (or outside) the opening of the cavity, while the ones buried inside the host remain inaccessible. Treatment of the host-guest adduct with appropriate reactants results in the exclusive functionalization of the exposed moieties, while the others are left untouched. Hence, the host behaves as a stoichiometric "shadow mask" that shields some reactive positions and directs the transformation on others of comparable reactivity, modulating the typical site- or regio-selectivity of the reaction.

For instance, Fujita's team elegantly used such a non-covalent protection of reactive groups to control site-selectivity in the functionalization of a linear tetraterpene bearing four C=C bonds of comparable reactivity. This linear compound assumes a folded conformation upon encapsulation in **H5** that places three of the four double bonds buried inside the cavity and the terminal C=C moiety in the cage window. As a consequence, addition of peracids or *N*-bromo succinimide exclusively occurs

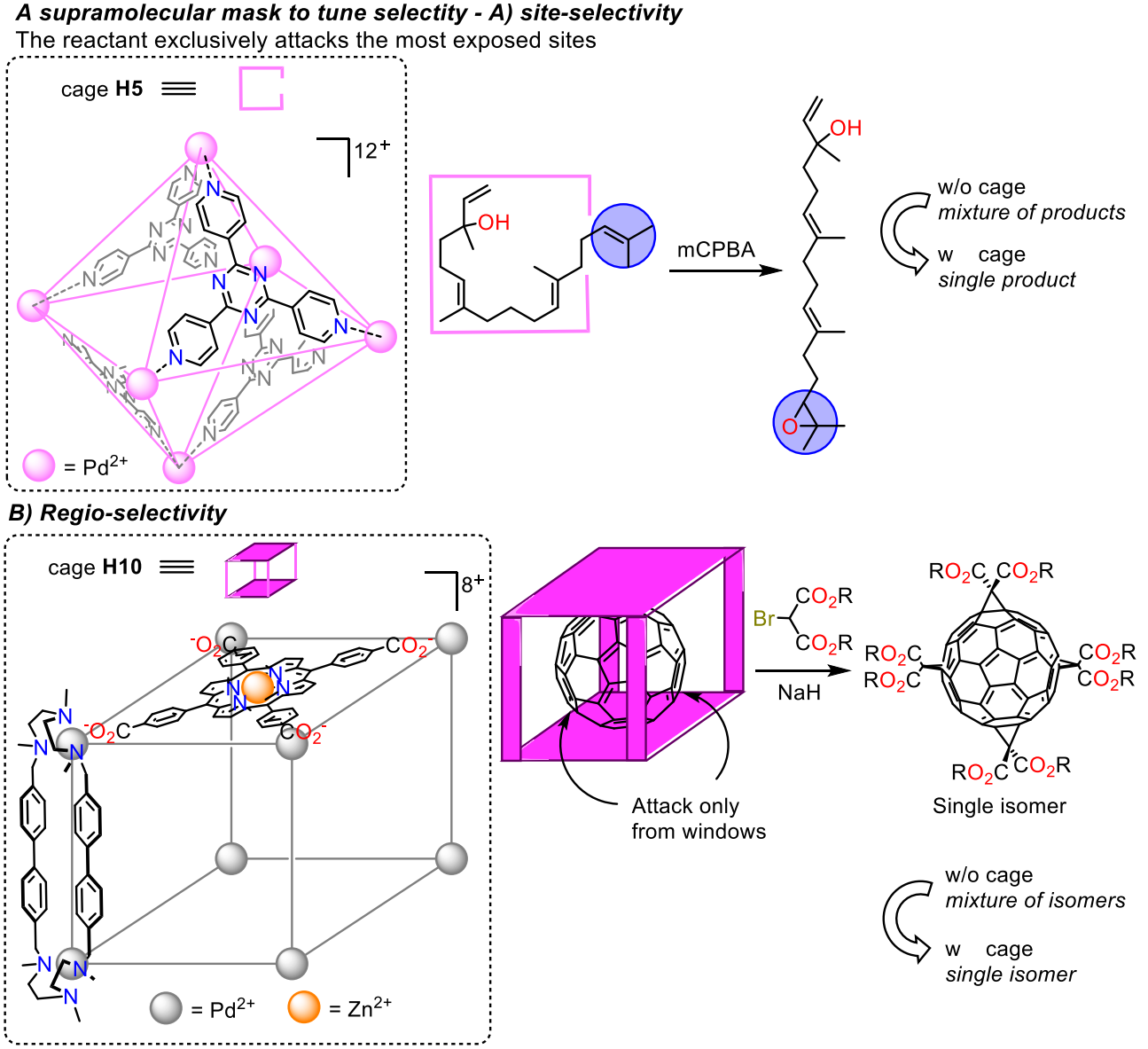

Fig.15. Modulation of site-selectivity via exclusive attack of the reactant on the exposed positions of an encapsulated guest: A) site-selective olefin oxidation (ref 62). B) regio-selective fullerene functionalization (ref 66).

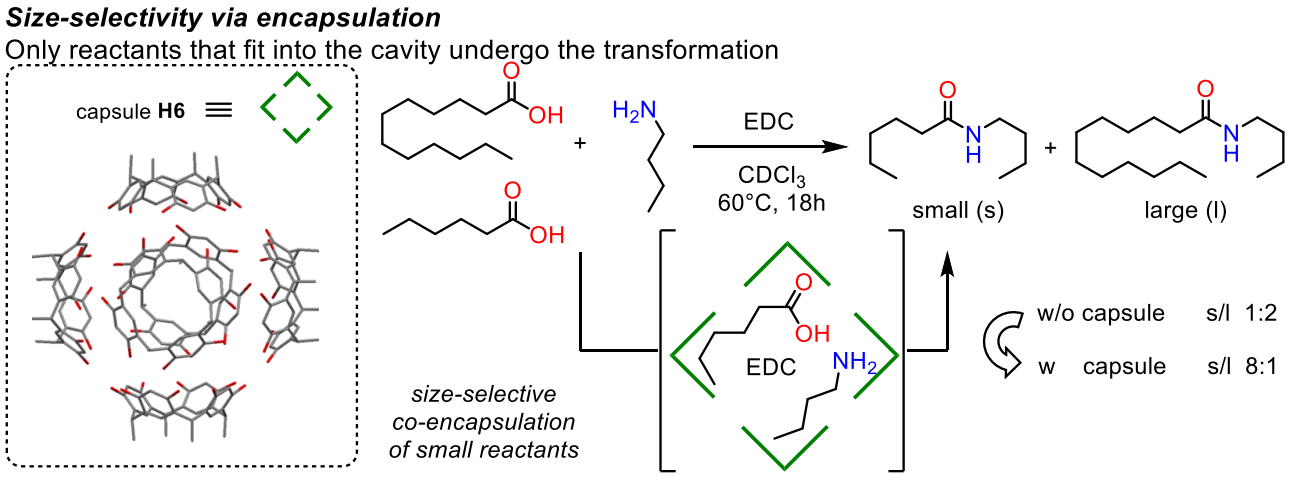

Fig.16. Size-selective coupling of amine and carboxylic acids to yield amides by selective encapsulation of small reactants (ref 68).

on the exposed, terminal double bond, while in bulk solution complex mixtures of products are obtained (Fig. 15A).[62] The same principle was used for other selective mono-functionalization reactions.[13,63,64] Remarkably, even polymers can be modified in a site-selective manner following this approach.[65]

Regio-selectivity can be modulated in a similar way. As an example, Ribas and coworkers recently applied this approach to accomplish a highly regio-selective poly-functionalization of fullerene (Fig. 15B).[66] Fullerene is a spherical molecule with multiple C=C bonds of comparable reactivity; as a consequence, formation of a single, poly-functionalized isomer requires to selectively target only specific positions and stands as an open problem. In fact, reactions in bulk solutions typically afford complex mixtures of regio-isomers, which are difficult to separate. However, when the fullerene is encapsulated inside cage **H10**, the reactants can approach it only from the windows disposed at 90° from one another. The first addition (a Bingel-Hirsch cyclopropanation reaction) occurs on one of the reactive equatorial C=C bonds and fixes the conformation of the mono-adduct inside the cavity, determining which (equatorial) C=C bonds are located close to the remaining windows. Hence, addition of other reactant equivalents selectively occurs at these positions, resulting in the formation of a single isomers for the bis-, tris- or tetra-adduct, respectively. Once the addition is complete, the tetra-adduct product can be displaced by the unsubstituted fullerene, which has a higher affinity for the host. In fact, this "supramolecular shadow mask" strategy, explored also by other groups, promises to be key for the elusive regio-selective functionalization of fullerenes.[67]

2.3.4 Substrate size selectivity. The precise size of the cavity and of its entrance channels imposes a strict filter to the size of the incoming substrates. In other words, the reactants need to fit into the cavity and its openings (windows) for the reaction to proceed, and therefore large molecules are excluded and do not react. This property enables the selective functionalization of a specific substrate among others of comparable reactivity but different size, i.e. size-selective reactions. Selection of a specific reactant is key for the functionalization of mixtures without previous separation and is a typical property of enzymes but remains challenging for conventional synthetic catalysts operating in bulk solution.

For instance, in water, the cavity of the hexameric resorcinarene capsule **H6** can host an amide coupling reactant (EDC) and only small coupling partners (amine and carboxylic acid). Thus, when multiple substrates of different size are added into the reaction mixture, the large ones are excluded and do not react, while the smaller ones are selectively converted into the amide product (Fig. 16).[68] The same principle has been applied to a large number of reactions,[69] and additional information can be found on more specific recent reviews.[70,71]

2.3.5 Product shape selectivity. Finally, a different strategy to control selectivity in chemical reactions exploits the defined shape of a cavity as a mold to define the shape of amorphous compounds formed in its interior. Confinement of an assembly process (typically nanoparticle growth) forces the aggregates to assume shape and size complementary to those of the cavity. As a consequence, the resulting nanoparticles have uniform and defined dimensions – i.e., are essentially monodisperse.[72]

Cage **H12** was used to control the shape and size of Pd nanoparticles (Fig. 17).[73a] The aniline nitrogens inside the cavity coordinate Pd salts. Then, addition of a reductant ($NaBH_4$) triggers Pd^{II} reduction and nanoparticle nucleation inside the cavity. The aggregate grows until it occupies all the available volume, assuming a defined shape and size complementary to the cavity which acts as a mold. As demonstrated in several reports,[73] the application of this strategy allows the synthesis of highly monodispersed nanoparticles with peculiar surface area that displays superior catalytic activity compared with those produced by conventional methods.

2.4 Catalyst site isolation

Confinement of reactants inside a cavity isolates them from the bulk solution. Transient, reactive species are therefore protected from the outside environment and can be stabilized enough to be observed or manipulated.[74] Analogously, encapsulation of a catalyst can protect it towards degradation processes that are spontaneous in bulk solution, enhancing

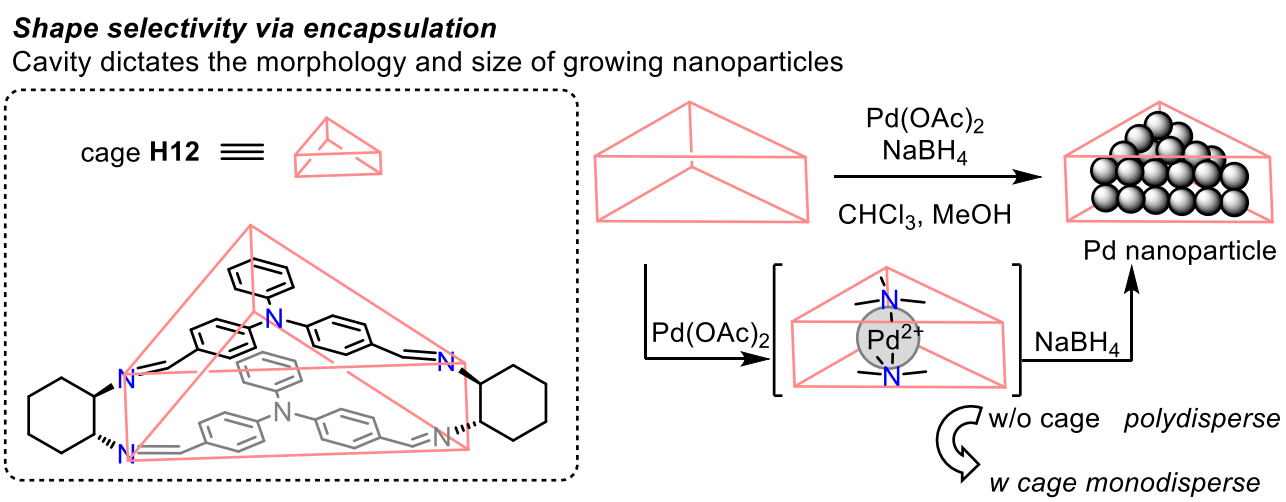

Fig.17. Formation of regular nanoparticles with a precise shape by localization of the nucleation and growth process inside a capsule (ref 73a).

both its activity and its tolerance to different reaction conditions.

2.4.1 Catalyst protection. Confinement has been long known to protect reactive, transient species by preventing access to external reactants, including air or water.[74] The same concept can be applied to catalysis. Encapsulation of an unstable catalyst can prevent or slow down its degradation, increasing its lifetime and its activity. This is especially effective when the decomposition pathway entails formation of dimers or reactions with the outside media.

For instance, Mn-porphyrin oxidation catalysts tend to deactivate via the formation of inactive μ-oxo dimers. However, encapsulation of these systems inside a cavity avoids the contact between two Mn-porphyrin units and prevents catalyst degradation. As a consequence, the catalytic activity of an epoxidation catalyst (its Turn Over Number, TON) undergoes a >20-fold enhancement – from 10 to 235 - upon encapsulation in cage **H13** (Fig. 18).[75] Similar considerations can also be applied to other catalysts,[76] and can be used to retain the activity of a catalyst even in an incompatible solvent (i.e. organometallic complexes in water).[77]

2.4.2 Sequential catalysis. Protection of an encapsulated catalyst from bulk solution unlocks the combination of incompatible catalysts to carry out sequential one-pot reactions on the same compound – i.e. sequential catalysis. This is what happens in living cells, where compartmentalization of enzymes (localization of different catalyzed reactions in separated environments) and control of substrate access allows multiple reactions to occur in sequence and converts simple starting materials into sophisticated products in a sort of assembly line. Catalyst protection via encapsulation enables artificial systems to display a similar behavior.

Fujita's group demonstrated that compartmentalization can be also transferred to the field of supramolecular catalysis. They anchored two incompatible catalysts, TEMPO and an imidazolidone-based Diels-Alder catalyst, to two different giant coordination cages (**H14** and **H15**, respectively, Fig. 19).[78] In the absence of confinement, oxammonium derived from oxidation of TEMPO oxidizes imidazolidone and prevents any reaction. However, encapsulation of the two catalysts unlocks an elegant cascade process to occur in one pot. Initial alcohol oxidation inside **H14** followed by a stereoselective Diels-Alder cyclization in **H15** affords a bicyclic product in good yield and excellent

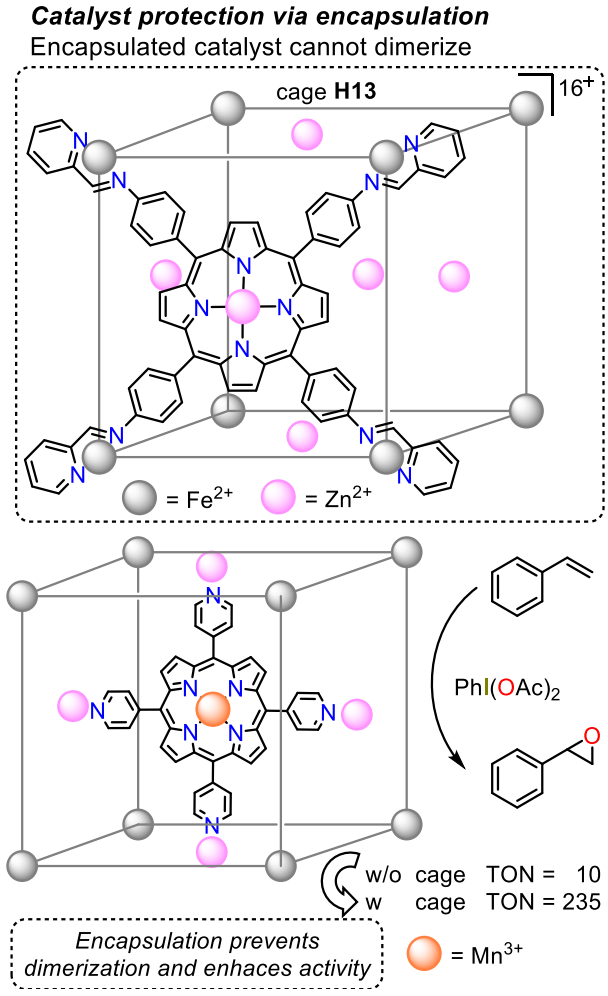

Fig.18. Improvement of catalytic activity (Turn Over Number, TON) by encapsulation that prevents degradation processes (ref 75).

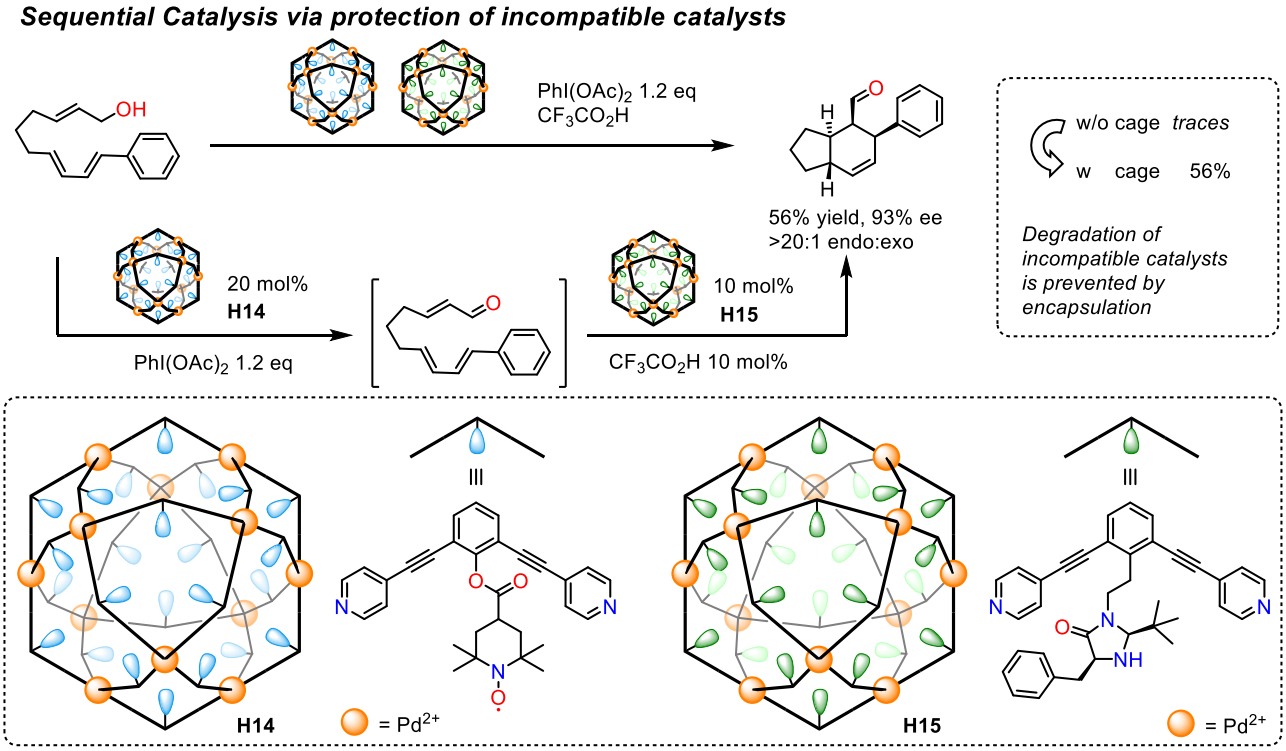

Fig.19. Sequential catalysis unlocked by localizing two incompatible catalysts into giant cages **H14** and **H15** that prevent their contact (ref 78).

stereoselectivity. Similar, elegant cascades that rely on typically incompatible catalysts have been described also by other groups.[77,79]

3 Recognition-driven Catalysis

When a reactant (the substrate) is bound to a supramolecular catalyst, an intermolecular reaction (reactant-catalyst) is converted into an intramolecular (intra-complex) one[17d] and the reaction rate can be greatly increased. In addition, pre-association may also offer a unique chance to control the selectivity of the reaction. The recognition event pre-organizes the catalyst-substrate adduct, drawing only a specific (or few) reactive position of the substrate near the catalytic centre.[80] This position is selectively functionalized even in the presence of multiple ones of comparable reactivity as long as the formation of the cycle-shaped transition state does not develop strain and/or require freezing the rotation about too many single bonds.[17] The transition state of the intra-complex reaction has indeed a pseudo cyclic skeleton whose structure consists of both covalent and supramolecular interactions (Fig. 18). Proper rationalization and quantification of such acceleration / selectivity can be again based on effective molarity (EM, see also section 2.1) provided that an intermolecular model reaction is available.[17d] The use of weak, labile supramolecular interactions for substrate recognition may then allow the facile release of the product after the reaction, ensuring catalytic turnover.[80,81] If the reaction product maintains affinity for the catalyst, the transformation may be product-inhibited. However, if the rate of the binding/dissociation process is higher or at least comparable to that of the catalysed reaction (reversible formation of labile bonds) and the association is not too strong, fast turnover and high catalytic activity are feasible. Indeed, recognition of substrate and transition state is key to the enzyme outstanding levels of activity and selectivity and has long been recognized as a powerful strategy for artificial catalysts.[81,82]

In this section, we describe a number of strategies to overcome the challenges of site-, regio-, stereo-, and substrate-selectivity with the tools offered by supramolecular chemistry (graphical index in Fig. 20). From a practical standpoint, the design of these supramolecular catalysts usually consists in the decoration of an already effective conventional catalyst with a supramolecular receptor such as urea, amide,[83] borolane,[84] crown-ether[85] and cyclodextrin[86] units connected through a fairly rigid spacer. We focus our discussion on works where the catalyst-substrate interaction i) occurs at a specific site (i.e. the recognition site) that is different from the catalytic centre and ii) has been investigated with some level of detail.

3.1 Geometric site-selectivity

Site-selectivity is the ability to preferentially transform a given functional group present in a molecule in the presence of others of the same kind.[87]

When such groups are present in a large number and display a similar intrinsic reactivity, conventional, undirected reactions usually afford mixtures of products. The benefits that a supramolecular approach brings to the table are clear. Pre-association of a substrate to the catalyst dictates which sites are exposed to the catalytic centre, allowing to single out and target a specific function at a precise distance from the binding site (geometric site-selectivity).[80] As a result, the

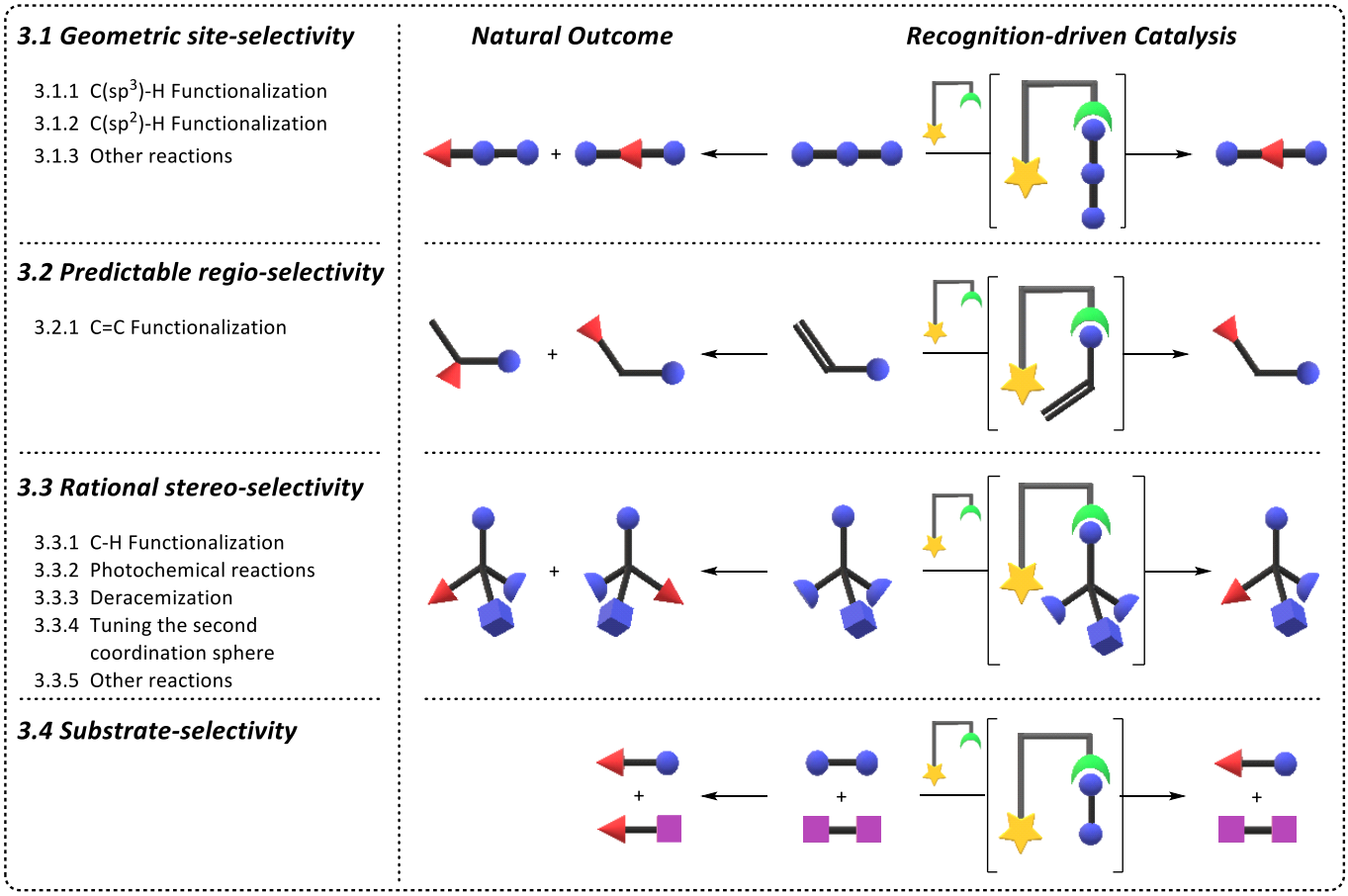

Fig. 20. Graphical summary for section 3 – Recognition-driven catalysis. In all cases, the catalysed reaction passes for a cycle-shaped transition state.

reaction is steered towards the production of a specific isomer even if the affected position is not the most intrinsically reactive in the molecule. This approach is especially attractive for the selective functionalization of the ubiquitous and scarcely reactive C-H bonds.

3.1.1. C(*sp*³)-H Functionalization. Achievement of a full control over hydrocarbon functionalization is one of the most sought-after goals in modern organic chemistry.[1a,88] C-H bonds are by far the most common bonds in organic compounds, therefore, the capability of selectively and predictively replacing one of them with another functional group would turn almost any organic molecule into a versatile building block, leading to a substantial simplification of many of the current synthetic routes.[88c] C-H positions with similar electronic and steric environments exhibit a comparable intrinsic reactivity[88a,89] making selective functionalization extremely difficult. Electronic, steric, stereoelectronic and medium effects can sometimes greatly activate or deactivate C-H bonds allowing for a certain degree of site-selectivity when appropriate reactants and conditions are employed,[1,88c,89,90] but targeting a C-H bond that is not the most reactive one usually remains an open challenge. This is particularly true for the positions located far away from other functional or directing groups (remote sites). In fact, direct remote functionalization remains elusive and alternative, complex synthetic routes must usually be designed to obtain the target molecule. A supramolecular, geometric approach can provide a way to overcome these challenges and virtually target any C-H bond in a substrate, disclosing new perspectives for C-H functionalization.

The Breslow group pioneered the use of supramolecular recognition to control site-selectivity in C-H oxidation using a bioinspired, geometry-based, supramolecular approach.[80,91] One of the earliest examples dates back to 1997, when the Mn porphyrin catalyst **C1** (Fig. 21) was endowed with four cyclodextrin binding sites which host *tert*-butylphenyl moieties *via* hydrophobic interactions in water. Binding of two of these apolar groups (G) located at both ends of a steroid substrate places the C6-H equatorial bond over the iron centre, enabling its exclusive hydroxylation, albeit with low turnovers (TON = 4). Furthermore, the over-oxidation to ketone is prevented since the axial C6-H bond points away from the catalytic centre. In stark contrast, undirected oxidation affords a complex mixture of products.[92] Later, different catalyst designs were explored leading to a much improved catalytic activity[93] and, in one case, to a shift of the oxidation site-selectivity on the same steroid.[94] Since this pioneering work, several advancements have been made, mainly devoted to a change and a simplification of the binding site (notably by Crabtree, Brudvig and co-workers[95]), and have been recently reviewed.[96]

In 2017, Olivo, Di Stefano, Costas and co-workers developed a supramolecular catalytic system for the selective, remote C-H

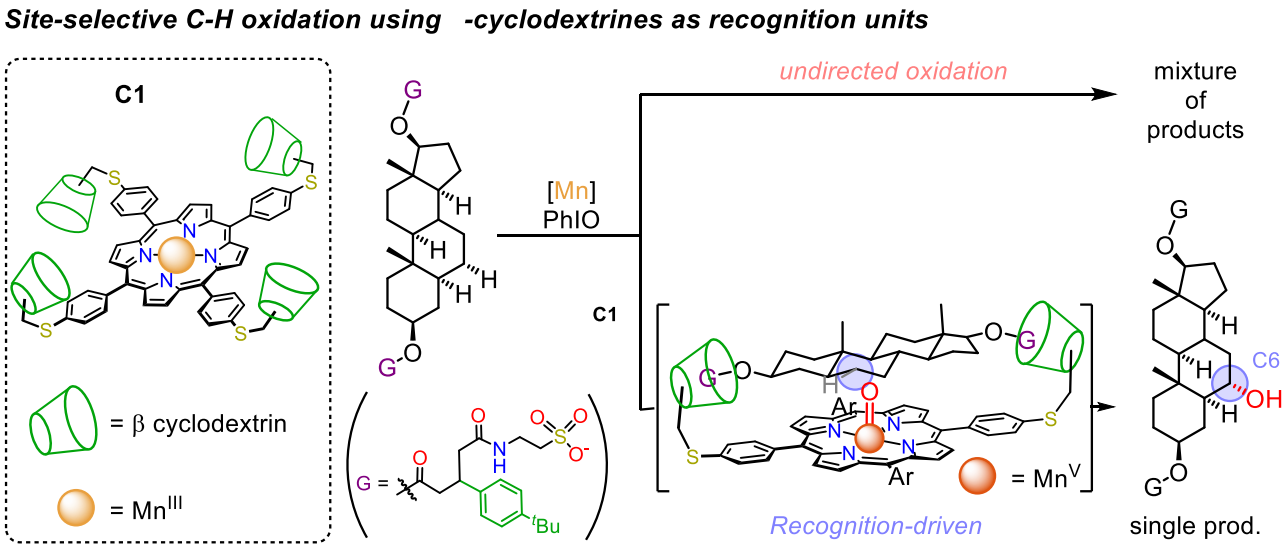

Fig. 21. Porphyrin-based catalyst **C1** and its use in the recognition and selective functionalization of a steroid substrate (ref 92).

oxidation of protonated aliphatic amines[97] (**C3,** Fig. 22). An iron or manganese complex based on the highly efficient pdp catalytic core[98] was endowed with benzo-18-crown-6 receptors to recognize the heads of primary, linear alkylammonium chains. The recognition pre-organizes the substrate to place the methylenes C8 and C9 (C1 being the CH_2-NH_3^+ one) close to the metal centre. The oxidation mainly occurs on the remote positions C8 and C9 of several alkylammonium tetrafluoroborate salts independently of their chain length, overriding intrinsic reactivity patterns even in these highly flexible systems. Later, a complementary selectivity (C3 and C4) on the same alkylammonium substrates was reported by Tiefenbacher *et al.*, who used a tweezer-like pdp-based supramolecular catalyst **C4** (Fig. 22). In this case, the shorter distance between the receptor and the catalytic center reverses the natural reactivity order of the methylenes on the chain enabling a selective oxidation of positions C3 and C4 that are strongly deactivated by the proximal positive charge.[99] Catalysts **C3** (M = Fe or Mn) were also shown to oxidize the C-H bonds of different steroids at remote D-ring with a high site-selectivity (>80%), modifying the innate selective of the reaction.[100] This selectivity can be predicted *a priori* via NMR analysis of the geometry of the catalyst-substrate adduct and is consistent with the one observed for linear amines (*i.e.,* C8 or C9 sites). Moreover, the inversion of catalyst chirality allows a fine tuning of the reaction site-selectivity, shifting the oxidation from one of the secondary position to the other in the same D-ring.

3.1.2. C(sp^2)-H Functionalization. Like aliphatic C-H bonds, aromatic C(sp^2)-H bonds often display similar reactivities and are therefore challenging to target in a selective fashion. This can be seen in the case of C-H borylation. The undirected reaction usually occurs at the most sterically accessible C-H bonds, rarely allowing to discriminate between the meta and para positions of a substituted arene (Fig. 23A).[101] Given the relevance of the resulting arylboronic esters as building blocks for Suzuki-Miyaura cross-coupling reactions,[102] the development of methodologies for site-selective C-H borylation is extremely attractive. A supramolecular approach was also shown effective in this field by several research groups.[103] The same catalytic core (Ir bipyridine) was equipped with different recognition units in order to vary the geometry of the catalyst-substrate adduct effecting the meta, ortho, or para borylation of different arenes.

In 2015, Kuninobu, Kanai and co-workers decorated an Ir bipyridine-based catalyst with a urea moiety. Such receptor could recognise aromatic amides and phosphonamides via hydrogen bonding and direct the borylation reaction towards the meta position (m/p increased from ~1:1 to >30:1; Fig. 23B).[104] Later, the scope of meta functionalization employing bipyridine-based ligands was greatly expanded by the Phipps[105] and Nakao groups (Fig. 23B).[106] Decoration of the same bipyridine ligand with a dioxaborolanyl ring allowed Kuninobu *et al* to perform the ortho-selective borylation of methylarylsulphides exploiting the Lewis acid-base interaction between the electron-deficient boron centre on the ligand and the sulphur atom in the thioanisoles to properly orient the substrate (Fig. 23B).[107] The Reek group was later capable of using hydrogen bonding interaction to obtain the ortho-borylation of (hetero)aromatic amides (Fig. 23B).[108] Finally, the Chattopadhyay group installed a 2-quinolone moiety on the same ligand and used its metal salt to recognise the carbonyl of ethyl benzoates, orienting the substrates to obtain para-selective borylation (Fig. 23B).[109]

Remarkably, the simple structure of the above supramolecular catalysts paves the way for practical use of these systems in preparative processes. A detailed review on these reactions can be found elsewhere.[103,110] A different strategy to increase the steric environment around the substrate and direct the reaction towards the most accessible *para* position relies on Lewis-base or electrostatic interactions between a functional group and a cofactor (a bulky counter-ion or Lewis acid) (Fig. 23C).[111] The inclusion of a supramolecular binding site is not limited to iridium catalysts but can also be expanded with Pd catalysed C-H activation.[112]

Recognition-driven C-H oxidations with Pdp-based supramolecular catalysts

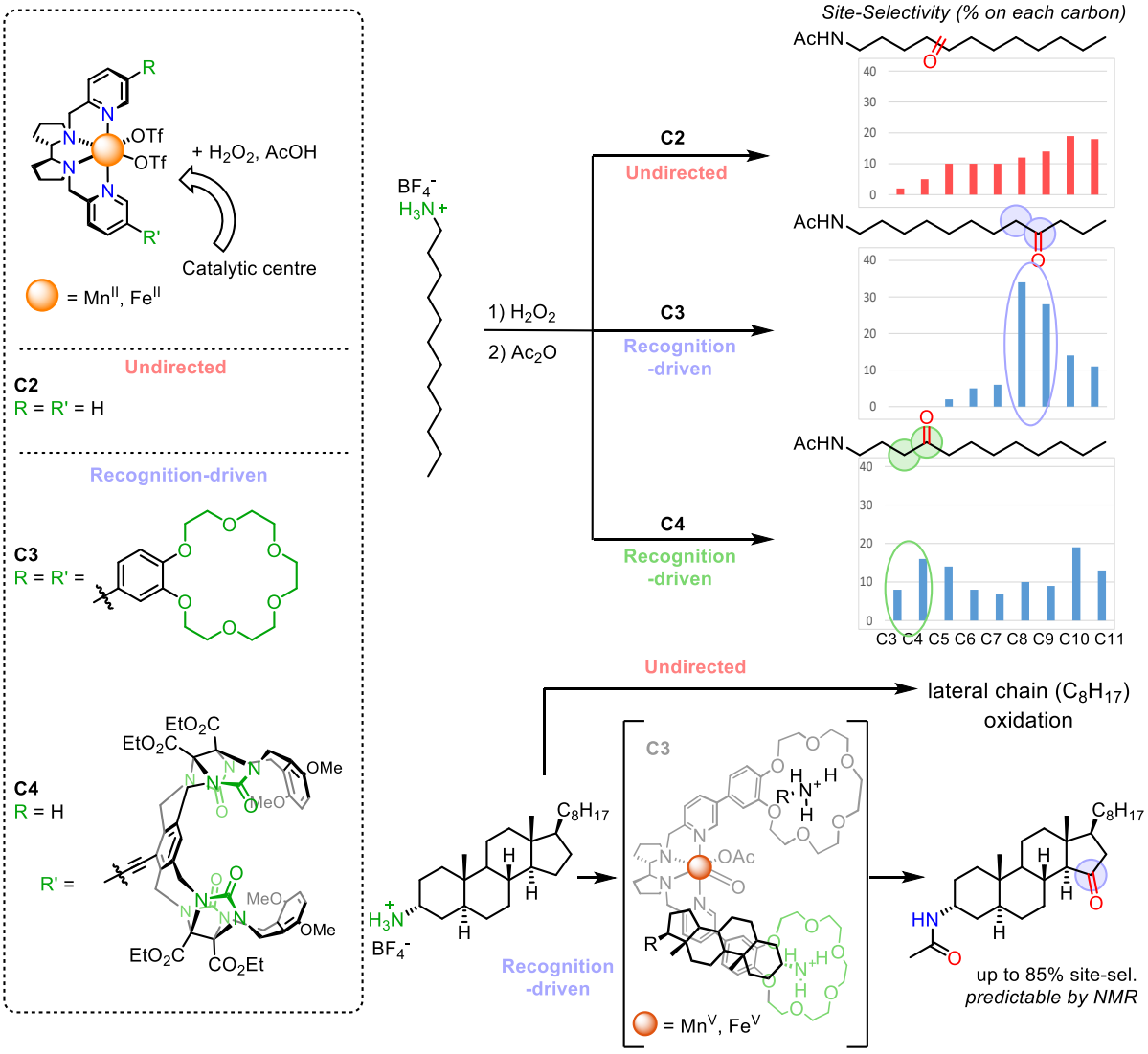

Fig. 22. Use of pdp-based catalysts in the site-selective oxidation of alkylammonium chains and steroid substrates. (refs 97, 99 and 100).

3.1.3. Other reactions. The geometric, supramolecular approach to site-selectivity has also been extended to reactions other than C-H functionalization. For instance, a site-selective epoxidation of poly-olefins (terpene derivatives) was attained by the Miller group using aspartate-containing peptide catalysts **C6** or **C7** and H_2O_2 (Fig. 24).[113,114] The carboxylic acid and H_2O_2 are condensed with *N,N'*-diisopropylcarbodidimide (DIC) to form peracid intermediates, which in turn mediate the epoxidation. Recognition of the alcohol moiety by hydrogen bond partners in the peptide pre-organizes the substrate and allows the selective epoxidation of one of the C=C bonds, with a high enantioselectivity in one case.[114] Similarly, supramolecular recognition was also employed in the site-selective cross coupling of dichloroarenes, in which the metalation is directed towards one of the two reactive C-Cl bonds.[115]

3.2 Predictable regio -selectivity

A regio-selective reaction is a process that effects the preferential making (or breaking) of a chemical bond at a specific atom of a functional group.[116] As an example, the addition of hydrogen halide to a monosubstituted alkene is usually regio-selective and follows the Markovnikov's rule. In several cases, altering the intrinsic regio-selectivity of a reaction with conventional strategies is challenging and requires extra steps or different reactants. On the other hand, the geometry-based approach of supramolecular chemistry offers an opportunity to elegantly modulate or even reverse this preference.

3.2.1 C=C Functionalization. Olefin hydroformylation is a process of significant industrial relevance and is catalysed by Rh-phosphine complexes. Terminal alkenes are converted in a mixture of linear (l) or branched (b) aldehydes, with a low preference for one isomer over the other.[117] Since the rate- and selectivity-determining step is the hydrometallation, a precise control over the position of the substrate double bond in this step can alter the regio-selectivity of the reaction. In 2008, Breit and co-workers showed that the l/b ratio for the rhodium-catalysed hydroformylation of vinylacetic acid could be largely

Undirected and directed Ir catalyzed aromatic C(sp^2)-H Borylation

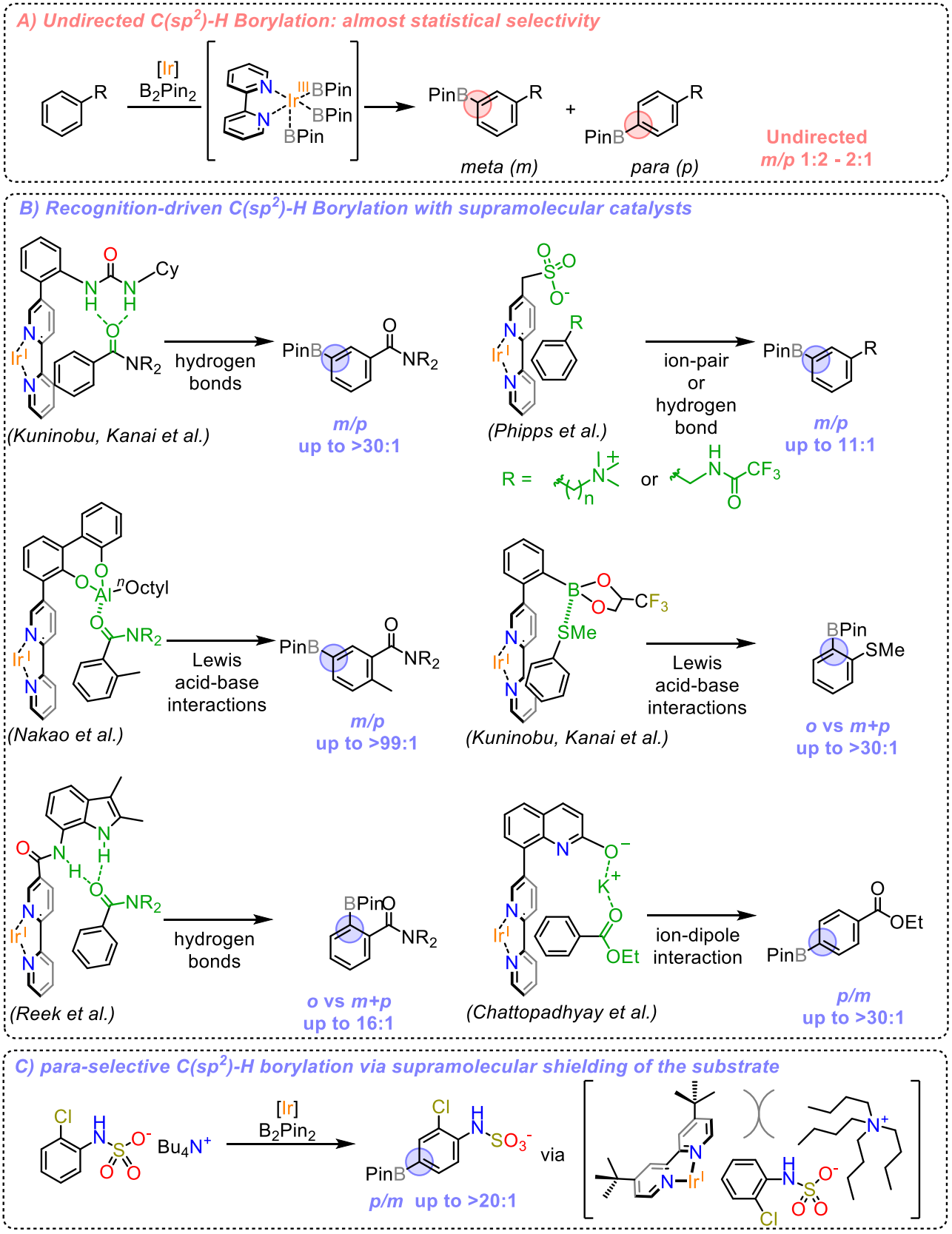

Fig. 23. (A) Undirected, non-selective, C(sp^2)-H borylation. (B) *meta*, *ortho* or *para* borylation arenes enabled by bipyridine-based iridium catalysts functionalised with various supramolecular directing groups (refs 104-109). (C) *para*-selective borylation *via* supramolecular shielding of the substrate (ref 112).

Terpene derivatives site-selective epoxidation with peptide-based catalyst

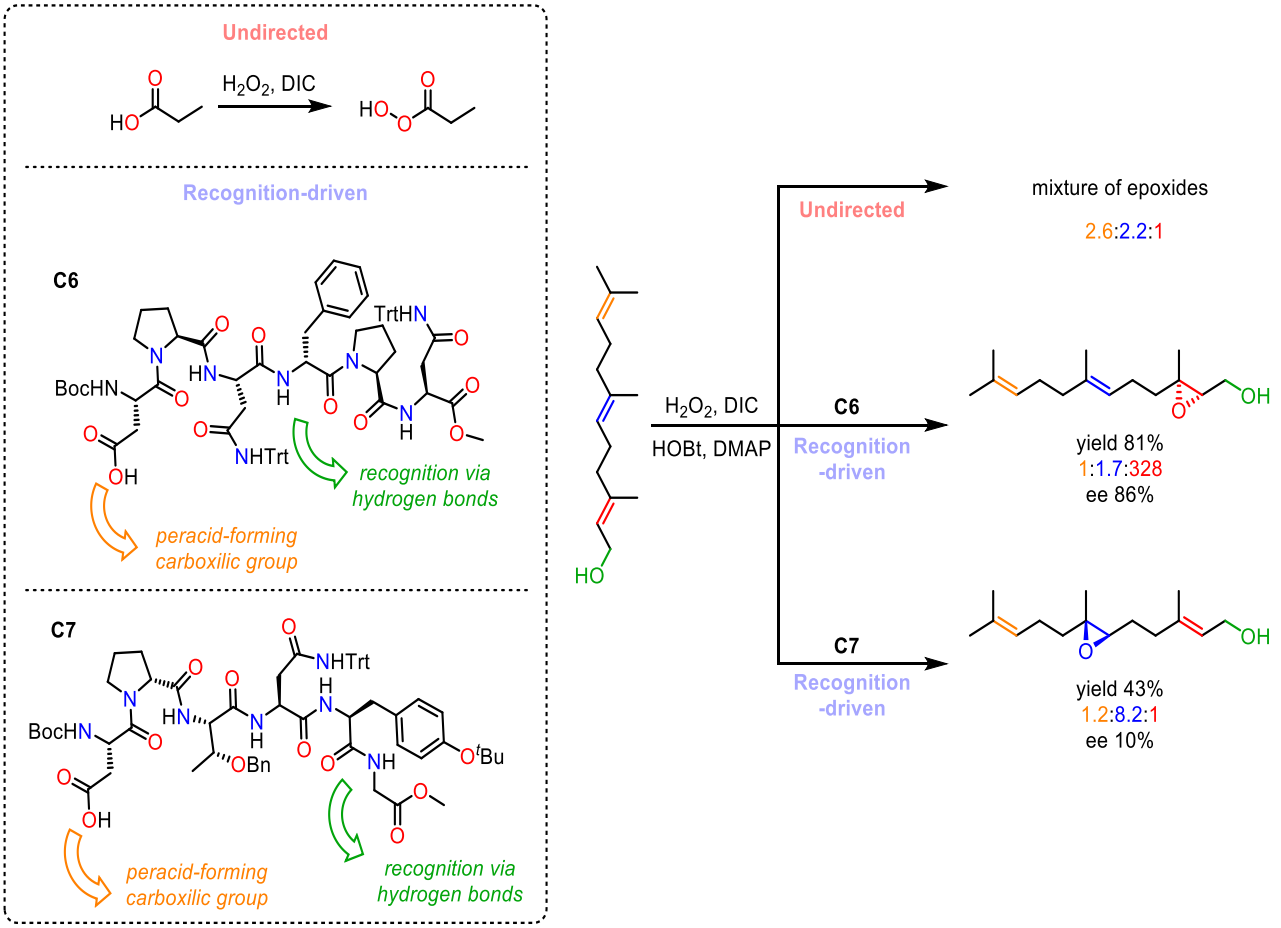

Fig. 24. Peptide-based catalysts employed for the site-selective oxidation of terpenoid alcohols (ref 113). Trt = triphenylmethyl.

improved via recognition of the carboxylate present in the substrate by a guanidinium motif installed on the ligand (Fig. 25).[118] In the presence of the simple triphenylphosphine ligand (catalyst **C8**), hydroformylation of vinylacetic acid is not regio-selective (l/b = 1.5), but use of supramolecular catalyst **C9** accelerates the reaction and selectively furnishes the linear product (l/b = 23; Fig. 25).[118] Later, the reaction was extended to internal alkenes.[119] However, longer terminal alkenes do not fit properly in this catalyst. Reek and co-workers designed the related Rh catalyst **C10** endowed with a receptor for carboxylates and phosphates that engage in multiple hydrogen bonding with four N-H groups (Fig. 25). In this case, the distance between the binding and the reaction site is longer, but catalyst **C10** is still highly regioselective for the linear product (l/b > 50:1).[120] In fact, different linkers between the olefin and the acid are tolerated, as long as they are not too short (i.e., vinyl acetic acid does not fit properly and the reaction displays a low regio-selectivity). Remarkably, a recent report shows that moving the recognition group further away in the backbone of catalyst **C11** allows to control the hydroformylation regioselectivity on C=C bonds located as far as 10 carbon atoms away (Fig. 25).[120e] Further details on recognition-driven hydroformylation can be found in a recent review.[121]

3.3 Rational stereo-selectivity

The binding of a symmetric substrate to a chiral supramolecular catalyst can differentiate two (or more) enantiotopic positions, allowing an improved enantio-selective functionalization. Conventional asymmetric catalysis typically relies on bulky, chiral species that selectively shield one face of the substrate from the approach of a reactant *via* repulsive, steric interactions (the TS for the formation of one enantiomer is destabilised with respect to the other).[122,123] In contrast, the use of supramolecular attractive interactions to control enantioselectivity often entails the selective stabilization of the TS leading to the desired product. Moreover, supramolecular recognition can simultaneously control stereo-selectivity and site- or regio-selectivity, greatly increasing the attractiveness of this approach. In this section we describe some recent asymmetric catalysts that rely on well-defined supramolecular interactions.

3.3.1 C-H Functionalization. The similarity of many of the C-H bonds typically present in organic compounds makes asymmetric C-H functionalization an even more challenging reaction, especially when the reaction implies distinguishing the two faces of the same methylene group. However, significant advances have been recently made,[123] and supramolecular recognition is emerging as a key strategy in this regard.

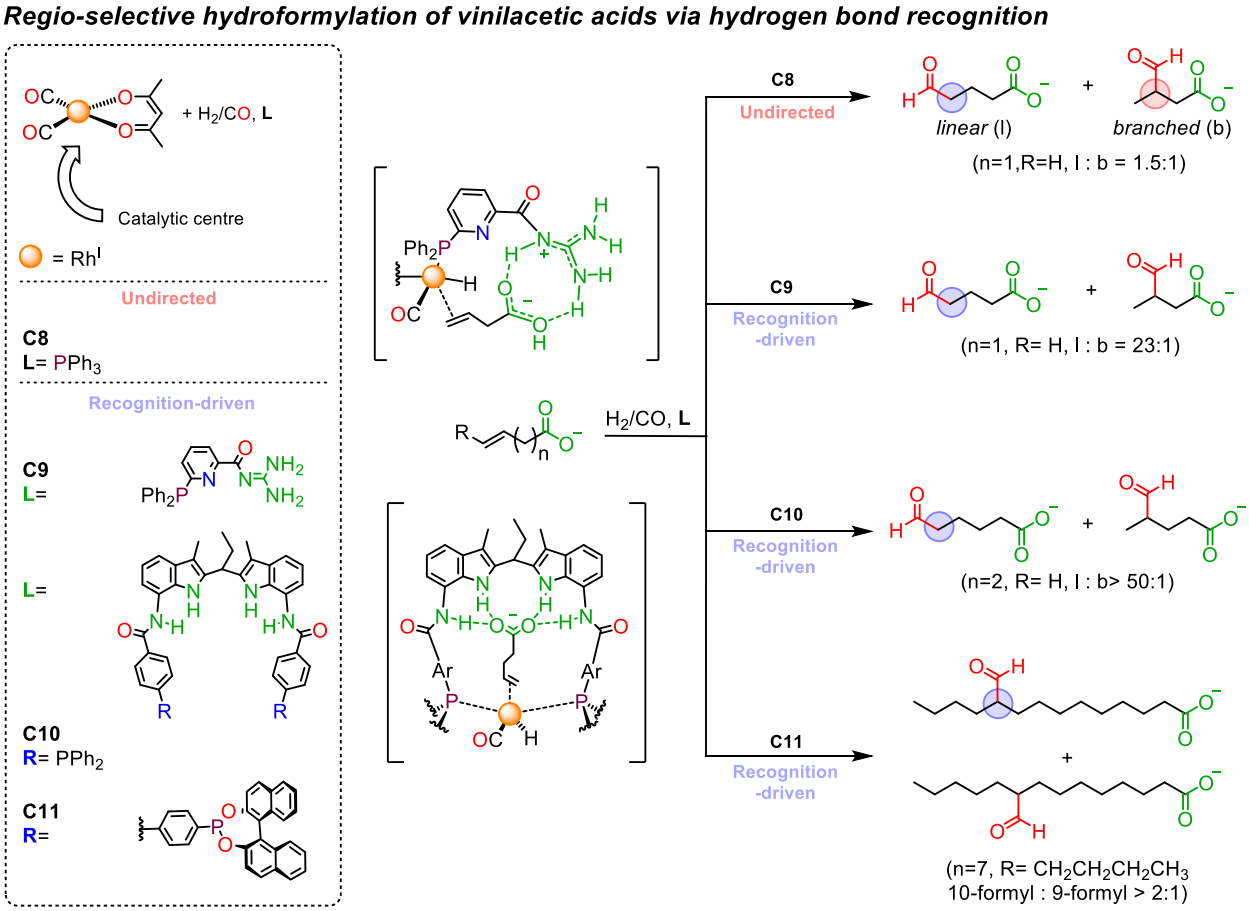

Fig. 25. Regio-selective hydroformylation of vinylacetic acid enabled by supramolecular recognition of the carboxylic acid moiety (refs 118-120).

Of particular note is the site- and enantio-selective borylation of aliphatic γ-C-H bonds with B_2Pin_2 recently reported by the Sawamura group. They designed an iridium catalyst (**C12**, Fig. 26) bearing a urea-containing pyridine recognition ligand (**RL**) and an asymmetric phosphite ligand (**L**).[124] The relative orientation of the two ligands is fixed by pyridine-naphthol π-π stacking. When the carbonyl function of the substrate engages in hydrogen bonding with the urea moiety, the substrate is forced by the chiral phosphite to assume a conformation where only one of the enantiotopic γ methylene C-H bonds is exposed to the metal centre. As a consequence, the C-H borylation occurs in a highly site- and enantio-selective fashion (>90% ee). Supramolecular recognition also allowed the development of an asymmetric version of other C(sp^3)-H functionalization reactions. Bach and co-workers designed a chiral receptor for secondary amides made up of a rigid lactam with a U-turn structure (Fig. 27). Binding of a rigid substrate to this receptor *via* complementary hydrogen bonding places one of the two enantiotopic faces close to the catalytic centre, allowing the asymmetric functionalization (Fig. 27). For instance, the Mn porphyrin catalyst **C13** in Fig. 27 catalyses the asymmetric C-H oxidation of enantiotopic methylenes in *spiro* compounds[125] and even the enantioselective hydroxylation of benzylic methylenes.[126] An analogous design was used also in asymmetric C-H amination of quinolone derivatives catalysed by silver[127] (**C14**, Fig. 27) and rhodium[128]complexes.

3.3.2 Photochemical reactions. Supramolecular recognition also proved its worth as a tool to induce chirality transfer in photochemical reactions. Photocyclization is a useful reaction for the stereoselective functionalization of olefins, since it can produce complex molecules with multiple stereo-centres in a single step.[129] The Bach group pioneered the use of supramolecular interactions in the field.[83b,130] They anchored the chiral lactam recognition unit described before (**L**, Fig. 27) on a benzophenone moiety, enabling formation of a chiral catalyst-substrate adduct (**C15**, Fig. 28). Irradiation with light at the proper wavelength promotes a photoinduced hydrogen atom transfer (HAT), which ultimately leads to the spiro-cycle with high enantiomeric excess.[130] A similar catalyst allowed the production of [2+2] cycloadducts with high enantio- and diastero-selectivity.[131] The reaction was found to be general for a broad range of substrates.[132]

3.3.3 Deracemization. More recently, supramolecular recognition by a chiral photosensitizer has been applied to the deracemization of allenes.[133] Chiral photocatalyst **C16** (Fig. 29) binds an allene substrate with a different affinity for the two enantiomers. Moreover, the geometry of the diastereomeric adducts is quite different. One enantiomer places its double bonds close to the photosensitizer, enabling the excitation transfer, while the other remains further away and is not efficiently sensitised. Upon irradiation, the enantiomer bound

Stereoselective C-H borylation with both recognition and asymmetric ligands

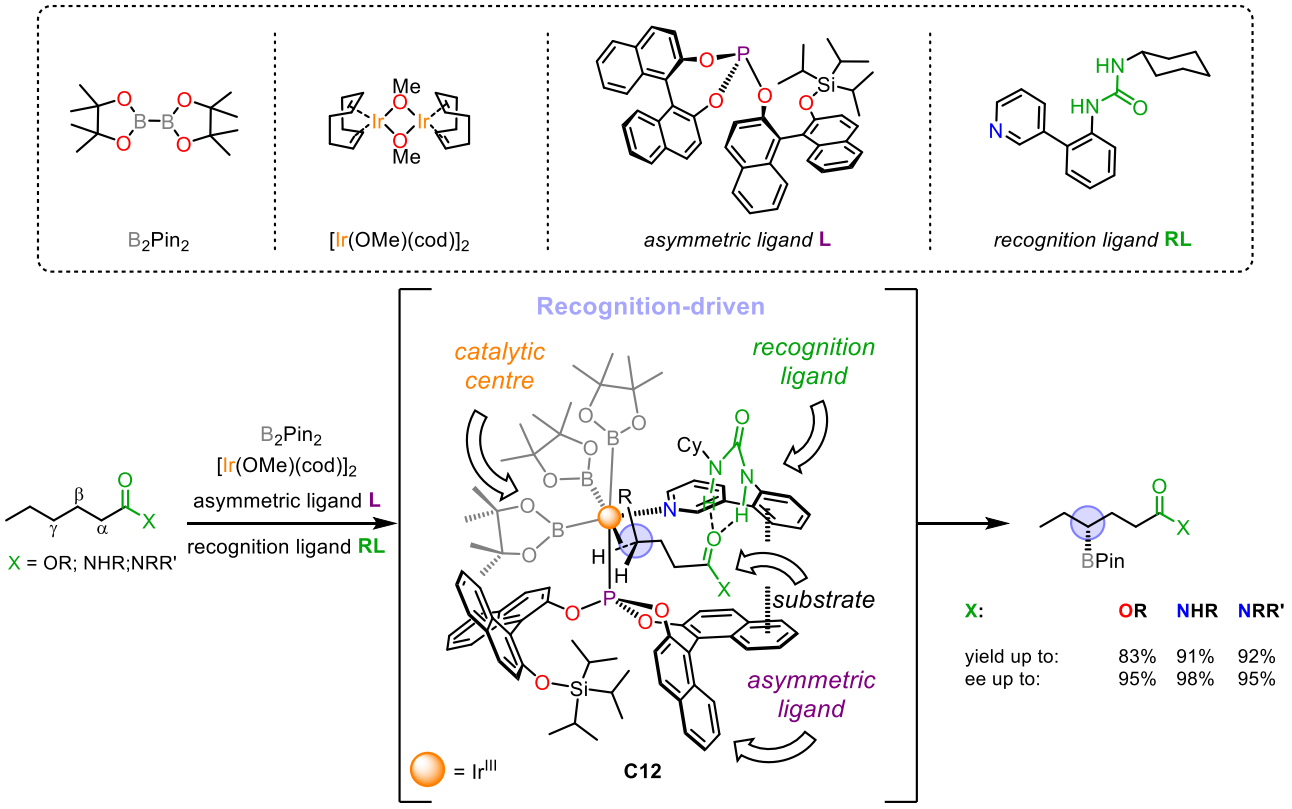

Fig. 26. Stereo-selective catalytic system for the B_2Pin_2 γ-borylation of carbonyl compounds. The phosphite cofactor generates a chiral pocket around the iridium centre (ref 124).

Asymmetric C-H functionalization with a chiral recognition unit

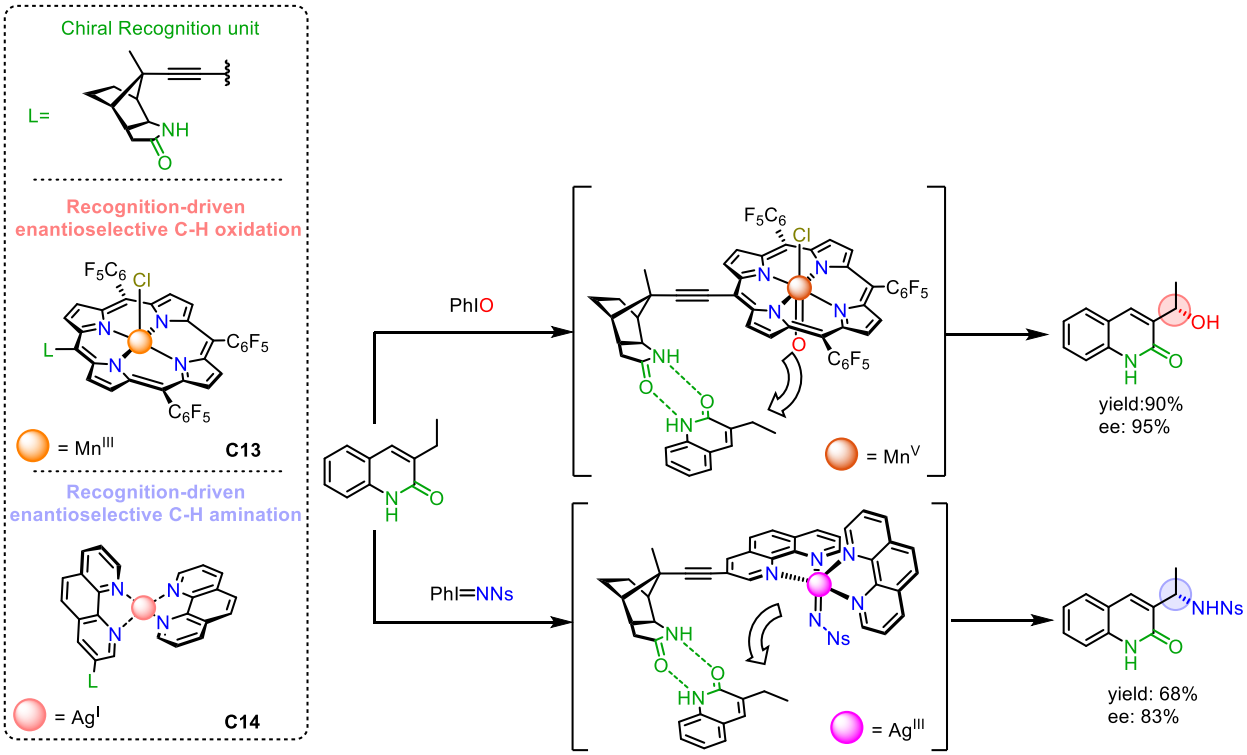

Fig. 27. Asymmetric oxidation or amination of C(sp^3)-H bonds in quinolone derivatives via supramolecular recognition with a chiral lactam receptor (refs 125-127). Ns = *p*-NO_2-benzenesulfonyl.

to the catalyst is excited *via* energy transfer. The allene in the triplet state now planarizes and racemizes *via* rotation around its stereogenic axis before returning to its fundamental state. As a consequence, the enantiomer that cannot be bound (and therefore sensitized) accumulates in solution, and after several cycles, the racemic mixture is converted into a highly optically pure solution (ee up to >99%). The same approach has also proved effective in the deracemization of 3-cyclopropylquinolones.[134]

Asymmetric photoinduced cyclization via supramolecular photosensitizer

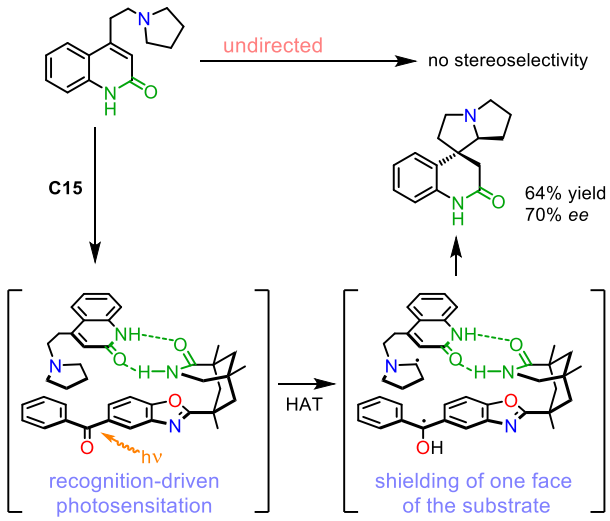

Fig. 28. Photoinduced cyclization of a 2-quinolone derivative catalysed by supramolecular photosensitiser **C15** (ref 130).

Allene deracemization via supramolecular photosensitizer

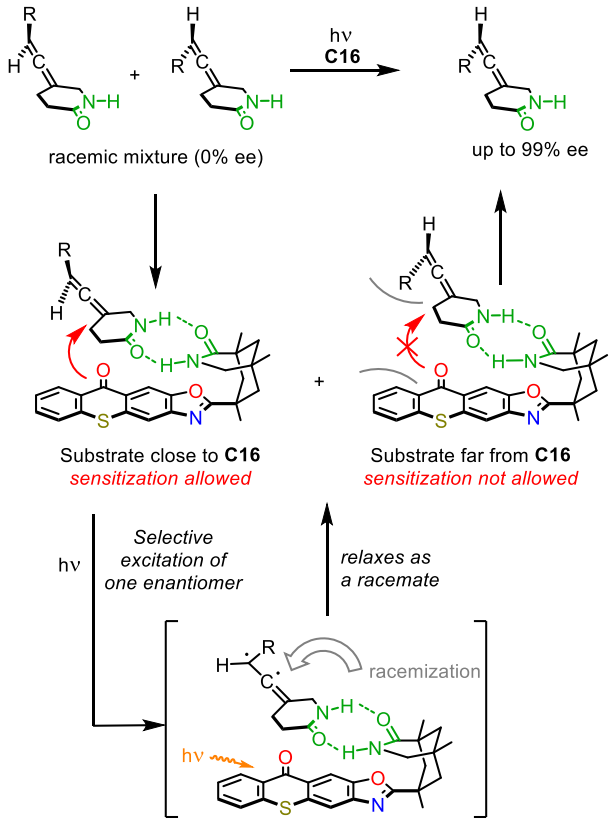

Fig. 29. Deracemization of a racemic allene mediated by chiral, supramolecular recognition (ref 133).

3.3.4 Tuning the second coordination sphere. Recognition of a chiral cofactor by a receptor is a simple yet powerful way to tune the environment around the reaction centre, i.e. the secondary coordination sphere of the catalyst. The trajectory of approach of the substrate to the catalytic site can be altered, modulating the reaction stereo-selectivity without varying the molecular structure of the catalyst. For instance, binding of a chiral cofactor to an achiral catalyst can transform the latter into an enantioselective catalyst. This approach allows to screen a large number of chiral catalytic systems reducing the synthetic effort, since a single supramolecular catalyst can be combined with multiple simple cofactors.

This approach was first explored by Reek *et al.* in asymmetric olefin hydrogenation. Binding of a (chiral) anionic aminoacid derivative to a supramolecular Rh catalyst has been used to control substrate orientation and to achieve the enantioselective hydrogenation of α,β-unsaturated amides (Fig. 30A).[135] More recently, a similar approach was used to place a chiral quinine derivative in proximity of a supramolecular Ir catalyst and unlock asymmetric C(sp^2)-H borylation of biaryls (Fig. 30B).[136] Such a strategy is being increasingly explored in the optimization of the catalyst efficiency and stereoselectivity.[137]

A) Asymmetric hydrogenation with a chiral cofactor

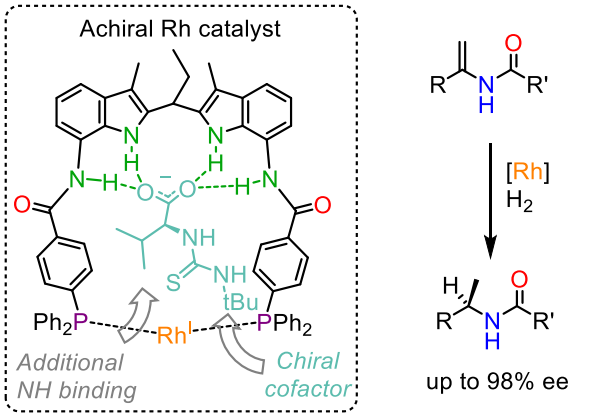

B) Asymmetric C-H borylation with a chiral cofactor

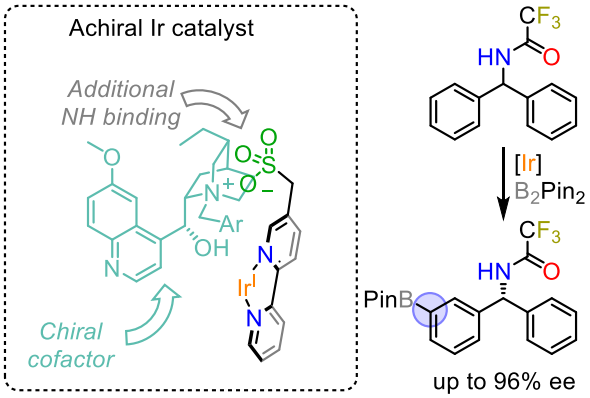

Fig. 30. Cofactor-controlled asymmetric hydrogenation of alkenes and aromatic C-H borylation (refs 135 and 136).

3.3.5 Other reactions. As stated before, preorganization of the substrate *via* supramolecular recognition by the catalyst is a powerful strategy to improve stereoselectivity. The examples described so far rely on "classical" supramolecular receptors which are known to bind specific functional groups. However, less common interactions (i.e. special ion-pairing, π-π stacking, C-H—π interactions, halogen bonding, etc.) can also be effective tools to orient the reactants. For example, incorporation of chiral ammonium pendant group on a Pd catalyst allows to fix the conformation of one reactant (the Pd-allyl fragment).[138] As a result, the addition of the second reactant occurs with high diastereo- and enantio-control (Fig. 31). A complete description of these systems with a less defined (and predictable) structure of the substrate-catalyst adduct is outside the scope of the present review, but we refer the interested reader to two thorough account that have recently been published.[82]

Asymmetric functionalization via ion pairing recognition

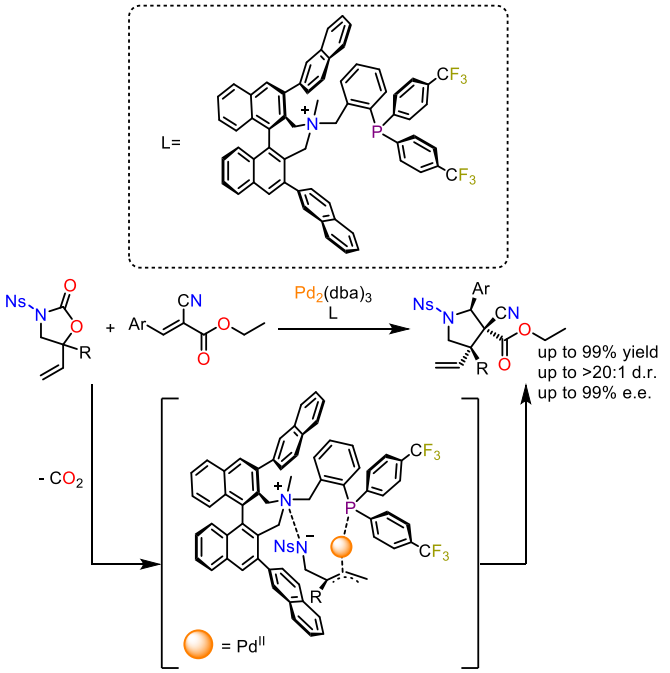

Fig. 31. Example of enantioselective allylic substitution directed by secondary substrate-catalyst interactions (ref 138). Ns = *p*-NO_2-benzenesulfonyl.

3.4 Substrate-selectivity.

The ability to discriminate among different competing substrates in a reaction is referred to as substrate-selectivity. The development of substrate-selective transformations would be key to use mixtures of compounds as practical feedstock materials. One particularly attractive application would be in the field of biomass valorisation.[139] Substrate-selectivity is a quite common property in nature, where enzymes select their natural substrates in the cytosol to avoid indiscriminate reactions that would affect vital cell structures.[140] This is achieved either by controlling which substrates can access to the active site through the entrance channels or by binding specific substrates inside the active site. Consequently, less-reactive compounds can be targeted by enzymes as long as they preferentially fit into the active site. The source of the enhanced reactivity and selectivity lies again in the intramolecularity of the reaction. In contrast, conventional artificial catalysts typically exhibit selectivity only for the substrates that are intrinsically the most reactive. The only way to alter such innate selectivity implies (i) substrate recognition or (ii) nanoconfinement of the catalyst (see section 2.4.1), and both require a supramolecular approach.

Again, this issue was pioneered by Breslow's group, which designed an iron-porphyrin complex **C17** (Fig. 32A) with quinoline moieties at the *meso* positions of the porphyrin ring[141] as a substrate-selective epoxidation catalyst. In the undirected reaction, monoester **1** is normally more reactive than the bis-nicotinate ester **2**. However, binding of two nicotinates to a Cu^{2+} /quinoline complex anchored to the porphyrin ligand inverts this relative reactivity and preferentially epoxides the bis-nicotinate ester.

More recently, crown ether-based catalyst **C3** (Fig. 32B) was shown to display an enzyme-like selectivity for C(sp^3)-H oxidation of undecylammonium in the presence of other intrinsically more reactive compounds,[142] even if added in a pool of four competing substrates (substrate-selectivity amplified from 3 to 77%). Analogously, a supramolecular approach also enabled other substrate-selective transformations,[82a,143] such as C(sp^2)-H borylation[144] and Suzuki-Miyaura coupling of bromopyridines.[145]

4 Catalysis Regulation by Molecular Machines

Supramolecular chemistry also offers the chance to modulate the activity and selectivity of the catalysts over time in a controlled manner. These catalysts are often molecular machines defined as molecules or supramolecular systems able to perform a task – catalysis in this case - in response to an appropriate stimulus.[146] The activation/deactivation of the task is coupled to defined, large-amplitude motions occurring within the machine. Such regulation discloses possibilities that are typically out of reach for conventional catalysts, going from simple switching ON/OFF (or *vice versa*) of the catalytic activity to the alternative operation of different catalytic units within the same machinery, or programmable selectivity that can be inverted *in situ*. Regulation of catalytic activity is indeed what allows cells and living organisms to carry out sophisticated tasks in complex mixtures without destructive interferences.

Catalysis regulation is accomplished by inducing *in situ* reversible molecular motions that shield, open, move or otherwise modify the active site upon addition of external stimuli. Then, the catalytic activity remains affected until another stimulus restores the initial conditions. This is what happens in natural enzymes, whose catalytic activity can be temporarily modified by pH or ionic strength variation, irradiation with light at a proper wavelength, addition or subtraction of cofactors that induce conformational changes in the protein structure and so on. This section showcases several examples of supramolecular catalytic systems that control the catalytic phenomenon, ranging from i) *in situ* ON/OFF switching the catalytic activity ii) *in situ* modulation of the catalyst

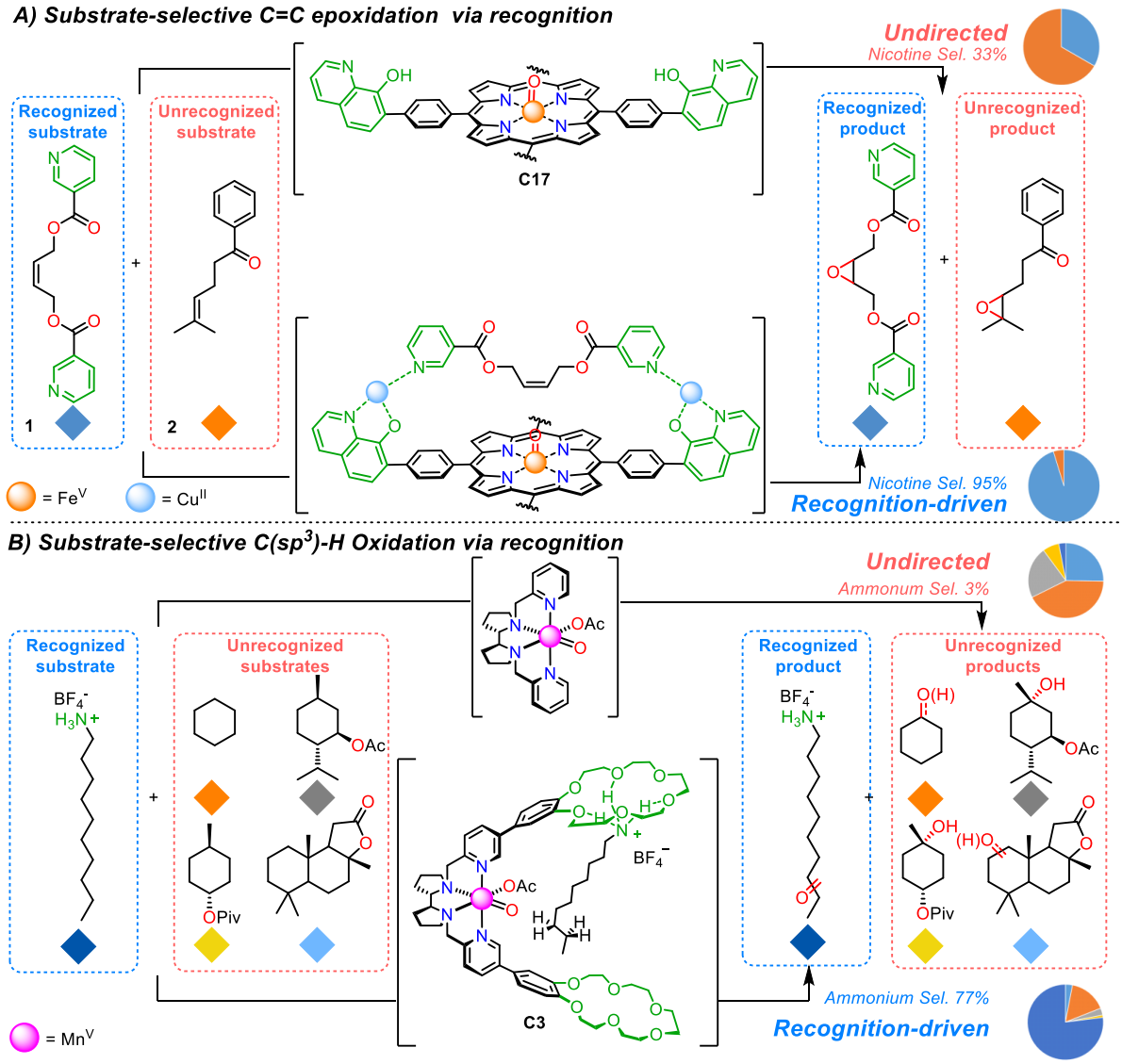

Fig. 32. A) Substrate-selective epoxidation and B) Oxidation of C(sp^3)-H bonds controlled by supramolecular recognition (refs 141 and 142).

selectivity and iii) dual catalysis (see Fig. 33). Again, we illustrate one or few examples for each concept, and refer the interested reader to other relevant articles or more exhaustive reviews.[147] Our purpose is to demonstrate that, like the catalysts described in the previous sections, molecular machines are unveiling new horizons in catalysis.

4.1. Switch ON/OFF of catalytic activity

Addition of an external stimulus (a chemical reactant or light) can trigger significant motions or other structural changes on the supramolecular catalyst that open or close the access to the active site in a reversible manner. As a consequence, catalysis can be chemically or photochemically switched ON or OFF at will, paving the way for the construction of sophisticated catalytic machineries able to perform different tasks at different times. The following examples of switchable catalysis are described on the basis of the nature of the stimulus employed.

4.1.1 Chemically-driven systems: acid/base switches. The external chemical stimulus is often an acid or a base that protonates/deprotonates the catalytic site, inducing a structural motion that makes the catalysis available/unavailable (or *vice versa*).

A series of outstanding works by Leigh and co-workers illustrated the key principles of switchable catalysis with molecular machines using acid/base chemical stimuli. The seminal work dates back to 2012.[148] In this case, the three-station, symmetric [2]-rotaxane **C18** is used as a switchable catalyst to accelerate the Michael reaction described in Fig. 34A. This reaction is catalyzed by secondary amines through an iminium-based mechanism. The positively charged, transient iminium intermediate formed in the reaction between the aldehyde and the amine is more reactive (more electrophilic) than the parent carbonyl compound and undergoes rapid attack by the sulfur-based nucleophile. In the absence of catalysts, no reaction is observed within 5 days. In contrast, the reaction smoothly occurs upon addition of **C18** (83% yield after 5 days), while doesn't occur at all when the protonated form **C18**H$^+$ is added in solution as PF_6^- salt. In the latter case, the crown-ether wheel sequesters the catalytic site

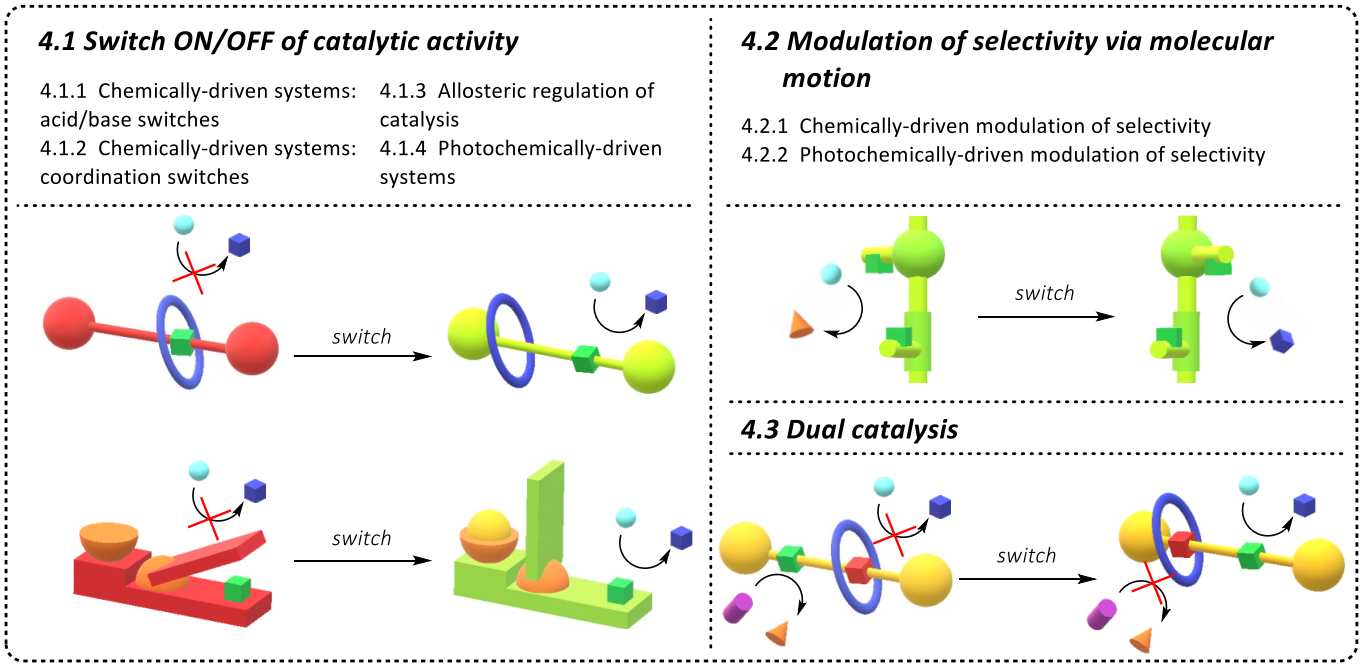

Fig. 33. Graphical summary of section 4 - Catalysis regulation by molecular machines.

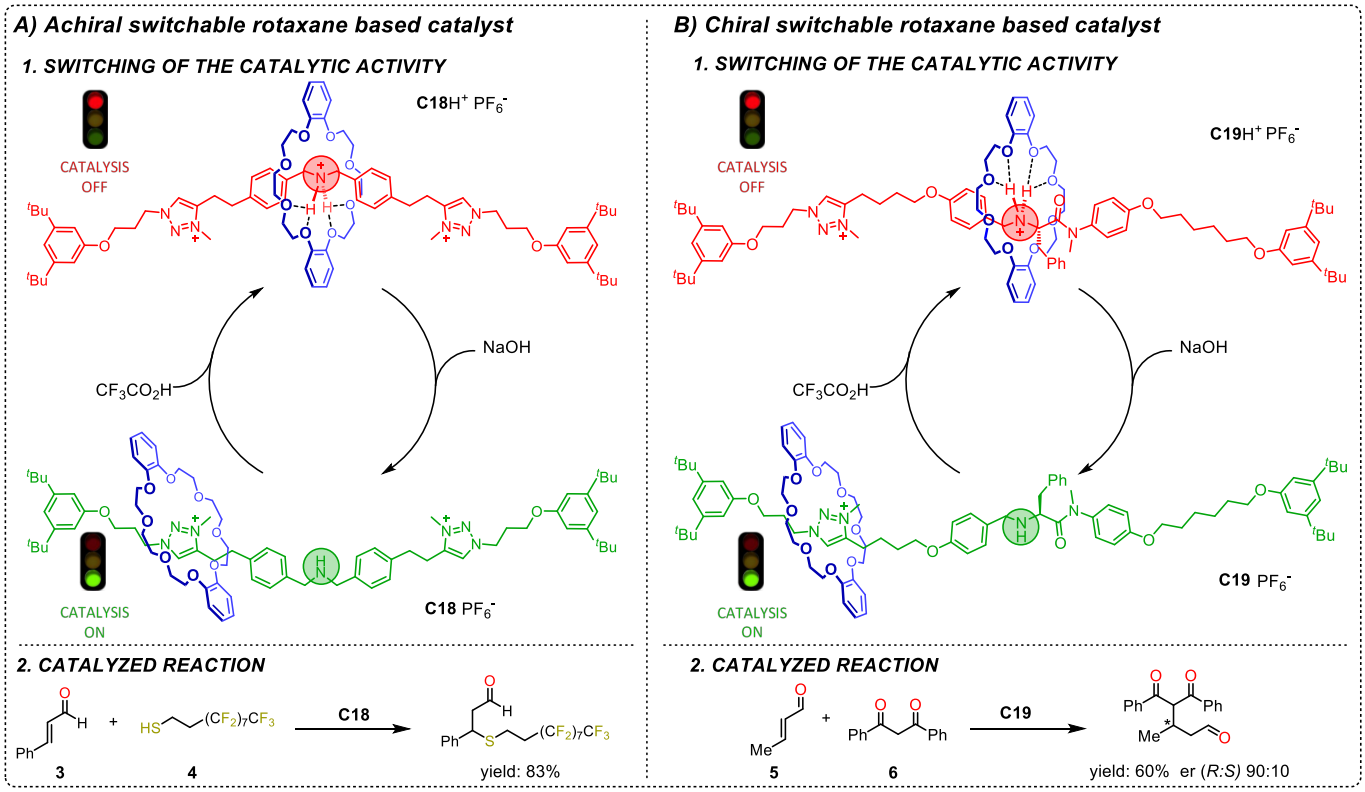

Fig. 34. A) Rotaxane **C18** and related acid-base equilibrium, which promotes the reaction between **3** and **4** (ref 148). B) *R* form of catalyst **C19** and the related acid-base equilibrium, which promotes the reaction between **5** and **6** (ref 149).

of the rotaxane (the secondary amine), preventing iminium formation and hence catalysis. Remarkably, the catalyst can be activated *in situ*. When the inactive protonated form **C18**H+ of the rotaxane is added to **3** and **4** in dichloromethane no reaction occurs but after washing with aqueous NaOH (1M), the Michael addition is complete in just 1h. Under these conditions the reaction is even faster because of the deprotonation of the thiol nucleophile.

Using the same principle, Leigh and co-workers also showed[149] that the enantiomeric forms of the OFF/ON switchable chiral catalyst **C19**, based on a two-station [2]-rotaxane catalyze an enantioselective Michael addition between **5** and **6**(up to 98:2 er, Fig. 34B). Again, the activation of **C19**H+ can be triggered by washing the dichloromethane solution with aqueous NaOH (1M). Similarly, the same group designed and implemented other intriguing catalysts that can be switched *in situ*.[150]

Recently, Leigh *et al.* reported the first case of dissipative catalysis by a molecular machine.[151] Dissipative catalysis occurs when a transient external stimulus (fuel) drives the molecular motion turning on the catalytic activity, which is maintained until the fuel wears off. [151] In this case, OFF/ON/OFF switching of a bistable [2]rotaxane-based catalyst is driven by trichloroacetic acid used as a fuel[152] (Fig. 35). When the latter is added to pre-catalyst **C20**, the amine function is protonated and consequently the crown ether wheel migrates from the thiourea station to the ammonium station. The unmasked thiourea can now catalyze the hydride transfer from **8** to **7**. Subsequent spontaneous decarboxylation of trichloroacetate generates CCl_3^-, which takes back the proton from the protonated rotaxane and restores the catalytically inactive form of the catalyst. In other words, catalysis is OFF before addition of the fuel, ON after its addition, persists in the ON state until the fuel is present and turns OFF again when the fuel is exhausted. The time of catalyst permanence in the ON state can be finely controlled by varying the amount of added fuel.

4.1.2 Chemically-driven systems: coordination switches. The chemical stimulus that switches ON/OFF catalytic activity can rely on the rapid association of metal cations with their ligands.[153]

Goldup and coworkers used Zn^{2+} or Cu^+ as chemical stimuli to drive the motions and catalytic activity of a molecular machine (rotaxane **C21**, Fig. 36). Addition of $AgSbF_6$ to a solution of **9**, **10** and axis **C22** abstracts the chloride ligand and unmasks the Au^+

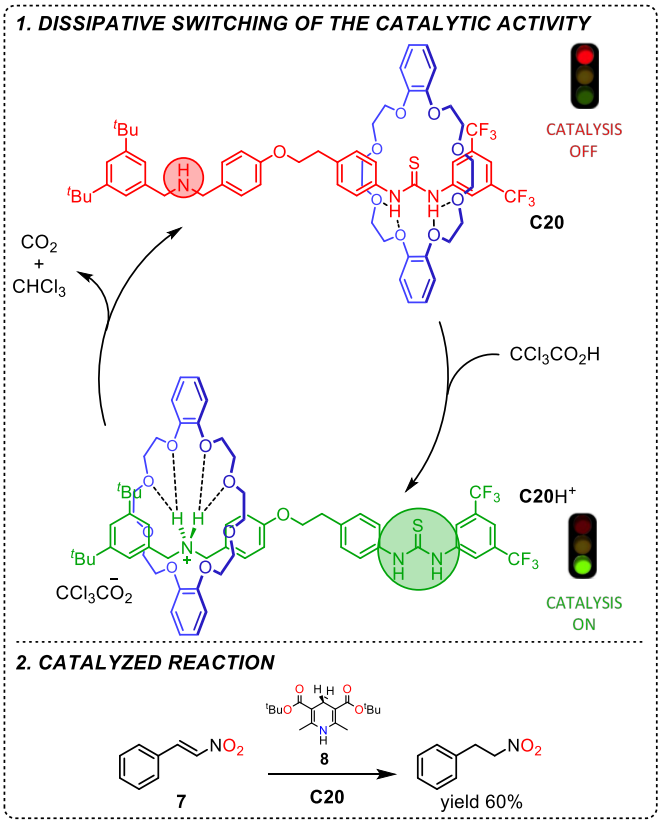

Fig. 35. Dissipative catalysis for the reduction of nitrostyrene. The catalyst is active as long as the fuel (CCl_3CO_2H) is present (ref 151).

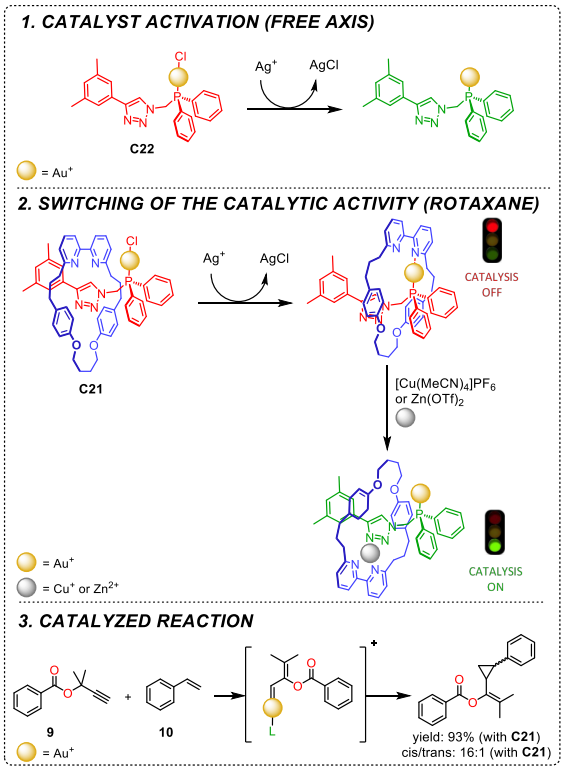

Fig. 36. In situ switch ON of rotaxane **C21** and catalyzed reaction (ref 154).

center, activating the cyclopropanation reaction.[154] In contrast, no reaction is observed upon addition of $AgSbF_6$ to rotaxane **C21**, as the Au^+ is sequestered by the bipyridine unit, inhibiting catalysis. In this case, activation of catalysis requires further addition of a cofactor such as $Zn(OTf)_2$ or $[Cu(MeCN)_4]PF_6$, that strongly interact with both the bipyridyl and triazole units, leaving the Au^+ center free for catalysis. Moreover, rotaxane **C21** provides the cyclopropane products with a diasteromeric selectivity (up to 16:1) higher than the free axis thanks to an improved definition of its secondary coordination sphere by the sterically crowded environment around the Au^+ center (the wheel). Similar, yet less efficient ON/OFF switches are also obtained when *p*-toluenesulfonic acid (TsOH) is used instead of the above salts as cofactor.

Schmittel and co-workers employed a different approach to control the catalyst activity by means of coordination driven switches. They reported several catalysts based on phenanthroline and terpyridine metal coordination, which allows the organization of sophisticated multicomponent self-sorting systems with switchable catalytic activity.[155] In one of their earliest works,[155b] they used nanoswitch **C23** bearing terpyridine and phenanthroline units to complete the coordination sphere of the Cu^I cation, thus making the copper center uncapable of catalyzing the cyclopropanation reaction **11** + **12** (Fig. 37). Addition of 0.5 mol equiv. of $Fe(ClO_4)_2$ leads to catalytic ON-state **C23$_2$** dimer, where the Fe^{II} ion engages two terpyridine moieties in an octahedral coordination leaving the coordinatively unsaturated Cu^I free to catalyze the **11** + **12**

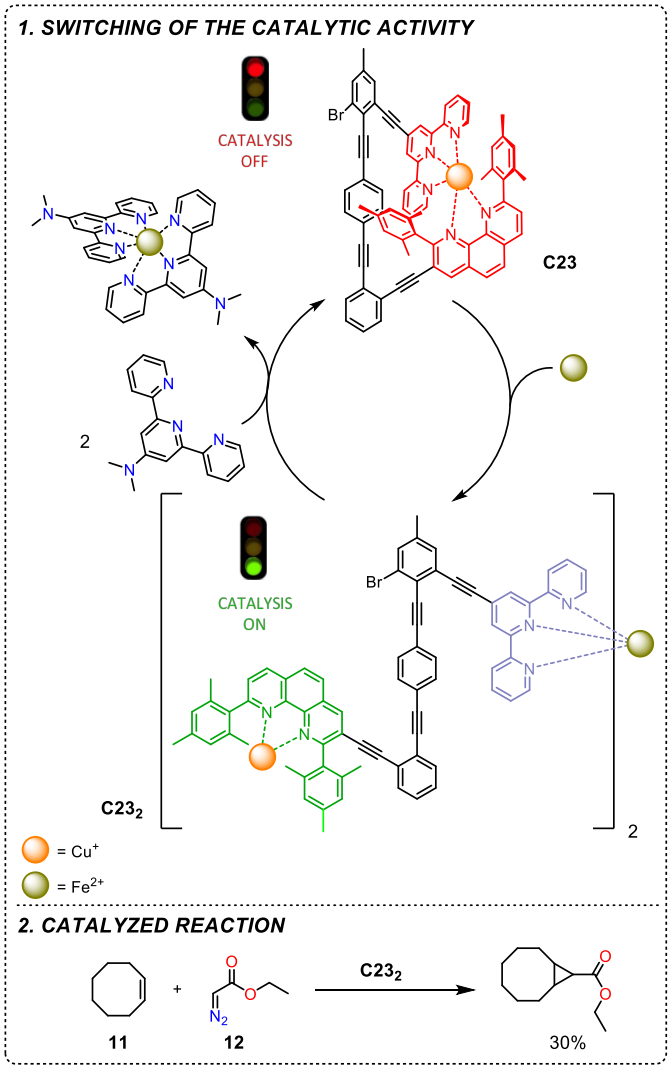

Fig.37. Switch ON / OFF of the catalysis due to addition and removal of Fe^{2+} ion to and from molecular machine **C23** (ref 155b).

reaction**.** The product is obtained in 30% yield after heating at 55°C for 4 hours. Catalyst **C23** can be deactivated again (OFF-state) by addition of 4-*N*,*N*-dimethylaminoterpyridine.

4.1.3 Allosteric regulation of catalysis. Control of supramolecular catalysis has been also achieved by interaction of simple ions or small molecules (effectors) with regulating molecular units located far from the catalytic site. In this case, the external stimulus translates into substantial conformational (allosteric) changes that modulate the access to the active site, switching ON or OFF its activity.

Mirkin's group designed an ON/OFF/ON regulation of the polymerization of *ε*-caprolactone **13** (Fig. 38).[156] The catalytic site is the Al salen-complex in the middle of the trimetallo-catalyst (**C24**) structure. Substrate access to the Al catalytic center is regulated by the presence/absence of bulky aromatic portions that act as a gate. The closed triple-layer form (*c*-**C24**) of the catalyst is inactive while the semi-open form (*so*-**C24**) is catalytically active, and the two can be transformed one into the other by addition of simple effectors. For example, addition of 2 molar equiv. of Cl^- or CH_3CN to a dichloromethane solution of *c*-**C24** causes its conversion into *so*-**C24**, due to the replacement of the weaker aniline ligand with the stronger Cl^- or CH_3CN ones in the Rh coordination sphere. In a proof-of-concept experiment, polymerization of *ε*-caprolactone is catalyzed by the *so*-**C24** form. Addition of Ag(BArF) (BArF = tetrakis[(3,5-trifluoromethyl)phenyl]borate) after 10 min (when the conversion of the substrate is about at 60%) transformed the catalytically active *so*-**C24** into the inactive *c*-**C24** by abstracting chloride ions, switching OFF the reaction. Addition of acetonitrile after 15 min restores the *so*-**C24** form of the catalyst, triggering the consequent polymerization to start over again. Analogous allosteric regulation of catalytic activity[157] has been masterfully used for analytic purpose[158] (determination of the concentration of the effector through an amplification

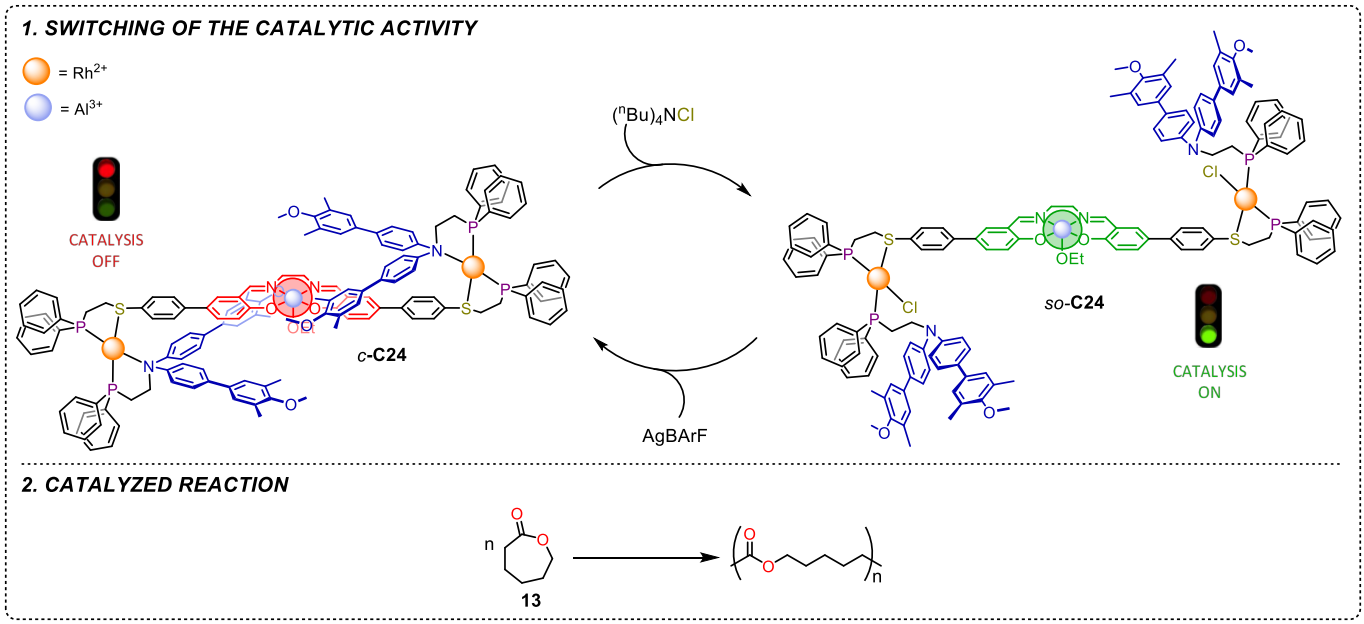

Fig.38. ON/OFF/ON catalyst modulation of *ε*-caprolactone polymerization. Subtraction or addition of effectors Cl^- or CH_3CN and Ag(BArF), respectively, turns off (*so*-**C24**→*c*-**C24**) or turns on (*c*-**C24**→*so*-**C24**) the catalyst (ref 156).

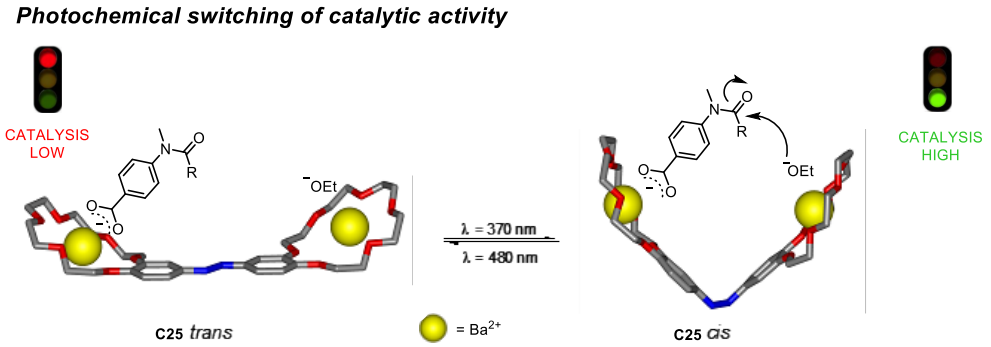

Fig.39. *In situ* activation and deactivation of the azobenzene based catalyst for the basic ethanolysis of amides (ref 162).

mechanism) or for a cascade autoactivation of the catalyst.[159] In other examples, allosteric modulation of catalyst geometry has been used to finely control the catalysis.[160]

4.1.4 Photochemically-driven systems. Irradiation with light at the proper wavelength can be exploited as a convenient stimulus to temporally change the geometry of a supramolecular catalyst with consequent activation of its catalytic properties, enabling ON/OFF switch of chemical reactions.

This concept was first put into practice by Rebek and coworkers in 1995,[161] who designed a photo-switchable promoter based on the azo-benzene unit for an aminolysis reaction, and then by one of us *et al*[162] in 2003 with the realization of the first repeatedly photo-modulable catalyst. In this case, the ditopic catalyst **C25** depicted in Fig. 39 catalyzes the ethanolysis of activated amides endowed with a carboxylate anchoring group. The latter function is bound by one of the two crown-ether-Ba^{2+} moieties by means of electrostatic interactions, pre-organizing the substrate to present the carbonyl function to the other crown-ether-Ba^{2+} moiety and its ethoxide counter anion, favoring the cleavage reaction. The *trans* form of the catalyst is much less efficient than the *cis* form for geometrical reasons (the *cis* configuration places the carbonyl group closer to the other Ba center, providing a better fit for the transition state structure), so irradiation of the solution at 370 nm (*trans*→*cis*, a photostationary state *trans*:*cis* 5:95 is reached) activates the catalysis. The inverse transformation, *cis*→*trans*, spontaneously occurs or can be photostimulated by irradiation with light at 480 nm (in the latter case a photostationary state *trans*:*cis* 81:19 is reached). Since the *trans* form still retains some catalytic activity, the system is better defined as a LOW/HIGH rather than an OFF/ON switch. However, the efficiency of the catalyst can be switched HIGH and LOW a number of times in the time course of the reaction, through alternate irradiations at 370 and 480 nm, respectively, with complete reversibility between the two photostationary states. In the last two decades, countless applications of this concept have been reported, which are exhaustively described in more specific reviews.[147c,e]

4.2 Modulation of selectivity via molecular motion

Addition of external stimuli can trigger geometrical changes around the catalytic site, modifying the microenvironment surrounding the reactants and hence modulating the selectivity (typically stereoselectivity) of the reaction.

4.2.1 Chemically-driven modulation of selectivity. Leigh and coworkers designed the programmable molecular robot **C26** that can be modulated *in situ* for the stereodivergent syntheses depicted in Fig. 40.[163] In this impressive example, addition of acid/base external stimuli can invert the stereoselectivity of two sequential reactions in a rationally programmable manner. The robot is endowed with two pyrrolidine based catalytic units with definite stereochemistry *S* and *R* (highlighted in blue and green, respectively).

The substrate, a masked unsaturated α,β-unsaturated aldehyde linked to the robot by means of an ester bond (Fig. 40, red portion), is held in proximity of one of the pyrrolidine units (the *S*-handed pyrrolidine in the *E*-form of the robot, the *R*-handed pyrrolidine in the *Z*-form). Addition of CF_3CO_2H (2.2 molar equiv.) in CH_2Cl_2 causes deprotection of the aldehyde function, triggering the reaction sequence. First, a nucleophilic addition of $CF_3(CF_2)_7CH_2CH_2SH$ (blue prism) to the unsaturated aldehyde substrate occurs via a (macro)cyclic iminium catalysis with the nearby pyrrolidine unit (setting the C3-stereocenter), and then the resulting sulfur substrate adds to $CH_2=C(SO_2Ph)_2$ (purple sphere) via a (macro)cyclic enamine catalysis, still catalyzed by the nearby pyrrolidine unit (setting the C2-sterocenter). Finally, the ester linkage is reduced to release the alcohol product **14**. In the *E*-form of the robot, the pyrrolidine unit close to the substrate is *S*-handed and generates 3*R* and 2*R* stereocenters in step A and B, respectively. However, the robot can be converted into its *Z* form via addition of excess CF_3CO_2H (6 molar equiv.), placing the substrate in proximity of the *R*-handed pyrrolidine that sets 3*S* and 2*S* stereocenters, respectively. Such isomerization can be reversed, restoring the *E*-form, by addition of trimethylamine (7 molar equiv.). As a result, the stereochemistry of the two additions is fully programmable: i) in the absence of acid-triggered isomerization (always *E*-form), a (2*R*,3*R*)-product is obtained; ii) if the robot is isomerized (*E* to *Z*) after the first step (step A in *E*-form, step B in *Z*-form), it furnishes (2*S*,3*R*)-**14**; iii) if initial *E* to *Z* isomerization is followed by a second *Z* to *E* isomerization after the first step (step A in *Z*-form, step B in *E*-form), (2*S*,3*S*)-**14** is produced; iv) if a single E to *Z* isomerization precedes the first reaction (always *Z* form), the robot yields the (2*R*,3*S*)-product. This example astonishingly demonstrates the potential of artificial molecular machines in the fine control of chemical reactivity and selectivity.

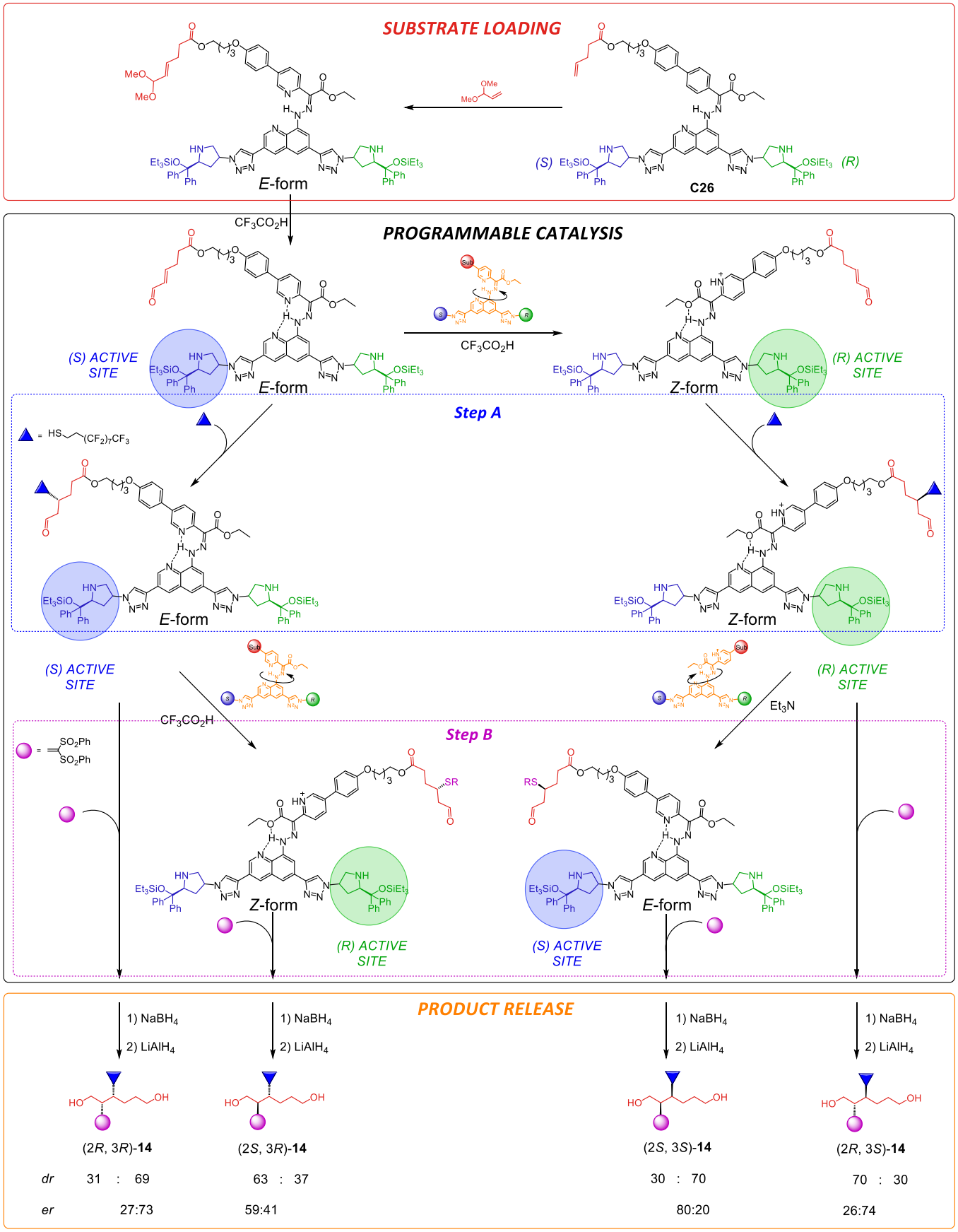

Fig. 40. Programmable molecular robot **C26** for stereodivergent syntheses (ref 163).

4.2.2 Photochemically-driven modulation of selectivity. In the extraordinary evolution of photoswitchable systems pioneered by the Feringa's group, an outstanding example exploits light to modulate the enantioselectivity of a catalytic reaction at will,[164] showcasing the exquisite level of sophistication reached by this chemistry and paving the way to many applications.[165]

Catalyst **C27** is endowed with a DMAP (dimethylaminopyridine) base (**A**) and a thiourea group (**B**) (Fig. 41).[164] In the *trans* form of the catalyst, **A** and **B** are located far from each other, separated by an indane pair containing two *R* stereocenters (see Fig. 41) that dictate the *P*-helicity of the structure. In this situation the **A** and **B** groups are too far to synergistically catalyze the Michael addition between *ortho*-methoxythioanisole (**15**) and cyclohexanone (**16**) (7% yield after 15 h and no enantioselectivity). This reaction is instead efficiently accelerated when unit **A**, which deprotonates **15**, and unit **B**, which activates the enone function of **16** through hydrogen bonding to the attack of the nucleophile, are in close proximity (see Fig. 41). Such proximity is achieved when *P-trans*-**C27** is transformed into *M-cis*-**C27** by *in situ* irradiation at 312 nm. Reaction **15** + **16** occurs more rapidly under these conditions (40% yield after 15 h) and **17** is obtained with a good enantioselectivity (er 75/25 *S*/*R*). Remarkably, when *P-cis*-**C27** obtained by heating *M-cis*-**C27** at 70 °C is used, the same reaction is catalyzed with even higher efficiency (83% yield after 15 h) but opposite enantioselectivity (er 23/77 *S*/*R*). Two subsequent steps, one photochemical and one thermal, allow the system to reversibly transforms *M-cis*-**C27** into *P-trans*-**C27**, closing the motion cycle. Operation of the system is guaranteed by the unidirectional clockwise motion (seen from the **B** site) in the catalyst, in turn dictated by the *R*-chirality of the two stereocenters on the indane cores. In fact, when the indane core pair has both stereocenters of the *S* configuration, the indane structure assumes a *M*-helicity, thus, irradiation and subsequent thermal treatment induce an anti-clockwise motion with consequent inversion of enantioselectivity during the motion cycle.

4.3 Dual catalysis

A special mention goes to those catalysts endowed with two distinct catalytic moieties which can be alternatively turned ON and OFF. The two moieties catalyse different reactions. Such systems are designed in such a way that when one catalytic site is available for catalysis (*cat1-ON)* the other is catalytically silent (*cat2*-OFF), and *vice versa*. In situ switching within the molecular machine turns on the initially silent catalytic site (*cat2*-ON) and deactivates (*cat1*-OFF) the initially active one. These systems are especially remarkable as the product distribution in a mixture of reactants can be controlled at will and in one-pot.

Leung et al described a rotaxane based dual organo-catalyst[166] endowed with two catalytic sites, namely a thiourea function and a secondary amine function. The latter is linked to an anthracene unit which acts both as a stopper and as a fluorescent probe to monitor the di-benzo-24-crown-8 wheel translocation along the axis (Fig. 42). The catalytic activity of the machine was investigated in the presence of a mixture of three component (**18**, **19** and **21**) and it was shown that the in situ switching of the rotaxane can selectively catalyses one of the two possible reactions at a time. Initially, the machine is present in the protonated form (**C28**H$^+$), with the secondary ammonium

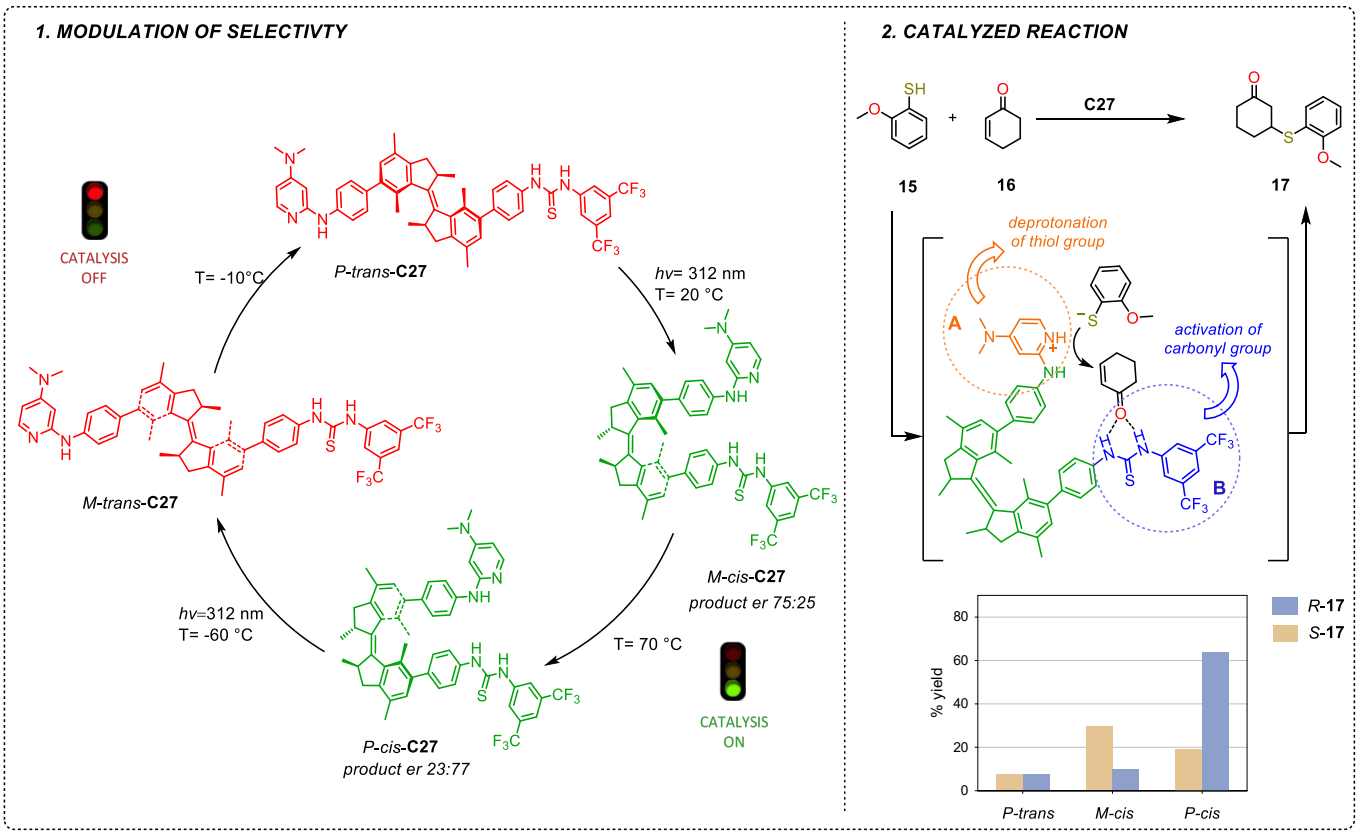

Fig. 41. Structure of catalyst **C27** (namely 2*R*,2*R'*-*P*,*P-trans*-**C27**), reaction between **15** and **16**, and proposed catalytic mechanism involving the *cis* form of the catalyst (ref 164).

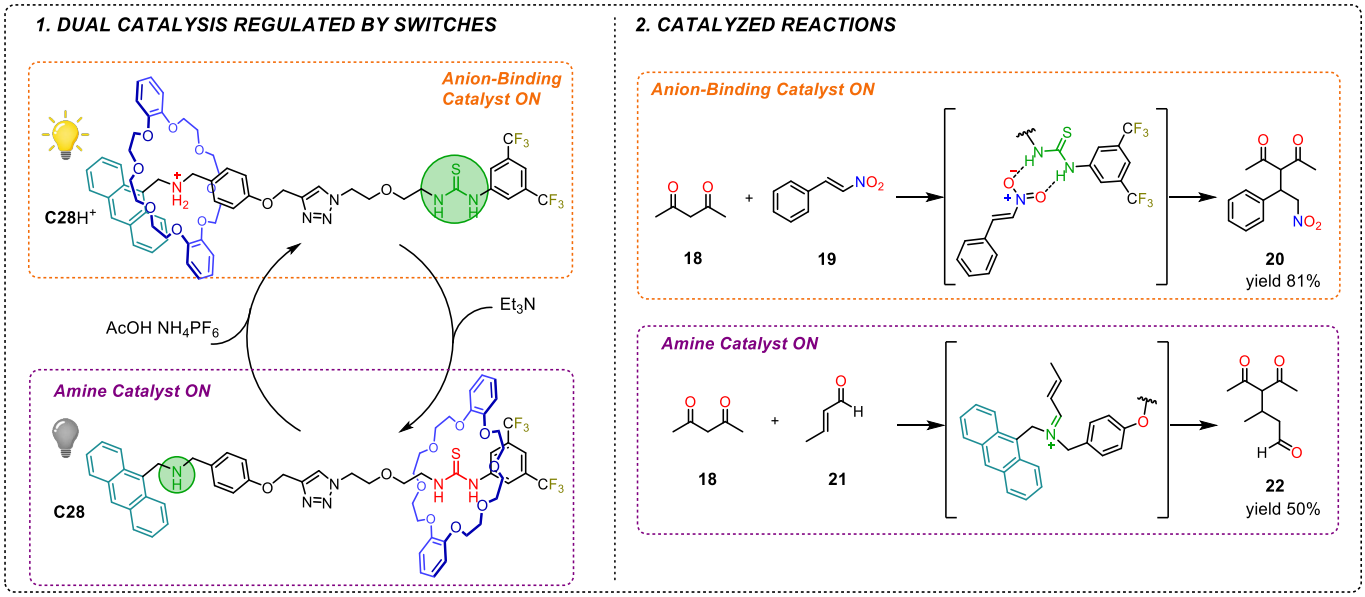

Fig.42. Dual catalysis enabled by catalyst **C28**. Two competitive reactions on the same substrate can be alternatively switched ON/OFF (ref 166).

site coordinating to the electron-rich macrocycle. Consequently, iminium catalysis is prevented and the thiourea group catalyses the reaction between **18** and **19** via hydrogen-bond activation of nitro group (product **20** is formed with a yield up to 81%). Addition of triethylamine converts the protonated **C28**H⁺ into the deprotonated form **C28**, where the urea catalytic site is masked by the macrocycle and the secondary amine is free to catalyse the addition **18** + **21**, leading to 50% of **22** via iminium catalysis.

Leigh's group designed some rotaxanes displaying dual, orthogonally-switchable organocatalysis,[167] one of which allows two consecutive functionalizations on the same substrate (Fig. 43). Rotaxane **C29** consists of a dibenzo-24-crown-8 macrocycle threaded on an axis bearing a dialkylamine station and two triazolium groups, whose cooperative action allows an anion-binding catalysis. NMR titrations of **C29**H⁺ with Bu_4NX (X= Br, Cl) show a high affinity of the triazolium units for halides, giving a 1:1 complex in CD_3CN, while no interaction takes place when **C29** is used as a receptor, indicating that both triazolium groups are involved in the anion coordination. Sequential functionalizations of **23** are then achieved by exploiting acid/base *in situ* switching of the catalyst. **C29**H⁺ catalyses the alkylation of **23** with **24** (product **25** is obtained with 70% yield after 12h) through an anion-binding catalysis that unmasks the carbocation intermediate, while dialkylammonium is concealed by the crown ether. Addition of NaOMe causes ammonium deprotonation and the displacement of the wheel to one of the positively charged triazolium units, switching OFF the anion-binding and ON the enamine catalysis, enabling the reaction between **25** and **26** (product **27** was obtained in 55% yield).

Dual catalysis systems employing coordination chemistry have been also designed by Schmittel and coworkers.[168] In one case,[168b] two reactions are competing in one pot, namely a 1,4-Michael addition catalyzed by a secondary amine (free

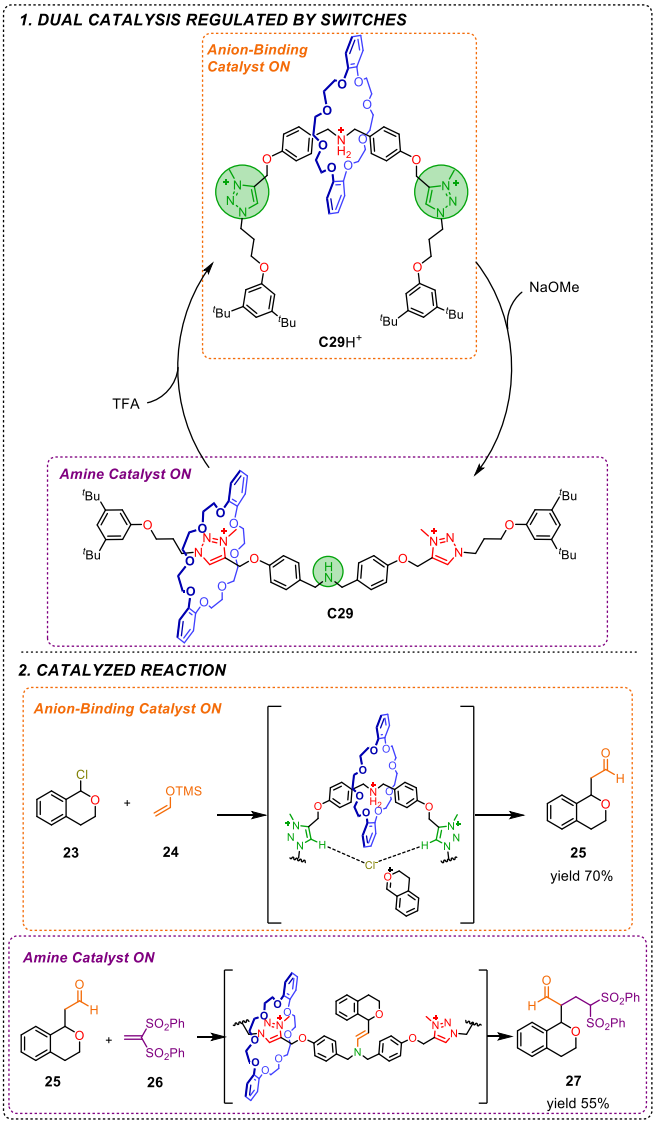

Fig.43. Consecutive nucleophilic substitution and conjugate addition one-pot catalysed by the two forms of rotaxane **C29** (ref 167b).

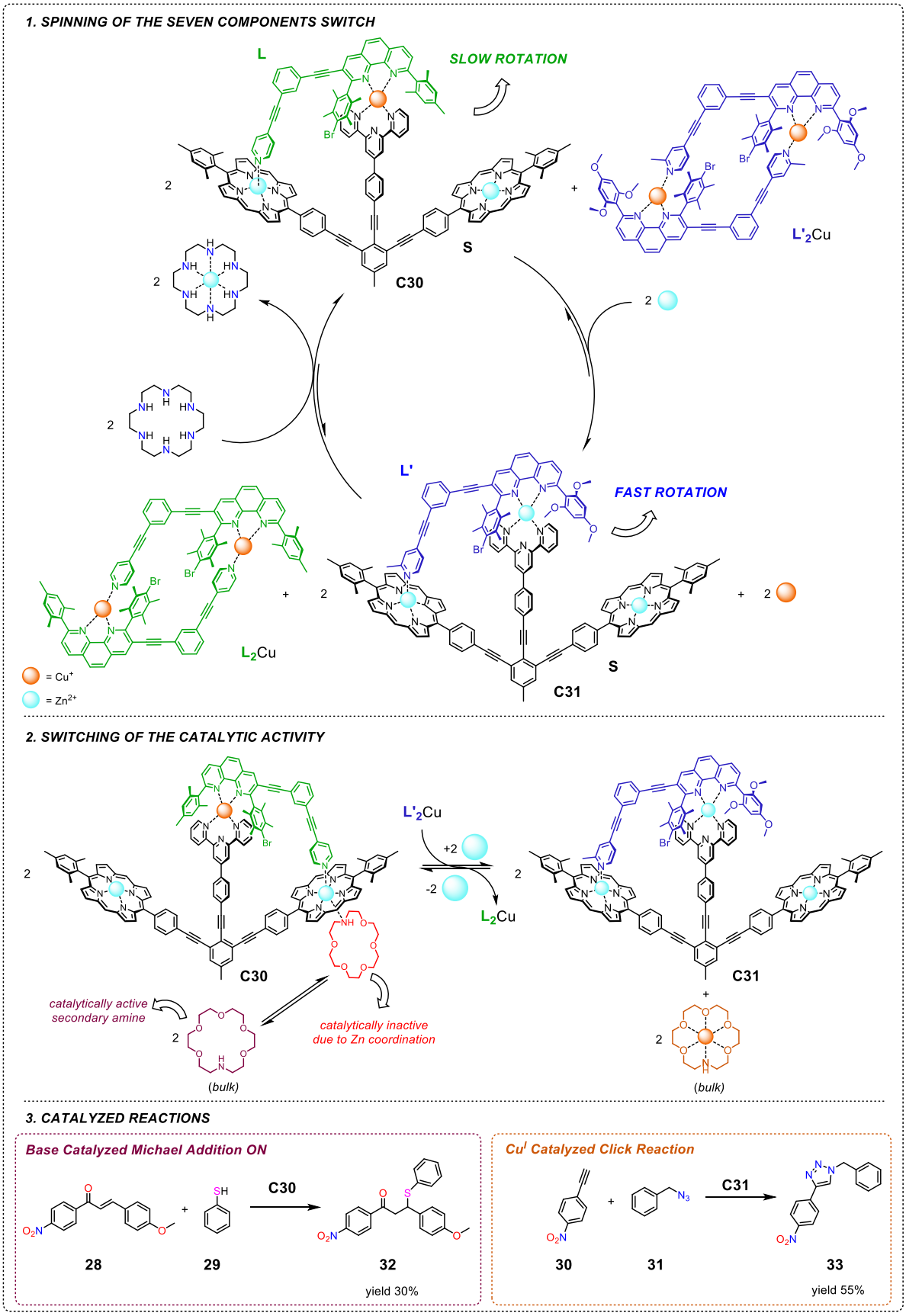

Fig.44. Seven component system realized by Schmittel and coworkers to switch from an aza-18-crown-6 catalysis to an aza-18-crown-6•Cu^{+} complex catalysis (ref 168b). Reactions carried out in CH_2Cl_2/CH_3CN 5:1, 50 °C, with the following ratio of reagent: **C30** : **L'**$_2$Cu : aza-18-crown-6 : **28** : **29** : **30** : **31** = 1:2:1:10:10:10:10:. Then 2 mol equiv. of Zn^{2+} as triflate salt were added and, subsequently, 2 mol equiv. of hexacyclen.

aza-18-crown-6) and a click reaction catalyzed by a Cu^{I} complex, and the motions of a molecular machine regulate which reaction occurs at a given time (see Fig. 44). A sophisticated, seven components switch was realized, which can be controlled by addition or subtraction of zinc cations. Semirotation of rotor **L** on stator **S** in **C30** (Cu complex) is 25-fold slower than that of rotor **L'** on stator **S** in **C31** (Zn complex; see Fig. 44). This semirotation displaces secondary amine ligands (aza-18-crown-6 ethers, amine catalysts) bound to the Zn-porphyrins, increasing the concentration of their free (unbound) form in solution. The spinning rate dictates the efficiency of such displacement.

In the initial state (**C30**), the spinning, although less rapid, allows a high enough concentration of the base aza-18-crown-6 in its free form in solution, that efficiently catalyzes the Michael addition between **28** and **29** (the reaction is instead completely inhibited in the presence of a simple monoporphyrin Zn^{2+} model). Addition of Zn^{2+} ions converts **C30** into **C31** liberating Cu^{+} ions and aza-18-crown-6 ligands that rapidly assemble together. Formation of complex aza-18-crown-6•Cu^{+} switches OFF the amine catalysis (Michael addition) but unlocks the catalysis of the click reaction between **30** and **31**. Then, addition of hexacyclen sequesters the Zn^{2+} cations, restores complex **C30** at the expense of **C31**, and reactivates Michael catalysis, interrupting the click one. In one experiment, starting with the system in the **C30** state, after 2 h, Michael adduct **32** was obtained in 30 % yield. Then Zn^{2+} was added and after 2 h the click product **33** was obtained in 55 % yield. Eventually, hexacyclen was added and after additional 2 h, extra 31 % yield of Michael product **32** was obtained. This way, the switch between two reactions (Michael addition and click [3+2] cycloaddition) can be regulated by addition of proper effectors.

5 Processive catalysis

"Catalysis can be called processive if the catalyst associates with its substrate and then performs multiple rounds of catalysis before dissociation"[169] (Fig. 45). It is one of the most promising attempts to successfully mimic complexity of natural systems. In fact, extraordinary examples of processive enzymes can be found in nature, which show the exquisite level of complexity reached by Nature during its billion year evolution.[169]

The Nolte and Rowan group has carried out pioneering studies on artificial models of processive enzymes, which, during the years, have led to astonishing results.[170] In this case the catalyst itself is not a molecular machine but the ensemble of the catalyst with its substrate constitutes a pseudo-rotaxane. As shown in Fig. 46, the polybutadiene (98% *cis*) polymer is threaded inside the cavity of a Mn porphyrin receptor, whose external face is shielded by addition of 4-*tert*-butylpyridine. In the presence of a terminal oxidant (PhIO), the system is able to catalyze the epoxidation of the double bonds present in the polymer skeleton with high yields and a marked preference for the *trans* form (80:20 *trans*/*cis*). The process is not sequentially processive – i.e., the epoxidation is random and occurs with a hopping mechanism, in which the Mn complex goes back and forth on the polymer track - however preludes to next developments including sequentiality.[171]

Other outstanding examples of processive catalysts have been reported by Harada,[172] who coupled α- and β-cyclodextrins to polymerize δ-valerolactone, by Leigh who prepared a pseudo-rotaxane in which, during its oriented dethread along the axis, the wheel iteratively and sequentially acquires three aminoacids[173] (or four in a more recent development[174]) to form a pendant peptidic chain, and lately by Li and Schneebeli who obtained the size-selective acylation of the amino groups present in the chains of polydisperse polymer mixtures by threading the polymer chains into hydrazone-based molecular tetrahedrons decorated with tryglime units.[65]

6 Conclusions and outlook

All the examples described in the previous sections give an overview of the current impact of the supramolecular approach in catalysis. In its essence, it implies binding of the substrate and the transition state to the catalyst via weak, reversible

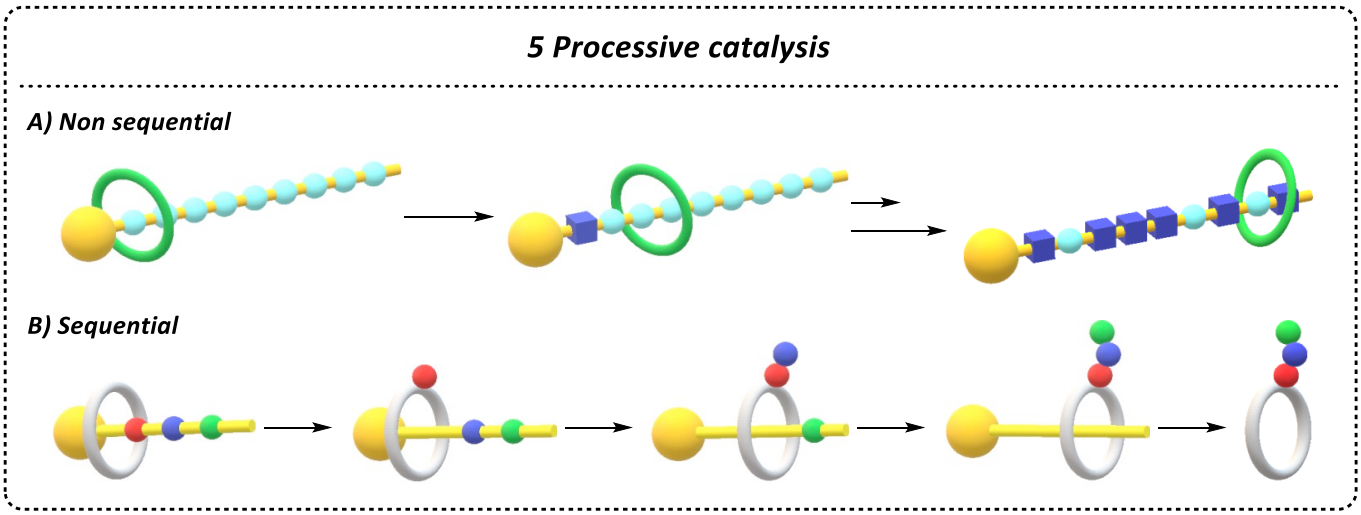

Fig. 45. Graphical summary for section 5 - Processive catalysis.

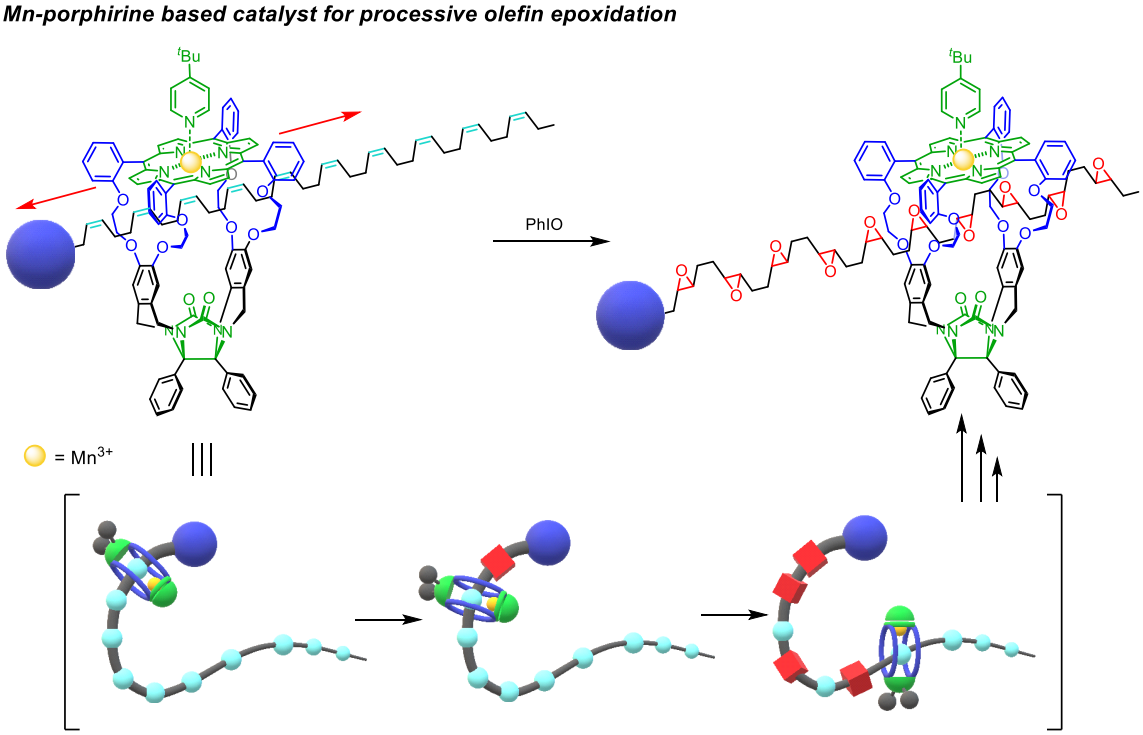

Fig. 46. Nolte and Rowan processive catalytic system. The polybutadiene polymer is threaded into the cavity of the Mn porphyrin catalyst. The oxidation occurs inside the cavity in the presence of 4-tert-butylpyridine with a hopping, random mechanism (ref 170a).

interactions, which favorably alter the energy profile of a reaction. Related consequences range from the acceleration of a reaction to the increase of its selectivity and even to the complete changeover of its mechanism, unlocking new reactivity or regulating its course. The potential of such an approach has long remained underexplored, as the early examples of supramolecular catalysis were mainly proof-of-principle studies,[175] often dealing with cleavage reactions. Conversely, current studies are turning their focus towards the selective formation of new bonds, paving the way for practical applications. These studies are now showcasing the unique advantages of the supramolecular strategy when compared to conventional catalysis, from the elegant cavity-assisted cyclization cascades[19b,24,36,38] to the recognition-driven remote or asymmetric functionalization[66,112,114,105a,118,120a,124,133,136] and the design of assembly lines for organic synthesis.[77-79,163,167,170] Given the similarity of the tools at disposal of supramolecular catalysis and biocatalysis and the inspiration of the former by the latter, a certain overlap among their outcomes has to be expected. Enzymes are typically far more efficient catalysts by virtue of their long evolution and sophistication, and have already found practical applications,[176] made even more feasible by the possibility to alter their natural reactivity via directed evolution[177] or the advent of artificial enzymes.[178] Notwithstanding, enzymes evolved as optimal catalysts in the cytosol, and their application in organic reactions faces some intrinsic problems, namely a too much high (substrate) specificity and a low tolerance to different reaction conditions (they usually work only in H_2O solvent, ambient temperature and narrow pH and ionic strength range). Conversely, artificial supramolecular catalysts have a simpler, more versatile structure that accommodates and tolerates multiple different substrates, reactants and reaction conditions, allowing for a broader scope. As a matter of fact, the two strategies can evolve to be complementary in scope and type of addressed problems. However, three open challenges still lie ahead of and limit the supramolecular approach:

i) The synthetic effort needed to prepare these catalysts has to be reduced. Although far less sophisticated than enzymes, molecular structures of supramolecular catalysts are often synthetically demanding, precluding their use on large scale. However, several steps have been already taken in this regard, and current supramolecular systems are already easier to prepare than early examples. Self-assembly, simplified designs and an improved recyclability are particularly promising.

ii) The scope of the catalyzed reactions needs to be broadened. So far, most examples have focused on simple or benchmark substrates, and have been too seldom applied to the problems typically faced in complex organic synthesis. Hence, the impact of supramolecular catalysis still remains limited and narrower than conventional catalysis approaches.

iii) The activity of most of the supramolecular catalysts needs to be substantially improved. No doubt, this step implies finding ways to avoid product inhibition. Given the pivotal role of this longstanding problem, a brief summary follows, which collect the main strategies successfully adopted so far for its solution.

- An evident change in the molecular shape going from the substrate to the product can reduce the affinity of the latter for the catalyst.[33,52] For instance, Zhang's group reported that cucurbit[8]uril hosts preferentially two molecules of Brooker's merocyanine with respect to their photodimerization

product.[179] As a result, effective turnover is achieved (almost quantitative yields at 1mol% cucurbituril loading, with multiple rounds of catalysis possible). Moreover, this concept also enabled the linear polymerization of difunctional merocyanine monomers, with the catalyst that threads along the chain.[180]

- Alternatively, turnover is facilitated when the product has a different electrostatic charge than the substrate(s). Such alteration can disrupt the product affinity for a charged supramolecular catalyst forcing its egress and replacement with new substrate molecules.[19c,22]
- Another strategy relies on the fast exchange of substrate and product on the supramolecular receptor.[16,82,96,103,121,16,82,83b,96,103,121] If the exchange rate is faster or at least comparable to the reaction rate and the catalyst does not significantly deactivate during the reaction,[100,181] the catalyst keeps working although the transformation slows down as it progresses due to the increase of the product concentration that saturate the reception. Nevertheless, the low amounts of substrate-catalyst adduct are still active and keep driving the reaction.
- Eventually, trapping the product in a final, irreversible step can also avoid inhibition. The free (unbound) product is subtracted from the equilibrium with its bound form by generating a new compound with no affinity for the supramolecular catalyst. Removal of the product from the catalyst allows catalytic turnover.[27]

In spite of these open challenges, supramolecular chemistry will certainly continue to disclose new opportunities for catalysis in the future and improve synthetic methods. It is not inconceivable the realization of an active complex consisting of assembled supramolecular catalysts, where a substrate is bound by the complex, subjected to subsequent, selective catalyzed reactions, and eventually released as the desired product like observed in enzymatic complexes. The seeds of such developments can be recognized throughout all this review.

Conflicts of interest

There are no conflicts to declare.

Acknowledgements

This work was supported by University of Roma La Sapienza (Progetti di Ricerca Grandi 2018, prot. n. RG1181641DCAAC4E) and Società Chimica Italiana.

References

1 (a) T. Brückl, R. D. Baxter, Y. Ishihara, P. S. Baran, *Acc. Chem. Res.*, 2012, **45**, 826–839; (b) J. F. Hartwig, *J. Am. Chem. Soc.*, 2016, **138**, 2–24.

2 (a) U. Biermann, W. Friedt, S. Lang, W. Lühs, G. Machmüller, J. O. Metzger, M. Rüsch gen. Klaas, H. J. Schäfer and M. P. Schneider, *Angew. Chem. Int. Ed.*, 2000, **39**, 2206–2224; (b) J. A. Gladysz, R. B. Bedford, M. Fujita, F. P. Gabbaï, K. I. Goldberg, P. L. Holland, J. L. Kiplinger, M. J. Krische, J. Louie, C. C. Lu, J. R. Norton, M. A. Petrukhina, T. Ren, S. S. Stahl, T. D. Tilley, C. E. Webster, M. C. White and G. T. Whiteker, *Organometallics*, 2014, **33**, 1505–1527.

3 J.-C. Wasilke, S. J. Obrey, R. T. Baker and G. C. Bazan, *Chem. Rev.*, 2005, **105**, 1001–1020.

4 (a) P. W. N. M. Van Leeuwen, Supramolecular Catalysis, Wiley-VCH, Mannheim, 2008; (b) M. Raynal, P. Ballester, A. Vidal-Ferran and P. W. N. M. van Leeuwen, *Chem. Soc. Rev.,* 2014, **43**, 1660–1773; (c) M. Raynal, P. Ballester, A. Vidal-Ferran and P. W. N. M. van Leeuwen, *Chem. Soc. Rev.,* 2014, **43**, 1734–1787.

5 See for example: (a) H. Eyring, R. Lowry and J. D. Spikes, *The Mechanism of Enzyme Action*, 1954, John Hopkins Press, Baltimore, (b) D. R. Storm and D. E. Koshland, Jr., *Proc. Nat. Acad. Sci. USA*, 1970, **66**, 445-452; (c) M. Page and W. P. Jencks, *Proc. Nat. Acad. Sci. USA*, 1971, **68**, 1678–1683; (d) W. P. Jencks, *Adv. Enzymol. Relat. Area Mol. Biol.* 1975, **43**, 219-410; (e) R. L. Schowen, "Catalytic Power and Transition State Stabilization", in *Transition States of Biochemical Process*, 1978, Plenum Press, New York; (f) F. H. Westheimer, *Adv. Phys. Org. Chem*, 1985, **21**,1-35; (g) F. M. Menger, *Acc. Chem. Res.* **1985**, *18*, 128-134; (h) F. M. Bruice, *Acc. Chem. Res.* **2002**, *35*, 139-148.

6 E. V. Anslyn and D. A. Dougherty, *Modern Physical Organic Chemistry*, University Science Book, Sansalito, CA, 2006.

7 L. Pauling, *Nature*, 1948, **161**, 707-709.

8 A. Fersht, *Enzyme Structure and Mechanism*, II Edition, W. H. Freeman & Co, New York, USA, 1985.

9 (a) A. B. Grommet, M. Feller and R. Klajn, *Nat. Nanotechnol.*, 2020, **15**, 256–271; (b) B. Mitschke, M. Turberg and B. List, *Chem*, 2020, **6**, 2515-2532.

10 (a) C. J. Brown, F. D. Toste, R. G. Bergman and K. N. Raymond, *Chem. Rev.,* 2015, **115**, 3012–3035; (b) V. Mouarrawis, R. Plessius, J. I. van der Vlugt and J. N. H. Reek, *Front. Chem.*, 2018, **6**, 623; (c) Z. Liu, H. Xiao, B. Zhang, H. Shen, L. Zhu and C. Li, *Angew. Chem. Int. Ed*., 2019, **58**, 2510–2513. (d) M. Morimoto, S. M. Bierschenk, K. T. Xia, R. G. Bergman, K. N. Raymond and F. D. Toste, *Nat. Catal.,* 2020, **3**, 969-984; (e) K. Wang, J. H. Jordan, X. Y. Hu and L. Wang, *Angew. Chem. Int. Ed.*, 2020, **59**, 13712–13721.

11 G. Crini, S. Fourmentin, É. Fenyvesi, G. Torri, M. Fourmentin and N. Morin-Crini, *Environ. Chem. Lett.*, 2018, **16**, 1361–1375.

12 (a) K. I. Assaf and W. M. Nau, *Chem. Soc. Rev.*, 2015, **44**, 394–418; (b) B. Tang, J. Zhao, J.-F. Xu and X. Zhang, *Chem. – A Eur. J.*, 2020, **26**, 15446–15460.

13 Y. Yu, J. M. Yang and J. Rebek, Jr, *Chem*, 2020, **6,** 1265–1274.

14 D. Zhang, A. Martinez and J.-P. Dutasta, *Chem. Rev.*, 2017, **117**, 4900–4942.

15 R. Chakrabarty, P. S. Mukherjee and P. J. Stang, *Chem. Rev.*, 2011, **111**, 6810–6918.
16 (a) Q. Zhang, L. Catti and K. Tiefenbacher, *Acc. Chem. Res.*, 2018, **51**, 2107–2114; (b) C. Gaeta, P. La Manna, M. De Rosa, A. Soriente, C. Talotta and P. Neri, *ChemCatChem*, 2020, DOI:10.1002/cctc.202001570.
17 (a) A. J. Kirby, *Adv. Phys. Org. Chem.*, 1980, **17**, 183–278. (b) L. Mandolini,, in *Adv. Phys. Org. Chem.*, 1986, **22**, 1–111; (c) R. Cacciapaglia, S. Di Stefano and L. Mandolini, *Acc. Chem. Res.*, 2004, **37**, 113–122; (d) S. Di Stefano, R. Cacciapaglia and L. Mandolini, *Eur. J. Org. Chem.*, 2014, 7304–7315; (e) S. Di Stefano and G. Ercolani, *Adv. Phys. Org. Chem.*, 2016, **50**, 1–76; (f) P. Motloch and C. A. Hunter, *Adv. Phys. Org. Chem.*, 2016, **50**, 77–118; (g) S. Di Stefano and L. Mandolini, *Phys. Chem. Chem. Phys.*, 2019, **21**, 955–987.
18 F. Yu, D. Poole III, S. Mathew, N. Yan, J. Hessels, N. Orth, I. Ivanović-Burmazović and J. N. H. Reek, *Angew. Chem. Int. Ed.*, 2018, **57**, 11247–11251.
19 (a) J. Kang and J. Rebek, *Nature*, 1997, **385**, 50–52; (b) D. Samanta, S. Mukherjee, Y. P. Patil and P. S. Mukherjee, *Chem. Eur. J.*, 2012, **18**, 12322–12329; (c) Q.-Q. Wang, S. Gonell, S. H. A. M. Leenders, M. Dürr, I. Ivanović-Burmazović and J. N. H. Reek, *Nat. Chem.*, 2016, **8**, 225; (d) A. Palma, M. Artelsmair, G. Wu, X. Lu, S. J. Barrow, N. Uddin, E. Rosta, E. Masson and O. A. Scherman, *Angew. Chem. Int. Ed.*, 2017, **56**, 15688–15692; (e) J. A. Finbloom, K. Han, C. C. Slack, A. L. Furst and M. B. Francis, *J. Am. Chem. Soc.*, 2017, **139**, 9691–9697; (f) Gonell, X. Caumes, N. Orth, I. Ivanović-Burmazović and J. N. H. Reek, *Chem. Sci.*, 2019, **10**, 1316–1321.
20 (a) M. Yoshizawa, Y. Takeyama, T. Okano and M. Fujita, *J. Am. Chem. Soc.*, 2003, **125**, 3243–3247; (b) S. Horiuchi, Y. Nishioka, T. Murase and M. Fujita, *Chem. Commun.*, 2010, **46**, 3460–3462; (c) Y. Nishioka, T. Yamaguchi, M. Yoshizawa and M. Fujita, *J. Am. Chem. Soc.*, 2007, **129**, 7000–7001; (d) T. Murase, S. Horiuchi and M. Fujita, *J. Am. Chem. Soc.*, 2010, **132**, 2866–2867.
21 (a) Y. Fang, Z. Xiao, A. Kirchon, J. Li, F. Jin, T. Togo, L. Zhang, C. Zhu and H.-C. Zhou, *Chem. Sci.*, 2019, **10**, 3529–3534. (b) J. L. Bolliger, A. M. Belenguer and J. R. Nitschke, *Angew. Chem. Int. Ed.*, 2013, **52**, 7958–7962.
22 (a) W. Cullen, M. C. Misuraca, C. A. Hunter, N. H. Williams and M. D. Ward, *Nat. Chem.*, 2016, **8**, 231–236; (b) W. Cullen, A. J. Metherell, A. B. Wragg, C. G. P. Taylor, N. H. Williams and M. D. Ward, *J. Am. Chem. Soc.*, 2018, **140**, 2821–2828. (c) M. D. Ward, C. A. Hunter and N. H. Williams, *Acc. Chem. Res.*, 2018, **51**, 2073–2082; (d) C. G. P. Taylor, A. J. Metherell, S. P. Argent, F. M. Ashour, N. H. Williams and M. D. Ward, *Chem. Eur. J.*, 2020, **26**, 3065–3073.
23 S. Mecozzi and J. Rebek, Jr, *Chem.Eur. J.*, 1998, **4**, 1016–1022.
24 (a) S. Mosca, Y. Yu, J. V Gavette, K.-D. Zhang and J. Rebek, *J. Am. Chem. Soc.*, 2015, **137**, 14582–14585; (b) Q. Shi, D. Masseroni and J. Rebek, Jr, *J. Am. Chem. Soc.*, 2016, **138**, 10846–10848; (c) N.-W. Wu, I. D. Petsalakis, G. Theodorakopoulos, Y. Yu and J. Rebek Jr., *Angew. Chem. Int. Ed.*, 2018, **57**, 15091–15095.
25 (a) D. Fiedler, R. G. Bergman and K. N. Raymond, *Angew. Chem. Int. Ed.*, 2004, **43**, 6748–6751; (b) C. J. Hastings, D. Fiedler, R. G. Bergman and K. N. Raymond, *J. Am. Chem. Soc.*, 2008, **130**, 10977–10983; (c) C. J. Brown, R. G. Bergman and K. N. Raymond, *J. Am. Chem. Soc.*, 2009, **131**, 17530–17531.
26 C. M. Hong, R. G. Bergman, K. N. Raymond and F. D. Toste, *Acc. Chem. Res.*, 2018, **51**, 2447–2455.
27 C. J. Hastings, M. D. Pluth, R. G. Bergman and K. N. Raymond, *J. Am. Chem. Soc.*, 2010, **132**, 6938–6940.
28 C. J. Hastings, R. G. Bergman and K. N. Raymond, *Chem.Eur. J.*, 2014, **20**, 3966–3973.
29 C. M. Hong, M. Morimoto, E. A. Kapustin, N. Alzakhem, R. G. Bergman, K. N. Raymond and F. D. Toste, *J. Am. Chem. Soc.*, 2018, **140**, 6591–6595.
30 K. Wang, X. Cai, W. Yao, D. Tang, R. Kataria, H. S. Ashbaugh, L. D. Byers and B. C. Gibb, *J. Am. Chem. Soc.*, 2019, **141**, 6740–6747.
31 H. Eyring, R. Lowry and J. D. Spikes, *The Mechanism of Enzyme Action*, Baltimore, Md, 1954.
32 H. Takezawa, K. Shitozawa and M. Fujita, *Nat. Chem.*, 2020, **12**, 574–578.
33 M. D. Pluth, R. G. Bergman and K. N. Raymond, *Science*, 2007, **316**, 85–88.
34 M. D. Pluth, R. G. Bergman and K. N. Raymond, *J. Am. Chem. Soc.*, 2008, **130**, 11423–11429.
35 T. Murase, Y. Nishijima and M. Fujita, *J. Am. Chem. Soc.*, 2012, **134**, 162–164.
36 Q. Zhang and K. Tiefenbacher, *Nat. Chem.*, 2015, **7**, 197–202.
37 (a) Q. Zhang and K. Tiefenbacher, *J. Am. Chem. Soc.*, 2013, **135**, 16213–16219; (b) S. Merget, L. Catti, G. Piccini and K. Tiefenbacher, *J. Am. Chem. Soc.*, 2020, **142**, 4400–4410.
38 (a) Q. Zhang, L. Catti, J. Pleiss and K. Tiefenbacher, *J. Am. Chem. Soc.*, 2017, **139**, 11482–11492; (b) Q. Zhang, J. Rinkel, B. Goldfuss, J. S. Dickschat and K. Tiefenbacher, *Nat. Catal.*, 2018, **1**, 609–615; (c) Q. Zhang and K. Tiefenbacher, *Angew. Chem. Int. Ed.*, 2019, **58**, 12688–12695; (d) L.-D. Syntrivanis, I. Némethová, D. Schmid, S. Levi, A. Prescimone, F. Bissegger, D. T. Major and K. Tiefenbacher, *J. Am. Chem. Soc.*, 2020, **142**, 5894–5900.
39 L. Catti and K. Tiefenbacher, *Angew. Chem. Int. Ed.*, 2018, **57**, 14589–14592.
40 W. Zhang, G. Cheng, G. L. Haller, Y. Liu and J. A. Lercher, *ACS Catal.*, 2020, **10**, 13371–13376.
41 P. La Manna, C. Talotta, G. Floresta, M. De Rosa, A. Soriente, A. Rescifina, C. Gaeta and P. Neri, *Angew. Chem. Int. Ed.*, 2018, **57**, 5423–5428.
42 D. M. Kaphan, M. D. Levin, R. G. Bergman, K. N. Raymond and F. D. Toste, *Science* 2015, **350**, 1235–1238.
43 T. A. Bender, M. Morimoto, R. G. Bergman, K. N. Raymond and F. D. Toste, *J. Am. Chem. Soc.*, 2019, **141**, 1701–1706.
44 W. Cullen, H. Takezawa and M. Fujita, *Angew. Chem. Int. Ed.*, 2019, **58**, 9171–9173.
45 (a) M. Yoshizawa, S. Miyagi, M. Kawano, K. Ishiguro and M. Fujita, *J. Am. Chem. Soc.*, 2004, **126**, 9172–9173; (b) T. Furusawa, M. Kawano and M. Fujita, *Angew. Chem. Int. Ed.*, 2007, **46**, 5717–5719; (c) T. Yamaguchi and M. Fujita, *Angew. Chem. Int. Ed.*, 2008, **47**, 2067–2069; (d) D. M. Dalton, S. R. Ellis, E. M. Nichols, R. A. Mathies, F. D. Toste, R. G. Bergman and K. N. Raymond, *J. Am. Chem. Soc.*, 2015, **137**, 10128–10131; (e) J. Guo, Y.-W. Xu, K. Li, L.-M. Xiao, S. Chen, K. Wu, X.-D. Chen, Y.-Z. Fan, J.-M. Liu and C.-Y. Su, *Angew. Chem. Int. Ed.*, 2017, **56**, 3852–3856.
46 W. M. Hart-Cooper, K. N. Clary, F. D. Toste, R. G. Bergman and K. N. Raymond, *J. Am. Chem. Soc.*, 2012, **134**, 17873–17876.
47 A. Cavarzan, A. Scarso, P. Sgarbossa, G. Strukul and J. N. H. Reek, *J. Am. Chem. Soc.*, 2011, **133**, 2848–2851.
48 A. C. H. Jans, X. Caumes and J. N. H. Reek, *ChemCatChem*, 2019, **11**, 287–297.
49 C. Zhao, F. D. Toste, K. N. Raymond and R. G. Bergman, *J. Am. Chem. Soc.*, 2014, **136**, 14409–14412.
50 (a) P. Restorp and J. Rebek, Jr, *J. Am. Chem. Soc.*, 2008, **130**, 11850–11851; (b) S. R. Shenoy, F. R. Pinacho Crisóstomo, T. Iwasawa and J. Rebek, Jr, *J. Am. Chem. Soc.*, 2008, **130**, 5658–5659; (c) F. R. Pinacho Crisóstomo, A. Lledó, S. R. Shenoy, T. Iwasawa and J. Rebek, Jr, *J. Am. Chem. Soc.*, 2009, **131**, 7402–7410; (d) P. Howlader, P. Das, E. Zangrando and P. S. Mukherjee, *J. Am. Chem. Soc.*, 2016, **138**, 1668–1676.
51 C. Ngai, C. M. Sanchez-Marsetti, W. H. Harman and R. J. Hooley, *Angew. Chem. Int. Ed.*, 2020, **59**, 23505–23509.

52 M. Yoshizawa, M. Tamura and M. Fujita, *Science*, 2006, **312**, 251–255.

53 (a) V. Martí-Centelles, A. L. Lawrence and P. J. Lusby, *J. Am. Chem. Soc.*, 2018, **140**, 2862–2868. (b) K. Ono, M. Niibe and N. Iwasawa, *Chem. Sci.* 2019, **10**, 7627–7632.

54 (a) Y. Nishioka, T. Yamaguchi, M. Kawano and M. Fujita, *J. Am. Chem. Soc.*, 2008, **130**, 8160–8161; (b) C. Tugny, N. del Rio, M. Koohgard, N. Vanthuyne, D. Lesage, K. Bijouard, P. Zhang, J. Meijide Suárez, S. Roland, E. Derat, O. Bistri-Aslanoff, M. Sollogoub, L. Fensterbank and V. Mouriès-Mansuy, *ACS Catal.*, 2020, **10**, 5964–5972.

55 (a) A. Nakamura and Y. Inoue, *J. Am. Chem. Soc.*, 2003, **125**, 966–972; (b) X. Wei, W. Wu, R. Matsushita, Z. Yan, D. Zhou, J. J. Chruma, M. Nishijima, G. Fukuhara, T. Mori, Y. Inoue and C. Yang, *J. Am. Chem. Soc.*, 2018, **140**, 3959–3974; (c) M. Rao, K. Kanagaraj, C. Fan, J. Ji, C. Xiao, X. Wei, W. Wu and C. Yang, *Org. Lett.*, 2018, **20**, 1680–1683; (d) J. Ji, W. Wu, W. Liang, G. Cheng, R. Matsushita, Z. Yan, X. Wei, M. Rao, D.-Q. Yuan, G. Fukuhara, T. Mori, Y. Inoue and C. Yang, *J. Am. Chem. Soc.*, 2019, **141**, 9225–9238; (e) J.-S. Wang, K. Wu, C. Yin, K. Li, Y. Huang, J. Ruan, X. Feng, P. Hu and C.-Y. Su, *Nat. Commun.*, 2020, **11**, 4675.

56 P. Zhang, J. Meijide Suárez, T. Driant, E. Derat, Y. Zhang, M. Ménand, S. Roland and M. Sollogoub, *Angew. Chem. Int. Ed.*, 2017, **56**, 10821–10825.

57 (a) M. Kuil, T. Soltner, P. W. N. M. van Leeuwen and J. N. H. Reek, *J. Am. Chem. Soc.*, 2006, **128**, 11344–11345; (b) V. Bocokić, A. Kalkan, M. Lutz, A. L. Spek, D. T. Gryko and J. N. H. Reek, *Nat. Commun.*, 2013, **4**, 2670; (c) S. S. Nurttila, P. R. Linnebank, T. Krachko and J. N. H. Reek, *ACS Catal.*, 2018, **8**, 3469–3488.

58 M. Guitet, P. Zhang, F. Marcelo, C. Tugny, J. Jiménez-Barbero, O. Buriez, C. Amatore, V. Mouriès-Mansuy, J.-P. Goddard, L. Fensterbank, Y. Zhang, S. Roland, M. Ménand and M. Sollogoub, *Angew. Chem. Int. Ed.*, 2013, **52**, 7213–7218.

59 C. García-Simón, R. Gramage-Doria, S. Raoufmoghaddam, T. Parella, M. Costas, X. Ribas and J. N. H. Reek, *J. Am. Chem. Soc.*, 2015, **137**, 2680–2687.

60 T. M. Bräuer, Q. Zhang and K. Tiefenbacher, *Angew. Chem. Int. Ed.,* 2016, **55**, 7698–7701.

61 T. A. Bender, R. G. Bergman, K. N. Raymond and F. D. Toste, *J. Am. Chem. Soc.*, 2019, **141**, 11806–11810.

62 H. Takezawa, T. Kanda, H. Nanjo and M. Fujita, *J. Am. Chem. Soc.*, 2019, **141**, 5112–5115.

63 D. Masseroni, S. Mosca, M. P. Mower, D. G. Blackmond and J. Rebek Jr., *Angew. Chem. Int. Ed.*, 2016, **55**, 8290–8293.

64 R. Breslow and P. Campbell, *J. Am. Chem. Soc.*, 1969, **91**, 3085.

65 M. Sharafi, K. T. McKay, M. Ivancic, D. R. McCarthy, N. Dudkina, K. E. Murphy, S. C. Rajappan, J. P. Campbell, Y. Shen, A. R. Badireddy, J. Li and S. T. Schneebeli, *Chem*, 2020, **6**, 1469–1494.

66 C. Fuertes-Espinosa, C. García-Simón, M. Pujals, M. Garcia-Borràs, L. Gómez, T. Parella, J. Juanhuix, I. Imaz, D. Maspoch, M. Costas and X. Ribas, *Chem*, 2020, **6**, 169–186.

67 (a) W. Brenner, T. K. Ronson and J. R. Nitschke, *J. Am. Chem. Soc.*, 2017, **139**, 75–78; (b) Y. Xu, R. Kaur, B. Wang, M. B. Minameyer, S. Gsänger, B. Meyer, T. Drewello, D. M. Guldi and M. von Delius, *J. Am. Chem. Soc.*, 2018, **140**, 13413–13420. (c) V. Leonhardt, S. Fimmel, A.-M. Krause and F. Beuerle, *Chem. Sci.*, 2020, **11**, 8409–8415; (d) E. Ubasart, O. Borodin, C. Fuertes-Espinosa, Y. Xu, C. García-Simón, L. Gómez, J. Juanhuix, F. Gándara, I. Imaz, D. Maspoch, M. von Delius and X. Ribas, *Nat. Chem.*, 2021, DOI:10.1038/s41557-021-00658-6.

68 S. Giust, G. La Sorella, L. Sperni, G. Strukul and A. Scarso, *Chem. Commun.*, 2015, **51**, 1658–1661.

69 (a) A. Cavarzan, J. N. H. Reek, F. Trentin, A. Scarso and G. Strukul, *Catal. Sci. Technol.*, 2013, **3**, 2898–2901; (b) L. R. Holloway, P. M. Bogie, Y. Lyon, C. Ngai, T. F. Miller, R. R. Julian and R. J. Hooley, *J. Am. Chem. Soc.*, 2018, **140**, 8078–8081; (c) S. S. Nurttila, W. Brenner, J. Mosquera, K. M. van Vliet, J. R. Nitschke and J. N. H. Reek, *Chem. Eur. J.*, 2019, **25**, 609–620.

70 M. Otte, *ACS Catal.*, 2016, **6**, 6491–6510.

71 E. Lindbäck, S. Dawaigher and K. Wärnmark, *Chem. Eur. J.*, 2014, **20**, 13432–13481.

72 K. Suzuki, S. Sato and M. Fujita, *Nat. Chem.*, 2010, **2**, 25–29.

73 (a) B. Mondal, K. Acharyya, P. Howlader and P. S. Mukherjee, *J. Am. Chem. Soc.*, 2016, **138**, 1709–1716. (b) S. Wang, X. Gao, X. Hang, X. Zhu, H. Han, W. Liao and W. Chen, *J. Am. Chem. Soc.*, 2016, **138**, 16236–16239; (c) B. Chen, C. Fang, P. Liu and J. M. Ready, *Angew. Chem. Int. Ed.*, 2017, **56**, 8780–8784; (d) Y.-T. Xu, X. Xiao, Z.-M. Ye, S. Zhao, R. Shen, C.-T. He, J.-P. Zhang, Y. Li and X.-M. Chen, *J. Am. Chem. Soc.*, 2017, **139**, 5285–5288; (e) B. Mondal and P. S. Mukherjee, *J. Am. Chem. Soc.*, 2018, **140**, 12592–12601; (f) Y. Fang, J. L. Li, T. Togo, F. Y. Jin, Z. F. Xiao, L. J. Liu, H. Drake, X. Z. Lian and H. C. Zhou, *Chem*, 2018, **4**, 555–563; (g) N. Sun, C. Wang, H. Wang, L. Yang, P. Jin, W. Zhang and J. Jiang, *Angew. Chem. Int. Ed.*, 2019, **58**, 18011–18016.

74 (a) A. Galan and P. Ballester, *Chem. Soc. Rev.*, 2016, **45**, 1720-1737; (b) D. J Cram, M. E. Tunner and R. Thomas*, Angew. Chem. Int. Ed.*, 1991, **30**, 1024-1027; (c) P. Mal, B. Breiner, K. Rissanen and J. R. Nitschke, *Science*, 2009, **324**, 1697-1699; (d) T. Iwasawa, R. J. Hooley and J. Rebek, Jr., *Science*, 2007, **317**, 493–496

75 M. Otte, P. F. Kuijpers, O. Troeppner, I. Ivanović-Burmazović, J. N. H. Reek and B. de Bruin, *Chem.Eur. J.*, 2014, **20**, 4880–4884.

76 (a) P. F. Kuijpers, M. Otte, M. Dürr, I. Ivanović-Burmazović, J. N. H. Reek and B. de Bruin, *ACS Catal.*, 2016, **6**, 3106–3112; (b) G. Qiu, P. Nava, A. Martinez and C. Colomban, *Chem. Commun.*, 2021, **57**, 2281-2284.

77 Z. J. Wang, K. N. Clary, R. G. Bergman, K. N. Raymond and F. D. Toste, *Nat. Chem.*, 2013, **5**, 100–103.

78 Y. Ueda, H. Ito, D. Fujita and M. Fujita, *J. Am. Chem. Soc.*, 2017, **139**, 6090–6093.

79 A. G. Salles, S. Zarra, R. M. Turner and J. R. Nitschke, *J. Am. Chem. Soc.*, 2013, **135**, 19143–19146.

80 R. Breslow, *Acc. Chem. Res.,* 1995, **28**, 146–153.

81 (a) J. Meeuwissen and J. N. H. Reek, *Nat. Chem.,* 2010, **2**, 615–621; (b) P. P. Dydio and J. N. H. Reek, *Chem. Sci.,* 2014, **5**, 2135–2145; (c) H. J. Davis and R. J. Phipps, *Chem. Sci.,* 2017, **8**, 864–877.

82 (a) J. Trouve and R. Gramage-doria, *Chem. Soc. Rev.,* 2021, **50**, 3565–3584; (b) A. Fanourakis, P. J. Docherty, P. Chuentragool and R. J. Phipps, *ACS Catal.* 2020, **10**, 10672–10714.

83 N. R. Mote and S. H. Chikkali, *Chem. Asian J.,* 2018*,* **13***,* 3623-2646; (b) F. Burg and T. Bach, *J. Org. Chem.* 2019, **84**, 8815-8836.

84 M. Li, J. S. Fossey, T. D. James, Boron: Sensing, Synthesis and Supramolecular Self-Assembly Meng Li, John S Fossey, Tony D James, Royal Society of Chemistry, London, 2015.

85 S. Di Stefano, G. Capocasa and L. Mandolini, *Eur. J. Org. Chem.*, 2020, **23**, 3340-3350.

86 (a) G. Crini, *Chem. Rev.*, 2014, **114**, 10940–10975; (b) C. C. Bai, B. R. Tian, T. Zhao, Q. Huang and Z. Z. Wang, *Molecules*, 2017, **22**, 1475-1691; (c) L. Marinescu and M. Bols, *Curr. Org. Chem.*, 2010, **14**, 1380-1398.

87 G. Huang and G. Dong, *Acc. Chem. Res*., 2017, **50**, 465–471.

88 (a) J. A. Labinger and J. E. Bercaw, *Nature*, 2002, **417**, 507–514; (b) T. Newhouse and P. S. Baran*, Angew. Chem. Int. Ed.*, 2011, **50**, 3362–3374; (c) K. Godula, D. Sames, *Science*, 2006, **312**, 67–73; (d) B. A. Arndtsen, R. G. Bergman, T. A. Mobley and T. H. Peterson, *Acc. Chem. Res.* 1995, **28**, 154–162; (e) S. R. Neufeldt and M. S. Sanford, *Acc. Chem. Res.* 2012, **45**, 936–946.

89 (a) D. H. R. Barton and D. Doller, *Acc. Chem. Res.,* 1992, **25**, 504-512; (c) R.Breslow, A. B. Brown, R. D. McCullough and P. W. White, *J. Am. Chem. Soc.,* 1989, **111**, 4517-4518; (d) W. R. Gutekunst and P. S. Baran, *Chem. Soc. Rev.,* 2011, **40**, 1976–1991. (e) J. F. Hartwig, *J. Am. Chem. Soc.,* 2016, **138**, 2–24; (f) J. F. Hartwig and M. A. Larsen, *ACS Cent. Sci.,* 2016, **2**, 281–292; (g) M. Milan, M. Salamone, M. Costas and M. Bietti, *Acc. Chem. Res.,* 2018, **51**, 1984–1995; (h) M. Bietti, *Angew. Chem. Int. Ed.,* 2018, **57**, 16618–16637.

90 (a) M.C. White, *Science,* 2012, **335**, 807-809; (b) K. Godula and D. Sames, *Science,* 2006, **312**, 67-72 (c) J. A. Labinger and J. E. Bercaw, *Nature,* 2002, **417**, 507-514; (d) H. Kunz and H. Waldmann, *Comprehensive Organic Chemistry,* 1991, **6**, 631-701.

91 R. Breslow, *Chem. Soc. Rev.,* 1972, **1**, 553-580.

92 R. Breslow, X Zhang and Y. Huang, *J. Am. Chem. Soc.,* 1997, **119**, 4535-4536.

93 J. Yang, B. Gabriele, S. Belvedere, Y. Huang and R. Breslow, *J. Org. Chem.,* 2002, **67**, 5057–5067.

94 J. Yang and R. Breslow, *Angew. Chem. Int. Ed.,* 2000, **39**, 2692–2695.

95 S. Das, C. D. Incarvito, R. H. Crabtree and G. W. Brudvig, *Science,* 2006, **312**, 1941–1943.

96 D. Vidal, G. Olivo and M. Costas, *Chem. Eur. J.,* 2018, **24**, 5042–5054.

97 G. Olivo, G. Farinelli, A. Barbieri, O. Lanzalunga, S. Di Stefano and M. Costas, *Angew. Chem. Int. Ed.,* 2017, **56**, 16347-16351.

98 (a) M. C. White and J. Zhao, *J. Am. Chem. Soc.,* 2018, **140**, 13988–14009; (b) L. Vicens, G. Olivo and M. Costas, *ACS Catal.,* 2020, **10**, 8611–8631.

99 M. Knezevic, M. Heilmann, G. M. Piccini and K. Tiefenbacher, *Angew. Chem. Int. Ed.,* 2020, **59**, 12387 -12391.

100 G. Olivo, G. Capocasa, B. Ticconi, O. Lanzalunga, S. Di Stefano and M. Costas, *Angew. Chem. Int. Ed.,* 2020, **59** 12703-12708.

101 J. F. Hartwig, *Chem. Soc. Rev.,* 2011, **40**, 1992-2002.

102 N. Miyaura, T. Yanagi and A. Suzuki, *Synth. Commun.* 1981, **11**, 513-519.

103 Y. Kuninobu and T. Torigoe, *Org. Biomol. Chem.,* 2020, **18**, 4126-4134.

104 Y. Kuninobu, H. Ida, M. Nishi and M. Kanai, *Nat. Chem.,* 2015, **7**, 712-717.

105 H. J. Davis, M. T. Mihai and R. J. Phipps, *J. Am. Chem. Soc.,* 2016, **138**, 12759-12762; (b) M. T. Mihai, H. J. M. T. Mihai, H. J. Davis, G. R. Genov and R. J. Phipps, *ACS Catal.,* 2018, 8, 3764–3769 (c) H. J. Davis, G. R. Genov, and R. J. Phipps, *Angew. Chem. Int. Ed.,* 2017, **56**, 13351 –13355.

106 (a) S. Okumura, S. Tang, T. Saito, K. Semba, S. Sakaki and Y. Nakao, *J. Am. Chem. Soc.,* 2016, **138**, 14699–14704; (b) L. Yang, N. Uemura and Y. Nakao, *J. Am. Chem. Soc.,* 2019, **141**, 7972–7979.

107 (a) H. L. Li, Y. Kuninobu and M. Kanai, *Angew. Chem. Int. Ed.,* 2017, **56**, 1495-1499; (b) Y. Kuninobu, *Synlett,* 2018, **29**, 2093–2107; (c) Y. Kuninobu, *J. Synth. Org. Chem., Jpn.,* 2016, **71**, 1058-1068.

108 S.-T. Bai, C. B. Bheeter and J. N. H. Reek, *Angew. Chem. Int. Ed.,* 2019, **58**, 13039–13043.

109 M. E. Hoque, R. Bisht, C. Haldar, and B. Chattopadhyay, *J. Am. Chem. Soc.,* 2017, **139**, 7745-7748.

110 (a) Y. Kuroda and Y. Nakao, *Chem. Lett.,* 2019, **48**, 1092–1100.

111 (a) M. T. Mihai, B. D. Williams and R. J. Phipps, *J. Am. Chem. Soc.*, 2019, **141**, 15477–15482; (b) L. Yang, K. Semba and Y. Nakao, *Angew. Chem. Int. Ed.*, 2017, **56**, 4853–4857; (c) J. R. Montero Bastidas, T. J. Oleskey, S. L. Miller, M. R. Smith and R. E. Maleczka, *J. Am. Chem. Soc.*, 2019, **141**, 15483–15487.

112 (a) Z. Zhang, K. Tanaka and J.-Q. Yu, *Nature*, 2017, **543**, 538–542; (b) A. Dey, S. K. Sinha, T. K. Achar and D. Maiti, *Angew. Chem. Int. Ed.*, 2019, **58**, 10820–10843; (c) G. Meng, N. Y. S. Lam, E. L. Lucas, T. G. Saint-Denis, P. Verma, N. Chekshin and J.-Q. Yu, *J. Am. Chem. Soc.*, 2020, **142**, 10571–10591.

113 P. A. Lichtor and S. J. Miller, *ACS Comb. Sci.,* 2011, **13**, 321–326.

114 P. A. Lichtor and S. J. Miller, *Nat. Chem.,* 2012, **4**, 990-995.

115 (a) W. A. Golding, R. Pearce-Higgins and R. J. Phipps, *J. Am. Chem. Soc.,* 2018, **140**, 13570–13574; (b) W. A. Golding and R. J. Phipps, *Chem. Sci.*, 2020, **11**, 3022-3027.

116 *IUPAC. Compendium of Chemical Terminology, 2nd ed. (the "Gold Book"). Compiled by A. D. McNaught and A. Wilkinson. Blackwell Scientific Publications, Oxford (1997). Online version (2019-) created by S. J. Chalk. ISBN 0-9678550-9-8. https://doi.org/10.1351/goldbook.*

117 (a) R. Franke, D. Selent and A. Börner, *Chem. Rev.,* 2012, **112**, 5675–5732; (b) B. M. Trost, *Acc. Chem. Res.,* 2002, **35**, 695–705; (c) B. Breit and W. Seiche, *Synthesis,* 2001, **2001**, 1-3; (d) K. Weissermel, H.-J. Arpe, Industrial Organic Chemistry, WileyVCH, Weinheim, 2003, pp. 127–144; (e) J. J. Carbó, F. Maseras, C. Bo and P. W. N. M. van Leeuwen, *J. Am. Chem. Soc.*, 2001, **123**, 7630–7637; (f) S. A. Decker and T. R. Cundari, *J. Organomet. Chem.,* 2001, **635**, 132–141; (g) E. Zuidema, L. Escorihuela, T. Eichelsheim, J. J. Carbó, C. Bo, P. C. J. Kamer and P. W. N. M. van Leeuwen, *Chem. Eur. J.,* 2008, **14**, 1843–1853; (h) P. W. N. M. van Leeuwen, Homogeneous Catalysis: Understanding the Art, Kluwer Academic Publishers, Dordrecht, 2004.

118 T. Šmejkal and B. Breit, *Angew. Chem. Int. Ed.,* 2008, **47**, 311 –315.

119 T. Šmejkal, D. Gribkov, J. Geier, M. Keller and B. Breit, *Chem. Eur. J.,* 2010, **16**, 2470–2478.

120 (a) P. Dydio and J. N. H. Reek, *Chem. Sci.,* 2014, **5**, 2135-2145; (b) P. Dydio, W. I. Dzik, M. Lutz, B. de Bruin and J. N. H. Reek, *Angew. Chem. Int. Ed.,* 2011, **50**, 396 –400; (c) P. Dydio, R. J. Detz and J. N. H. Reek, *J. Am. Chem. Soc.,* 2013, **135**, 10817−10828; (d) P. Dydio and J. N. H. Reek, *Angew. Chem.,* 2013, **125**, 3970 –3974; (e) P. R. Linnebank, S. F. Ferreira, A. M. Kluwer and J. N. H. Reek, *Chem. Eur. J.*, 2020, **26**, 8214-8219.

121 S. S. Nurttila, P. R. Linnebank, T. Krachko and J. N. H. Reek, *ACS Catal.,* 2018, **8**, 3469–3488.

122 J. Halpern, *Science*, 1982, **217**, 401-407.

123 T. G. Saint-Denis, R. Zhu, G. Chen, Q. Wu and J. Yu, *Science,* 2018, **359**, 759-772.

124 R. L. Reyes, M. Sato, T. Iwai, K. Suzuki, S. Maeda and M. Sawamura, *Science,* 2020**, 369**, 970–974.

125 J. R. Frost, S. M. Huber, S. Breitenlechner, C. Bannwarth and T. Bach, *Angew. Chem. Int. Ed.,* 2015, **54**, 691 –695.

126 (a) F. Burg, M. Gicquel, S. Breitenlechner, A. Pöthig and T. Bach, *Angew. Chem. Int. Ed.,* 2018, **57**, 2953-2957; (b) F. Burg, S. Breitenlechner, C. Jandl and T. Bach, *Chem. Sci.,* 2020, **11**, 2121-2130.

127 R. R. Annapureddy, C. Jandl and T. Bach, *J. Am. Chem. Soc.* 2020, **142**, 7374-7378.

128 T. Höke, E. Herdtweck and T. Bach, *Chem. Commun.* 2013, **49**, 8009-8011.

129 (a) T. Bach, *Synthesis,* 1998, **5**, 683-703; (b) D. De Keukeleire and S.-L. He, *Chem. Rev.,* 1993, **93**, 359-380; (c)Y. Inoue, *Chem. Rev.,* 1992, *92*, 741-770; (d) S. L. Schreiber, *Science,* 1985, **227**, 857-863.

130 (a) A. Bauer, F. Westkämper, S. Grimme, and T. Bach, *Nature*, 2005, **436**, 1139–1140; (b) P. Wessig, *Angew. Chem. Int. Ed.,* 2006, **45**, 6640–6642.

131 T. Bach and H. Bergmann, *J. Am. Chem. Soc.,* 2000, **122**, 11525-11526.

132 (a) C. Müller, A. Bauer and T. Bach, *Angew. Chem. Int. Ed.,* 2009, **48**, 6640–6642; (b) S. Brandes, P. Selig and T. Bach, *Synlett,* 2004, **14**, 2588-2590; (c) P. Selig and T. Bach, *J. Org. Chem.,* 2006, **71**, 5662-5673 (d) T. Bach, H. Bergmann and K. Harms, *Org. Lett.,* 2001, **3**, 601-603 (e) A. Tröster, R. Alonso, A. Bauer and T. Bach, *J. Am. Chem. Soc.,* 2016, **138**, 7808–7811.

133 A. Hölzl-Hobmeier, A. Bauer, A. V. Silva, S. M. Huber, C. Bannwarth and T. Bach, *Nature,* 2018, **564**, 240-243.

134 A. Tröster, A. Bauer, C. Jandl and T. Bach, *Angew. Chem. Int. Ed.,* 2019, **58**, 3538–3541.

135 P. Dydio, C. Rubay, T. Gadzikwa, M. Lutz and J. N. H. Reek, *J. Am. Chem. Soc.,* 2011, **133**, 17176–17179.

136 G. R. Genov, J. L. Douthwaite, A. S. K. Lahdenperä, D. C. Gibson and R. J. Phipps, *Science,* 2020, **367**, 1246–1251.

137 (a) V. Dhayalan, S. C. Gadekar, Z. Alassad and A. Milo, *Nat. Chem.* 2019, **11**, 543–551; (b) I. L. Zak, S. C. Gadekar and A. Milo, *Synlett*, 2020, **32**, 329-336; (c) A. Camp, M. Kita, P. T. Blackburn, H. Dodge, C. H. Chen and A. J. M. Miller, *J. Am. Chem. Soc.*, 2021, **143**, 2792-2800.

138 (a) K. Ohmatsu, N. Imagawa and T. Ooi, *Nat. Chem.*, 2014, **6**, 47-51; (b) K. Ohmatsu, S. Kawai, N. Imagawa and T. Ooi, *ACS Catal.*, 2014, **4**, 4304-4306.

139 (a) R. Kumar, F. Hu, C. A. Hubbell, A. J. Ragauskas and C. E. Wyman, *Bioresour. Technol.,* 2013, **130**, 372–381; (b) T. Pfenning, A. Chemburkar, S. Cakolli, M. Neurock and B. H. Shanks, *ACS Sustainable Chem. Eng.,* 2018, ***6***, 12855–12864; (c) S. Dutta, *RSC Adv.,* 2012, **2**, 12575-12593; (d)Y. Nakagawa and K. Tomishige, *Catal. Today,* 2012, **195**, 136-143; (e) I. K. M. Yu and D. C. W. Tsang, *Bioresour. Technol.,* 2017, **238**, 716-732; (f) V. V. Vu, J. A. Hangasky, T. C. Detomasi, S. J. W. Henry, S. T. Ngo, E. A. Span and M. A. Marletta, *J. Biol. Chem.,* 2019, **294**, 12157-12166; (g) X. Jin, B. Yin, Q. Xia, T. Fang, J. Shen, L. Kuang and C. Yang, *ChemSusChem,* 2019, **12**, 71-92.

140 (a) D. H. Sherman, S. Li, L. V. Yermalitskaya, Y. Kim, J. A. Smith, M. R. Waterman and L. M. Podust, *J. Biol. Chem.*, 2006, **281**, 26289–26297; (b) S. Li, H. Ouellet, D. H. Sherman and L. M. Podust, *J. Biol. Chem.* , 2009, **284**, 5723–5730 (c) A. T. Larsen, E. M. May and K. Auclair, *J. Am. Chem. Soc.*, 2011, **133**, 7853–7858.

141 R. Breslow, A. B. Brown, R. D. McCullough and P. W. White, *J. Am. Chem. Soc.,* 1989, **111**, 4517-4518.

142 G. Olivo, G. Capocasa, O. Lanzalunga, S. Di Stefano and M. Costas, *Chem. Commun.*, 2019, **55**, 917-920.

143 (a) R. Breslow, X. Zhang, R. Xu, M. Maletic and R. Merger, *J. Am. Chem. Soc.* 1996, **118**, 11678–11679; (b) O. Perraud, A. B. Sorokin, J.-P. Dutasta, and A. Martinez, *Chem. Commun.,* 2013, **49**, 1288–90.

144 X. Lu, Y. Yoshigoe, H. Ida, M. Nishi, M. Kanai and Y. Kuninobu, *ACS Catal.,* 2019, **9**, 1705–1709.

145 P. Zardi, T. Roisnel and R. Gramage-Doria, *Chem. Eur. J.*, 2019, **25**, 627–634.

146 S. Erbas-Cakmak, D. A. Leigh, C. T. McTernan and A. L. Nussbaumer, *Chem. Rev.*, 2015, **115**, 10081–10206.

147 (a) D. A. Leigh, V. Marcos and M. R. Wilson, *ACS Catal.* 2014, **4**, 4490−4497. (b) E. A. Neal and S. M. Goldup, *Chem. Commun.,* 2014, **50**, 5128-5142. (c) V. Blanco, D. A. Leigh and V. Marcos, *Chem. Soc. Rev.* 2015, **44**, 5341-5370. (d) L. van Dijk, M. J. Tilby, R. Szpera, O. A. Smith, H. A. P. Bunce and S. P. Fletcher, *Nat. Rev. Chem.*, 2018, **2**, 0117; (e) R. Dorel and B. L. Feringa, *Chem. Commun.,* 2019, **55**, 6477-6486; (f) A. Goswami, S. Saha, P. K. Biswas and M. Schmittel, *Chem. Rev.*, 2020, **120**, 125–199; (g) A. Martinez-Cuezva, A. Saura-Sanmartin, M. Alajarin and J. Berna, *ACS Catal.*, 2020, **10**, 7719–7733; (h) A. W. Heard and S. M. Goldup, *ACS Cent. Sci.*, 2020, **6**, 117–128; (i) C. Kwamen and J. Niemeyer, *Chem. Eur. J.*, 2021, **27**, 175–186.

148 V. Blanco, A. Carlone, K. D. Hänni, D. A. Leigh and B. Lewandowski, *Angew. Chem. Int. Ed.,* 2012, **51**, 5166-5169.

149 V. Blanco, D. A. Leigh, V. Marcos, J. A. Morales-Serna and A. L. Nussbaumer, *J. Am. Chem. Soc.*, 2014, **136**, 4905-4908.

150 (a) G. De Bo,D. A. Leigh, C. T. McTernan and S. Wang, *Chem. Sci.*, 2017, **8**, 7077-7081. (b) K. Eichstaedt, J. Jaramillo-Garcia, D. A. Leigh, V. Marcos, S. Pisano and T. A. Singleton, *J. Am. Chem. Soc*., 2017, **139**, 9376−9381.

151 C. Biagini, S. D. P. Fielden, F. Schaufelberger, D. Thomas, S. Di Stefano and D. A. Leigh, *Angew. Chem. Int. Ed.*, 2019, **58**, 9876-9880.

152 C. Biagini and S. Di Stefano, *Angew. Chem. Int. Ed.*, 2020, **59**, 8344-8354.

153 (a) A. Martinez-Cuezva, M. Marin-Luna, D. A. Alonso, D. Ros-Ñiguez, M. Alajarin and J. Berna, *Org. Lett.*, 2019, **21**, 5192−5196. (b) M. Calles, J. Puigcerver, D. A. Alonso, M. Alajarin, A. Martinez-Cuezva and J. Berna, *Chem. Sci.*, 2020, **11**, 3629-3935. (c) A. Martinez-Cuezva, A. Saura-Sanmartin, T. Nicolas-Garcia, C. Navarro, R.-A. Orenes, M. Alajarina and J. Berna, *Chem. Sci.*, 2017, **8**, 3775-3780. (d) A W. Heard and S. M. Goldup, *Chem.*, 2020, **6**, 994–1006. (e) G. H. Ouyang, Y. M. He, Y. Li, J. F. Xiang and Q. H. Fan, *Angew. Chem. Int. Ed.*, 2015, **54**, 4334-4337. (f) Y. J. Lee, K. S. Liu, C.C. Lai, Y. H. Liu, S. M. Peng, R. P. Cheng and S. H. Chiu, *Chem. Eur. J.*, 2017, **23***,* 9756-9760.

154 M. Galli, J. E. M. Lewis and S. M. Goldup, *Angew. Chem. Int. Ed.*, 2015, **54**, 13545-13549.

155 (a) M. Schmittel, S. Pramanik and S. De, *Chem. Comm.*, 2012, **48**, 11730-11732; (b) S. De, S. Pramanik and M. Schmittel, *Dalton Trans.*, 2014, **43**, 10977-10982; (c) N. Mittal, S. Pramanik, I. Paul, S. De and M. Schmittel, *J. Am. Chem. Soc.*, 2017, **139**, 4270-4273; (d) I. Paul, N. Mittal, S. De, M. Bolte and M. Schmittel, *J. Am. Chem. Soc.*, 2019, **141**, 5139-5143; (e) S. Saha, A. Ghosh, T. Paululat and M. Schmittel, *Dalton Trans.*, 2020, **49**, 8693-8700; (f) I. Paul, A. Goswami, N. Mittal and M. Schmittel, *Angew. Chem. Int. Ed.*, 2018, **57**, 354-358; (g) P. K. Biswas, S. Saha, S. Gaikwd and M. Schmittel, *J. Am. Chem. Soc.*, 2020, **142**, 7889-7897.

156 H. J. Yoon, J. Kuwabara, J.-H. Kim and C. A. Mirkin, *Science*, 2010, **330**, 66-69.

157 J. R. Farrell, C. A. Mirkin, I. A. Guzei, L. M. Liable-Sands and A. L. Rheingold, *Angew. Chem. Int. Ed.*, 1998, **37**, 465-467.

158 N. C. Gianneschi, S. T. Nguyen Chad and A. Mirkin, *J. Am. Chem. Soc*., 2005, **127**, 1644-1645.

159 H. J. Yoon and C. A. Mirkin, *J. Am. Chem. Soc.*, 2008, **130**, 11590–11591.

160 (a) C. M. McGuirk, J. Mendez-Arroyo, A. I. d'Aquino, C. L. Stern, Y. Liu and C. A. Mirkin, *Chem. Sci.*, 2016, **7**, 6674-6683; (b) C. M. McGuirk, J. Mendez-Arroyo, A. M. Lifschitz and C. A. Mirkin, *J. Am. Chem. Soc*., 2014, **136**, 16594−16601; (c) C. M. McGuirk, C. L. Stern and C. A. Mirkin, *J. Am. Chem. Soc.*, 2014, **136**, 4689−4696; (d) A. M. Lifschitz, R. M. Young, J. Mendez-Arroyo, Charlotte L. Stern, C Michael McGuirk, M. R. Wasielewski and C. A. Mirkin, *Nat. Commun*., 2015, **6**, 6541-6546.

161 F. Würthner and J. Rebek, Jr, *Angew. Chem. Int. Ed. Engl.*, 1995, **34**, 446-448.

162 R. Cacciapaglia, S. Di Stefano and L. Mandolini, *J. Am. Chem. Soc.*, 2003, **125**, 2224-2227.

163 S. Kassem, A. T. L. Lee, D. A. Leigh, V. Marcos, L I. Palmer and S. Pisano, *Nature*, 2017, **549**, 374-378.

164 J. Wang and B. L. Feringa, *Science*, 2011, **331**, 1429-1432.

165 Selected examples are: (a) M. Vlatković, L. Bernardi, E. Otten and B. L. Feringa, *Chem. Commun.,* 2014, **50**, 7773-7775; (b) D. Zhao, T. M. Neubauer and B. L. Feringa, *Nat. Commun.*, 2015, **6**, 6652; (c) S. F. Pizzolato, P. Štacko, J. C. M. Kistemaker, T. van Leeuwen, E. Otten and B. L. Feringa, *J. Am. Chem. Soc.*, 2018, **140**, 17278−17289; (d) K. Grill, H. Dube, *J.*

Am. Chem. Soc. 2020, **142**, 19300-19307; (e) O. B. Berryman, A. C. Sather, A. Lledó, J. Rebek, *Angew. Chem. Int. Ed.* 2011, **50,** 9400-9403.

166 C.-S. Kwan, A. S. C. Chan and K. C.-F. Leung, *Org. Lett.*, 2016, **18**, 976-979.

167 a) J. Beswick, V. Blanco, G. De Bo, D. A. Leigh, U. Lewandowska, B. Lewandowski and K. Mishiro, *Chem. Sci.*, 2015, **6**, 140-143; b) K. Eichstaedt, J. Jaramillo-Garcia, D. A. Leigh, V. Marcos, S. Pisano and T. A. Singleton, *J. Am. Chem. Soc.*, 2017, **139**, 9376-9381.

168 S. De, S. Pramanik and M. Schmittel, *Angew. Chem. Int. Ed.*, 2014, **53***,* 14255-14259; (b) A. Goswami, T. Paululat and M. Schmittel, *J. Am. Chem. Soc.*, 2019, **141**, 15656-15656.

169 S. F. M. van Dongen, J. A. A. W. Elemans, A. E. Rowan and R. J. M. Nolte, *Angew. Chem. Int. Ed.*, 2014, **53**, 11420–11428.

170 (a) P. Thordarson, E. J. A. Bijsterveld, A. E. Rowan and R. J. M. Nolte, *Nature*, 2003, **424**, 915-918; (b) C. Monnereau, P. Hidalgo Ramos, A. B. C. Deutman, J. A. A. W. Elemans, R. J. M. Nolte and A. E. Rowan, *J. Am. Chem. Soc.*, 2010, **132**, 1529-1531; (c) A. B. C. Deutman, C. Monnereau, J. A. A.W. Elemans, G. Ercolani, R. J. M. Nolte and A. E. Rowan, *Science*, 2008, **322**, 1668-1671.

171 (a) S. Varghese, J. A. A. W. Elemans, A. E. Rowan and R. J. M. Nolte, *Chem. Sci.* 2015, **6**, 6050-5058; (b) P. J. Gilissen, P. B. White1, J. A. Berrocal, N. Vanthuyne, F. P. J. T. Rutjes, B. L. Feringa, J. A. A. W. Elemans and R. J. M. Nolte, *Nat. Commun*. 2020, **11**, 5291.

172 Y. Takashima, M. Osaki, Y. Ishimaru, H. Yamaguchi and A. Harada, *Angew. Chem.*, 2011, **123**, 7666-7670.

173 B. Lewandowski, G. De Bo, J. W. Ward, M. Papmeyer, S. Kuschel, M. J. Aldegunde, P. M. E. Gramlich, D. Heckmann, S. M. Goldup, D. M. D'Souza, A. E. Fernandes and D. A. Leigh, *Science*, 2013, **339**, 189-193.

174 G. De Bo, S. Kuschel, D. A. Leigh, B. Lewandowski, M. Papmeyer and J.W. Ward, *J. Am. Chem. Soc.*, 2014, **136**, 5811-5814.

175 Here follows reference to some selected pioneering examples of supramolecular catalysts. (a) J.-P. Behr and J.-M. Lehn, *J. Chem. Soc., Chem. Commun.*, 1978, 143–146; (b) D. J. Cram, H. E. Katz, I. B. Dicker, *J. Am. Chem. Soc.*, 1984, **106**, 4987–5000; (c) W. L. Mock, T. A; Irra, J. P. Wepsiec, M. Adhya, *J. Org. Chem.*, 1989, **54**, 5302-5308; (d) M. W. Hosseini, A. J. Blacker and J.-M. Lehn, *J. Am. Chem. Soc.*, 1990**, 112**, 3896-3904; (e) T. Tjivikua, P. Ballester and J. Rebek, Jr, *J. Am. Chem. Soc.*, 1990**, 112**, 1249-1250; (f) C. J. Walter, H. L. Anderson and J. K. M. Sanders, *Chem. Commun.*, 1993, 458-460 (g) I. Huc, R. J. Pieters and J. Rebek, Jr, *J. Am. Chem. Soc.*, 1994, **116**, 10296-10297; (h) W. H. Chapman, Jr. and R. Breslow, *J. Am. Chem. Soc.*, 1995, **117**, 5462-5469; R. G. Konsler, J. Karl and Eric N. Jacobsen, *J. Am. Chem. Soc.*, 1998, **120**, 10780-10781; (i) A. Robertson, D. Philp and N. Spencer, *Tetrahedron,* 1999, **55**, 11365–11384; (j) V. Van Axel, A. Dalla Cort, L. Mandolini, D. N. Reinhoudt and L. Schiaffino, *Chem. Eur. J.*, 2000, **6**, 1193-1198; (k) F. Cuevas, S. Di Stefano, O. J. Magrans, P. Prados, L. Mandolini and J. de Mendoza, *Chem. Eur. J.*, 2000, **6**, 3228-3234; (l) P. Molenveld, S. Kapsabelis, J. F. J. Engbersen and D. N. Reinhoudt *J. Am. Chem. Soc.*, 1997, **119**, 2948-2949.

176 a) A. Schmid, J. S. Dordick, B. Hauer, A. Kiener, M. Wubbolts and B. Witholt, *Nature*, 2001, **409**, 258–268; (b) U. T. Bornscheuer, G. W. Huisman, R. J. Kazlauskas, S. Lutz, J. C. Moore and K. Robins, *Nature*, 2012, **485**, 185–194.

177 (a) M. T. Reetz, *Angew. Chemie Int. Ed.*, 2010, **50**, 138–174; (b) F. H. Arnold, *Angew. Chemie Int. Ed.*, 2018, **57**, 4143–4148.

178 F. Schwizer, Y. Okamoto, T. Heinisch, Y. Gu, M. M. Pellizzoni, V. Lebrun, R. Reuter, V. Köhler, J. C. Lewis and T. R. Ward, *Chem. Rev.*, 2018, **118**, 142–231.

179 Y. Kang, X. Tang, H. Yu, Z. Cai, Z. Huang, D. Wang, J.-F. Xu and X. Zhang, *Chem. Sci.*, 2017, **8**, 8357–8361.

180 X. Tang, Z. Huang, H. Chen, Y. Kang, J.-F. Xu and X. Zhang, *Angew. Chemie Int. Ed.*, 2018, **57**, 8545–8549.

181 M. Petroselli, V. Angamuthu, F.-U. Rahman, X. Zhao, Y. Yu, J. Rebek, *J. Am. Chem. Soc.* 2020, **142**, 2396–2403.

ARTICLE

Table of contents entry

Recent advancements in supramolecular catalysis are reviewed, which show the high potential of related tools when applied to organic synthesis. Nanoconfinement of reactants, recognition driven and processive catalysis, regulation of catalysis by molecular machines are recognized as innovative instruments that can pave the way to alternative synthetic strategies.